DETERMINATION OF WATER QUALITY OF NGUUE SPRING AND RIVER MUTONGA IN THARAKA-NITHI, KENYA AND EVALUATION OF CORN-COB DERIVED CARBON POWDER IN REMEDIATION OF CONTAMINATED WATER

BERTHA KINYA MWENDA

A Thesis Submitted to the Graduate School in Partial Fulfillment of the Requirements for the Award of the Degree of Master of Science in Chemistry of Chuka University

CHUKA UNIVERSITY

OCTOBER, 2025

DECLARATION AND RECOMMENDATION

Declaration

This thesis is my original work that has not been presented for examination purpose in any other institution.

Signature..... Date.....24/10/2025.....
Bertha Kinya Mwenda
SM11/58123/22

Recommendation

This thesis has been examined, passed and submitted with our approval as University supervisors

Signature..... Date.....24/10/2025.....
Prof. Eric Njagi, PhD
Chuka University

Signature..... Date.....24/10/2025.....
Prof. Moses Mahugu Muraya, PhD
Chuka University

COPYRIGHT

DEDICATION

This work is dedicated to my dad Douglas Mwenda, my mum Lydia Wanja, my siblings Bettylord Gacheri, Brenda Kanana and my son Cassian Mutuma.

ACKNOWLEDGEMENT

My special thanks and honour goes to Almighty God for giving me mental and physical strength, throughout the study period without which I would not have made it. His presence has been my constant source of inspiration throughout the study.

I would like to express my heart most felt and sincere gratitude to my Supervisors, Prof. Eric Njagi and Prof. Moses Mahugu Muraya whose expertise, guidance, patience, dedication and invaluable input has been instrumental in completion of this thesis. I also acknowledge my lecturers for mentorship and general contribution throughout the study.

I also extend my sincere gratitude towards Chuka University for provision of resources during the study. I also extend my appreciation to members of Physical Sciences department in Meru University too for accepting me to use their laboratory. Special thanks to Meru University laboratory technicians Julius Mutiria, Clare, Kazungu and Joshua for their devotion, guidance and technical support that made my experimental work possible.

My special appreciation to my wonderful family. To my amazing parents, Douglas Mwenda and Lydia Wanja, I can't thank you enough for your unfailing love, prayers and endless inspiration has been fundamental for my success. To my loving and caring sisters Bettylord and Brenda words alone are not enough to express my gratitude to you for endless encouragement and all assistance that prompted this achievement. To my amazing son Cassian Mutuma, your whispers of love and company was my constant source of inspiration. I sincerely thank you for understanding my absence when you needed me most and for your co-operation during study period, gave me inner strength to carry on.

To my course mates Liz Murugi and Miriam Wanjiru receive my special appreciations for not only being course mates but for sacrifice and encouragements accorded. To my friends Juster Kiende and Dolly Kathure I can't thank you enough for sacrifice and all kind support you offered towards this incredible journey. My appreciations also go to all who were part of this journey for any form of contribution.

ABSTRACT

Water quality is a pressing global concern, since water pollution negatively impacts water bodies and poses severe threats to both human and aquatic life.The aim of this study was to, determine physico-chemical and bacteriological parameters of Nguue spring and river Mutonga, and compare to the limits set by WHO and KEBS. The performance of low-cost adsorbent in removal of zinc and iron from contaminated water was also evaluated. Sampling was done each at six points along the river and the spring approximately 500 metres apart, in the dry and wet season in the months of September and November 2024. The physical parameters of water such as temperature, pH, DO, TDS and EC were measured using multiparameter. Total hardness was estimated by titrimetry. Anions of NO_3^- and PO_4^{3-} were determined by UV spectrophotometric method. The heavy metals of Zn^{2+} and Fe^{3+} in water samples were determined by Atomic Absorption Spectrophotometer. In the dry season, River Mutonga recorded a temperature between 25.9-26.6 °C, pH of 7.1-7.4 , electrical conductivity was 172.8-202 µS/cm, total dissolved solids 0.838-0.886 mg/L , dissolved oxygen, 3.19-3.25 mg/l, however, total hardness 0.838-0.886 mg/L, nitrate concentrations 16.57-19.35 mg/L, while phosphate was 1.95-2.12 mg/L. Nguue Spring during the dry season exhibited a temperature of 25.9-26.5 °C, pH was 5.21-6.58 indicating slight acidity, electrical conductivity of 147.6-193.6 µS/cm and total dissolved solids 0.552-1.2 mg/L, total hardness wa 58-160 mg/L, well Similar to Mutonga River, nitrate levels 16.83-19.47 mg/L. In the wet season, River Mutonga recorded a lower temperature of 21 °C compared to the dry.4 and 6.5-8.5 respectively, indicating increased acidity in sampling point M1. Electrical conductivity 57.2-60.4 µS/cm and total dissolved solids 31.3-36.6 mg/L were markedly lower than in the dry season, reflecting dilution effects of rainfall. Dissolved oxygen was 8.72-8.92 mg/L increased substantially and was well above the WHO minimum standard 4.0 mg/l. Total hardness decreased to 87.3-122 mg/L but remained within permissible limits. Nitrate levels dropped to 7.25-12.35 mg/L, now falling within KEBS standards which is 10 mg/l, while phosphates was 2.01-2.29 mg/L remained above WHO limits 0.5 mg/L. Nguue Spring in the wet season showed a temperature of 20.5-21 °C, pH was4.210-5.724 was consistently below both WHO and KEBS ranges, suggesting acidic conditions. Electrical conductivity was 37.8-55.6 µS/cm and total dissolved solids 27.7-59.5 mg/L decreased compared to the dry season, reflecting rainwater dilution. Dissolved oxygen was 8.58-8.86 mg/L was significantly elevated and met WHO standards, total hardness was 22.6-84 mg/L remained within permissible limits. Nitrate concentration was 7.8-14.65 mg/Lwas marginally above the KEBS guideline, while phosphate was 1.95-2.23 mg/L exceeded WHO standards but was acceptable under KEBS. Batch adsorption was carried out by varying the parameters of temperature, pH, intial concentration, contact time and adsorbent dosage. The total coliforms count in Mutonga were 11-460 and 36-1100 MPN per 100 ml in dry and wet season repectively and exceeded KEBS and WHO limits. In Nguue spring the toal coliform counts were 36-1100 and 43->1100 MPN per 100 ml in dry and wet season respectively exceeding KEBS and WHO limits. Adsorption of zinc and iron on CCAC and CCC was successfully represented by Freundlich and Lngmuir isotherm models. Adsorption of zinc on CCAC and CCC was best described by Freundlich with KF=2.35 mg/g, n=1.387, R^2=0.9359 and KF=116.84mg/g, n=0.1634, R^2= 0.9497 respectively indicating a favourable multilayer adsorption on heterogenous surface. Adsorption of iron on CCAC and CCC also Freundlich gave a reasonable fit with KF=1.1498mg/g, n=0.5826, R^2=0.90703 and KF=1.8034mg/g, n=0.9063, R^2=0.97692 respectively

TABLE OF CONTENTS

LIST OF TABLES

LIST OF FIGURES

LIST OF ABBREVIATIONS AND ACRONYMS

AAS	**:**	Atomic absorption spectrophotometer
AC	**:**	Activated carbon
ANOVA	**:**	Analysis of variance
APHA	**:**	American public health association
BAM	**:**	Bacteriological analytical manual
BOD	**:**	Biochemical oxygen demands
CCAC	**:**	Corn-cob Activated Charcoal
CCC	**:**	Corn-cob Charcoal
CUEC	**:**	Chuka university ethics committee
DO	**:**	Dissolved oxygen
EDTA	:	Ethylenediaminetetraacetric acid
GPS	**:**	Global positioning system
ISO	**:**	International organization for standardization
LEMB	**:**	Levine eosin methylene broth
LSD	**:**	Least significance difference
MPN	**:**	Most probable number
NACOSTI	**:**	National commission for science technology and innovation
SAS	**:**	Statistical analysis software
SDG	**:**	Sustainable development goals
TDS	**:**	Total dissolved solids
TS	**:**	Total solid
UV-VIS	**:**	Ultraviolet visible
WHO	**:**	World health organization
XRD	**:**	X-ray diffraction spectroscopy
XRF	**:**	X-ray fluorescence

CHAPTER ONE
INTRODUCTION

1.1 Background to the Study

Water resources are essential for life powering human consumption, food production and environmental systems (Akhtar, 2021). Globally over 5 billion inhabitants are dependent on ground water and surface water system (Khatri, 2014). Water quality depends on it physico-chemical and biological parameters. Changes in parameters such as pH, temperature and essential and non-essential trace metals in water can render it unfit for human use. The degradation of water resources is a much studied phenomena and can be caused by natural processes (climate change, water-rock interaction and geological factors) and human activities (agricultural practices and urban waste) as well as considerable chemical compounds due to industrial revolution (Nagaruju *et al*., 2016).

In Kenya water resources are progressively getting polluted from both point and nonpoint sources; the significant contamination is horticultural that produce silt and agrochemicals deposits; industrial solid waste and homegrown effluent (Omunyala, 2017). Water pollution remains as significant challenge on water quality. Thus, it has become very hard to get clean safe and potable water in most of developing countries (Dara and Mishra, 2011; Idibie *et al*., 2018). During, wet season there is increased surface run off of agricultural chemicals from farms, raw sewage from neighboring learning institutions, quarry run-off drains into the river Mutonga and Nguue spring thus affecting the quality of this water. The water taken from the river and spring does not undergo through any treatment before use for any activity. There is no integrated or seasonal assessment of physico-chemical and bacteriological parameters done. Thus, this study reviewed the water quality of Nguue spring and Mutonga river water and low-cost bioremediation approach to ensure its suitability and safety among its users.

Water is also susceptible to contamination by micro-organism, from different sources (Oldairo and Aiyedun, 2016). Significantly, microbial contaminants such as coliforms, *E. coli*, *Cryptosporidium parvum* and *Giardia lamblia* compromise the safety of water (Opara and Nnodium, 2014). Presence of *Escherichia coli*, *Klebsiella spp.* and *Enterobacter* species in water is an indicator of possible presence of pathogenic

organism such as *Clostridium pafrigens*, *Salmonella* and protozoa (Opara and Nnodium, 2014). These pathogens cause diarrhea, giardiasis, dysentery and gastroenteritis which are common among the rural dwellers of developing nations (Isikwe and Chikezie, 2014; Oludairo and Aiyedun, 2016). Infections by bacterial contaminants may be symptomized by stomach cramps, nausea, vomiting and fevers occurring within ten days upon consumption of contaminated water (Ugwuzor and Ifeanyi, 2015).

Some inorganic substances such as zinc, copper, iron and nickel are necessary for development of plants and animals but they are harmful when the concentration go above the acceptable limits (Vardhan *et al*., 2019). The contamination of surface water with heavy metals like zinc, copper, iron, lead, chromium, nickel and cadmium is responsible for several health issues in human like renal dysfunction, mental disorders, cancers and harmful effects on reproductive system. Hence there is need for evaluation and removal of such contaminants in water.

There are several physicochemical methodologies with varying degrees of success that have been developed to remove contaminants from water though they are expensive and generate large amounts of secondary pollutants (Miretzky *et al*., 2006). Biological methods such as biosorption, bioaccumulation, bioreduction, phytoremediation and mycoremediation are effective to physicochemical methods because they are cost-effective and eco-friendly.

Among other technologies for water pollution treatment, adsorption is considered better than other methods because of convenience, easy operation and simplicity of design (Amit and Minocha, 2006). Activated carbon adsorption is also a well-known method for removal of heavy metals (Ajamal *et al*., 2003). It is considered to be a particularly competitive process for the removal of heavy metals at trace quantities however; the use of activated carbon is not suitable in developing countries due to high cost of production and regeneration of spent carbon (Bailey *et al*., 1999).

The use of alternative low-cost materials as potential adsorbent for the removal of natural materials, industrial waste and agricultural wastes which are generally available

and have little cost compared to activated carbon (Feng and Guo, 2012). This has been necessitated by the fact that the methods used currently for water treatment such as chemical oxidation, chemical precipitation, evaporation, electrochemical treatment and use of ion exchange resins have significant demerits such as incomplete metal removal, high reagent or energy requirements, generation of toxic sludge and are generally ineffective especially when the ion concentration is low (Liang *et al*., 2009).

Disposal of waste materials is increasingly becoming a great concern (Amit and Minocha, 2006) because these wastes represents unused resources and are also an environmental hazard. A large volume of solid waste is produced in agricultural sector in many countries includes rice husks, saw-dust, maize cob, maize husks, fluted pumpkin stem, okra stem derived cellulose, coca pods, coconut fiber, yam, cassava, banana, sweet potato and plantain peels, among others (Okoro *et al*., 2006). A large portion of these wastes are normally used as domestic fuels; however, this cheap abundant waste can be explored as low-cost alternative adsorbents owing to relatively high fixed carbon content and porous structure (Amit and Minocha, 2006).

1.2 Statement of Problem

Rapid expansion of agriculture, livestock keeping, industrial activities, health care facilities, car wash operations and learning institutions has led to increased discharge of hazardous waste into rivers and other water bodies. In Igoji and Maara sub counties, most residents draw water directly from such surface sources for domestic use, with limited or no household-level treatment. Consequently, consumption of untreated water poses serious health risks to consumers. Nguue spring and River Mutonga are particularly vulnerable to pollution due to intensified anthropogenic activities in their catchments, including agricultural runoff and quarry drain off. Despite this, there is no intergrated, seasonal assessment of physico-chemical, bacteriological quality and no evaluation of corn-cob derived adsorbent for removal of zinc and iron in this catchment. Water from these sources pose potential health implications for surrounding communities. At the same time, maize is the dominant subsistence crop in Kenya, but post-harvest maize cobs are largely underutilized, commonly discarded or used as low-grade fuel, leading to accumulation in homesteads. Valorization of this agricultural by-product into activated carbon could provide a low-cost, environmentally friendly

adsorbent for water purification. Therefore, this study seeks to assess the quality of water from Nguue spring and Mutonga River and to design a simple cost-effective remediation method using corn-cob-derived carbon powder.

1.3 Objective of the Study

1.3.1 General Objectives

To investigate the water quality of Nguue spring and river Mutonga in dry and wet seasons and to evaluate the effectiveness of corn-cob derived carbon powder in removal of zinc and iron from contaminated water.

1.3.2 Specific Objectives

i. To determine the physico-chemical properties and the total coliforms present in Nguue spring and Mutonga river water
ii. To determine the structural and elemental properties of corn-cob carbon powder
iii. To evaluate the performance of corn-cob carbon powder adsorbent on removal of zinc and iron from contaminated water

1.4 Research Questions

i. What are the physico-chemical properties and the total coliforms present in Nguue spring and Mutonga river water?
ii. What is the structural and elemental properties of corn-cob carbon powder?
iii. What is performance of corn-cob carbon powder adsorbent on removal of zinc and iron from contaminated water ?

1.5 Significance of the Study

This study is of great significance both scientifically and socially. It generates empirical data on the physico-chemical and microbial quality of water from Nguue Spring and River Mutonga, thereby contributing to the existing body of knowledge in environmental and analytical chemistry. In addition, it advances the application of locally available biomass, specifically maize cobs, in water remediation. Since maize is a major subsistence crop in Kenya and maize cobs are largely discarded as waste, their conversion into carbon powder for bio-adsorption not only offers a low-cost water

treatment option but also promotes sustainable waste management and circular economy practices.

From a public health perspective, the study provides health practitioners and public health officials with evidence-based information on the risks associated with consumption of untreated water from surface sources. Such knowledge is useful in developing preventive strategies to reduce the incidence of waterborne diseases and the mortality associated with them. This directly supports SDG 3 (Good Health and Well-Being) by contributing to the reduction of illnesses caused by unsafe water.

The findings of this research are also valuable to the County Government of Tharaka-Nithi and other stakeholders in the water sector by providing a basis for regular monitoring of water quality and guiding the design of interventions that ensure safe and reliable water for both human and animal consumption. Furthermore, the study has policy relevance as it informs environmental policymakers in defining legislative interventions aimed at maintaining water quality standards in line with national and international guidelines. This aligns with SDG 6 (Clean Water and Sanitation), which calls for universal access to safe water and effective management of water resources.

Beyond the local setting, the knowledge generated from this study can be applied to other communities facing similar challenges of water contamination and limited access to affordable treatment technologies. By demonstrating the effectiveness of corn-cob-derived carbon powder in water purification, the study offers a sustainable and low-cost alternative to conventional treatment methods, which are often expensive and inaccessible to rural communities. he valorization of maize cobs into useful adsorbents also contributes to SDG 12 (Responsible Consumption and Production) by promoting resource recovery and reducing agricultural waste, while indirectly supporting SDG 13 (Climate Action) through sustainable environmental management practices. Ultimately, this research contributes to scientific innovation, public health protection, environmental conservation, and sustainable development by addressing both local and global concerns on water safety and resource utilization.

From seasonal variability point of view, water quality is crucial for effective water resource management, understanding impacts on aquatic ecosystems and human health, and developing adaptive stratergies to address seasonal pollution from natural and human sources.

1.6 Scope and Limitation of the Study

This study focused on the assessment of selected physico-chemical and microbial parameters of water from Nguue Spring and River Mutonga in Tharaka-Nithi County. The parameters analyzed were limited to those that could be reliably determined using the available laboratory facilities and were most relevant to assessing water quality in relation to human health.

The study further concentrated on evaluating the adsorption efficiency of carbon powder derived from corn-cobs as a low-cost bio-adsorbent for water remediation. Other agricultural wastes and alternative adsorbent materials were not explored. The adsorbent was chemically modified using nitric acid. Other activating agents were not explored. For batch adsorption experiments were evaluated by varying the parameters of pH, dosage, initial metal ion concentration, contact time and temperature. Additionally, the study was limited by time, financial resources, and the scope of available analytical instruments, which influenced the choice and number of parameters investigated.

CHAPTER TWO

LITERATURE REVIEW

2.1 Overview of Water Quality and Remediation Techniques

2.1.1 Importance of Water Quality

Water is the most vital natural resource for sustaining life on earth, whether in surface or underground reserves. It plays a critical role in hydro-geo-ecological systems and is central to metabolic, physiological, and ecological processes of living organisms (Nahyan, 2012; Akhtar, 2021). Water quality is typically assessed using established criteria that specify acceptable limits for different parameters to ensure safety for human and environmental health. For some parameters, such as dissolved oxygen, minimum thresholds are set to maintain essential biological functions (Hasan, 2018). The physicochemical properties of water, including pH, temperature, electrical conductivity, biochemical oxygen demand (BOD), chemical oxygen demand (COD), total dissolved solids (TDS), and mineral or heavy metal concentrations, are key determinants of its suitability for different uses. Since water is indispensable for domestic, agricultural, industrial, and ecological purposes, its quality is a fundamental determinant of environmental sustainability and public health.

2.1.2 Health Implications of Poor Water Quality

Access to safe and adequate drinking water remains a global challenge. Globally, 829,000 people are estimated to die each year from diarrhoea as a result of unsafe and or inadequate drinking water, sanitation and hygiene (WHO, 2022). In developing countries, it is estimated that at any given time, nearly half of the population suffers from water-related illnesses (WHO, 2010). The lack of safe water compromises not only public health but also socio-economic development, particularly in rural communities that depend directly on surface water sources (MacDonald and Calow, 2009).

Unsafe drinking water is strongly associated with diarrheal diseases, cholera, typhoid, and parasitic infections. Vulnerable populations, such as children, the elderly, and immunocompromised individuals, including those living with HIV/AIDS, face an even greater risk (Laurent, 2007). Consequently, the purity and cleanliness of water are

critical for reducing morbidity and mortality, especially in regions where waterborne diseases remain endemic (Vidyasagar, 2007).

2.1.3 Sources of Water Pollution

Water quality is influenced by both natural processes and human activities. Naturally, contamination can occur through geological leaching of minerals and trace elements into water systems, leading to elevated levels of fluoride, arsenic, or heavy metals (Singh *et al*., 2022). However, anthropogenic activities are the primary drivers of water pollution in most regions. Polluted surface waters often contain a wide range of pathogens, viruses, bacteria, and protozoa, mostly from faecal sources (Servais *et al*., 2007). Point sources include municipal wastewater discharges, effluents from industries, and runoff from livestock handling areas (Williams *et al*., 2012), while non-point sources include stormwater, sewage leaks, agricultural runoff, and domestic animal waste (Chigor *et al*., 2012).

In rural Kenyan catchments such as Nguue spring and Mutonga River, water quality is increasingly deteriorating due to immense agricultural practises leading to leaching of fertilisers and pesticides. Oher contributors include improper solid waste disposal, poorly managed sanitation systems, and domestic effluents. According to Hiscock (2014), common water contaminants include agrochemicals, industrial effluents, petroleum wastes, sewage sludge, and urban runoff, all of which pose both acute and chronic health risks to surrounding communities.

2.1.4 Limitations of Conventional Water Treatment Methods

Traditional water treatment technologies such as chlorination, coagulation-precipitation, reverse osmosis, ion exchange, solvent extraction, electrochemical treatments, and activated carbon adsorption have been widely used to remove contaminants (Amit and Minocha, 2006). While effective, these methods are often expensive, energy-intensive, and environmentally unsustainable. They also generate concentrated toxic sludge or secondary wastes that require specialized disposal (Chen *et al*., 2005). Furthermore, when contaminant concentrations are very low, conventional technologies may not be efficient, making them impractical for rural and low-resource

settings (Huang *et al*., 2003; Gaber *et al*., 2012). These limitations highlight the urgent need for cost-effective, sustainable, and locally adaptable water treatment solutions.

2.1.5 Potential of Agricultural Waste in Water Remediation

Recent research has focused on low-cost and environmentally friendly alternatives for water remediation, with agricultural wastes gaining considerable attention as effective adsorbents. Biomaterials such as rice husks, banana peels, sawdust, and corn cobs have been investigated for their ability to remove heavy metals, organic pollutants, and microorganisms due to their lignocellulosic composition and modifiable surface chemistry (Sen, 2023).

Corn (maize) is one of the most extensively cultivated crops worldwide and serves as a staple food in Kenya. After harvesting, maize cobs are usually discarded or burned, leading to waste management challenges (Bayou *et al*., 2023). However, corn cobs are rich in cellulose, hemicellulose, and lignin, making them suitable for modification into activated carbon or other adsorbents. Studies have demonstrated that modified corn cobs can effectively remove metals, dyes, and microbial contaminants from water, offering a sustainable and low-cost treatment option for rural communities. Due to their abundance, low cost, and underutilization in Kenya, corn cobs present a promising material for developing affordable remediation technologies for water treatment (Bayou *et al*., 2023).

2.2 Physico-Chemical and Bacteriological Parameters Influencing Water Quality

The availability of good quality water is an indispensable requirement for preventing diseases and improving quality of life. Water quality is commonly assessed through a range of physico-chemical parameters that serve as indicators of its suitability for human consumption, industrial use, and ecological sustainability (Kumar *et al*., 2021; WHO, 2022). These parameters include colour, odour, temperature, acidity, hardness, pH, sulphate, nitrates, phosphates, turbidity, dissolved oxygen (DO), biochemical oxygen demand (BOD), chemical oxygen demand (COD), electrical conductivity (EC), alkalinity, hardness and other chemical constituents. While some parameters such as temperature, colour, odour, pH, turbidity can be assessed through physical observation, while chemical tests for biochemical oxygen demand, chemical oxygen demand,

dissolved oxygen, alkalinity and hardness require chemical or instrumental analysis (Sharma, 2015; Sillanpää *et al*., 2018). Ensuring safe drinking water has been recognized globally as a fundamental human right (United Nations, 2010; WHO, 2022).

Temperature is among the most significant ecological factors influencing aquatic systems. It regulates seasonal and diurnal variations and directly affects biological and biochemical processes such as microbial activity, growth, mineralization, and decomposition (Van Vliet *et al*., 2011; Kaushal *et al*., 2021). Even minor thermal fluctuations can significantly alter DO levels and consequently affect aquatic biodiversity. Global warming and increased anthropogenic pressures have intensified thermal stress in freshwater ecosystems, amplifying water quality concerns (Arismendi *et al*., 2022).

Electrical conductivity (EC) measure the ability of water to conduct an electric current and reflects the concentration of dissolved ions such as chloride, nitrate, sulphate, phosphate, sodium, calcium, and magnesium. Higher EC is often associated with pollution from agricultural fertilizers, pesticides, and urban effluents (Bhat *et al*., 2020; Zhang *et al*., 2022). Because EC is highly temperature-dependent, values are standardized at 25°C for comparability (EPA, 2012). Land use practices, particularly intensive agriculture and urbanization, have been strongly linked to elevated EC in both surface and groundwater systems (Wang *et al*., 2018)

Alkalinity and pH are critical indicators of acid–base balance in aquatic ecosystems. Acidification may occur due to atmospheric deposition of sulfuric and nitric acids or through industrial effluents, leading to ecological imbalance and biodiversity decline (Oko *et al*., 2020). Natural waters often exhibit alkalinity due to carbonate and bicarbonate buffering, which helps resist pH fluctuations. Extreme deviations in pH disrupt physiological processes in aquatic organisms, while moderately alkaline waters are generally associated with higher primary productivity (Sharma, 2015; Rajiv *et al*., 2021).

Dissolved oxygen (DO) is a vital parameter reflecting the ecological health of aquatic systems. It influences microbial decomposition, nutrient cycling, photosynthesis, and

respiration (Morales *et al*., 2021). DO levels typically decrease in warm seasons due to higher temperatures and intensified microbial activity but rise under conditions of strong photosynthetic activity. Chronic oxygen depletion (hypoxia) can lead to fish kills, loss of biodiversity, and ecological imbalance (Rabalais *et al*., 2020).

Nitrates (NO_3^-), which are essential plant nutrients, often originate from inorganic fertilizers such as urea, ammonium nitrate,diammonium phosphates among others, animal manure, and sewage effluents. Elevated nitrate concentrations in drinking water have been linked to gastrointestinal disorders, eutrophication, and infant methemoglobinemia ("blue baby syndrome") (Ward *et al*., 2018). The World Health Organization (WHO, 2022) and Kenya Bureau of Standards (KEBS, 2015) set the permissible limit for nitrate in drinking water at 10 mg/L. However, recent studies show widespread exceedances in agricultural regions of Sub-Saharan Africa, posing significant health and environmental risks (Omondi *et al*., 2022).

Phosphates (PO_4^{3-}), similarly, are essential nutrients but can severely degrade aquatic ecosystems when present in excess. Agricultural runoff, industrial effluents, detergents, and untreated sewage are the main contributors to phosphate enrichment (Dodds and Smith, 2016). Elevated concentrations promote eutrophication, which leads to algal blooms, oxygen depletion, and disruption of aquatic life-support systems. KEBS (2015) recommends a limit of 2.2 mg/L for phosphate in drinking water. Recent studies confirm phosphate enrichment as a persistent threat to freshwater systems, particularly in urban and peri-urban catchments (Zhou *et al*., 2022).

Heavy metals are defined as metals having high atomic weight and density at least $5g/cm^3$ (Zhang et al., 2019). Heavy metals are naturally occurring elements with a large atomic weight at least five times the density of water (Tchounwou *et al*., 2012). Various heavy metals such as chromium, cadmium, nickel, copper, zinc, lead, mercury and arsenic are recognized as biologically dispensable and detrimental to the aquatic ecosystem (Jacob *et al*., 2018).

In terms of abundance, iron accounts for 5% of the earth's crust and comes second after aluminium. Elemental iron is not easily found in nature as Fe^{3+} and Fe^{2+} combines

readily with Sulphur- and oxygen- containing compounds leading to formation of carbonates, sulphides, oxides and hydroxides. In nature, iron is mostly found in oxide form. Rivers contain approximately 0.5-1.0mg/l of iron and groundwater contains 100mg/l. The naturally occurring iron minerals are magnetite, hematite, goethite and siderite. Weathering process release these elements into waters. Iron is a central component of haemoglobin and it binds oxygen and transport it from lungs to other body parts but however in it exceeds the required amounts it is stored in the liver and may damage vital organs. Iron deficits leads to anaemia, causing tiredness, headache, loss of concentration and affects immune system. In young children iron deficits negatively affects mental development, leads to irritability causing concentration disorder. High concentration of iron in drinking water imparts taste and odour. The recommended level of concentration of iron is usually 0.3mg/l (KEBS, 2015; WHO, 2022).

Zinc ions can be found in trace amounts in almost all igneous rocks and when excess in drinking water it produces undesirable taste and odour. The metal is used in the production of alloys as well as galvanizing iron and steel. Zinc oxide is used as white pigment in rubber and is the most used in compound of zinc. In natural surface water, the level of concentration of zinc is usually 10mg/l. The permissible level of zinc in water is 5mg/l (WHO, 2022).

Microbial contaminants in water encompass a diverse array of pathogens, including enteric bacteria, protozoa, and viruses, which pose significant public health risks. Enteric bacteria, particularly coliforms such as *Escherichia coli*, are widely used as indicators of faecal contamination in water (U.S. Environmental Protection Agency [EPA], 2021). While many strains of *E. coli* are harmless, certain pathogenic strains can cause severe gastrointestinal illnesses. The presence of *E. coli* in water suggests the potential presence of other harmful pathogens, including Salmonella spp., Shigella spp., and Vibrio cholerae, which are responsible for diseases like cholera, dysentery, and typhoid fever (WHO, 2023). Other micro-organisms are *Giardia lamblia* and *Cryptosporidium parvum* (Opara and Nnodium, 2014). Occurrence of Klebsliella, *Escherichia coli* and Enterobacter species in water may point at the existence of medically significance pathogens such as *Salmonella*, *Clostridium pafrigen* and

protozoa e.g *Entamoeba histolytica* (Anyamene and Osiagu, 2014). Consumption of contaminated water with these pathogens results in diarrhea, giardiasis, dysentery and gastroenteritis among other implications (Isikwue and Chikezie, 2014; Oludairo and Aiyedun, 2016).

Enteric viruses, including rotavirus, norovirus, and hepatitis A virus, can be transmitted through contaminated water. These viruses are typically resistant to conventional water treatment methods and can cause a range of illnesses, from mild gastroenteritis to severe liver disease. The presence of these viruses in water is often associated with inadequate sanitation and water treatment practices (CDC, 2024).

The consumption of water contaminated with these microbial pathogens can lead to various health issues, particularly in vulnerable populations such as children, the elderly, and immunocompromised individuals. Infections can result in symptoms ranging from mild gastrointestinal discomfort to severe dehydration and even death if not properly managed. The WHO estimates that microbiologically contaminated drinking water can transmit diseases such as diarrhoea, cholera, dysentery, typhoid, and polio, causing approximately 505,000 diarrheal deaths each year (WHO, 2023).

In addition to traditional pathogens, emerging contaminants such as antimicrobial-resistant (AMR) bacteria pose new challenges to water safety. Recent studies have shown that AMR bacteria can persist in water sources, complicating treatment efforts and posing serious health risks (Izah and Ogwu, 2025). The presence of these resistant bacteria in water highlights the need for enhanced monitoring and treatment strategies to address this growing concern.

Furthermore, environmental factors play a crucial role in the prevalence and persistence of waterborne pathogens. Climatic conditions, soil characteristics, and water quality parameters can influence the survival and transmission of these microorganisms. Understanding these environmental influences is essential for developing effective water quality management practices (Wang *et al*., 2023). The presence of microbial contaminants in water remains a significant public health issue. Ongoing research and monitoring are essential to identify emerging pathogens, understand environmental

influences, and develop effective strategies to ensure safe drinking water for all populations.

2.3 Structural and Elemental Analysis of Corn-cob

2.3.1 Powder X-ray diffraction

X-ray Diffraction is used to probe internal crystalline and amorphous structure of corn-cob by analysing how the X-rays are diffracted by the atoms in the material. The theory is based on Bragg's law, where X-rays of a specific wavelength (λ) diffract at certain angles (θ) when they encounter planes of atoms separated by distance (d). The resulting resulting pattern of peaks and troughs is then analysed to identify the materials atomic arrangement and crystallinity. For corn-cob this helps to understand its fundamental structure and how it becomes more crystalline after treatment (Assirey and Altamimi, 2021).

2.3.2 X-ray Fluorescence

XRF is an elemental analysis technique used that is capable of analysing and even quantifying elements in the sample. The specific X-ray photons produced in the sample have specific energy which get absorbed on the way to the detector by other atoms in the sample (Palmer, 2022).

The analytical results, therefore, depends on the energy of the elements of interest and the sample state. XRF is non-destructive when the sample can be analysed without any sample preparation. Additionally, XRF can also be used to determine the chemical composition of a wide variety of sample states including solids, liquids and powder. It can also be used to determine the thickness and composition of layers and coating and is effective for rapid screening. XRF analysis is known for high precision and accuracy with fast sample preparation. No solvents are necessary since the samples don't need to be dissolved into a liquid or to have been diluted (Palmer, 2022). However, XRF is an elemental analysis technique and therefore quantifies the total concentration of each element in a sample. XRF can't distinguish between different oxides (Palmer, 2022).

2.4 Adsorption Mechanisms for Water Remediation Using Agricultural Wastes, Kinetics, and Isotherms

2.4.1 Adsorption

Adsorption is the transfer of ions from water to the solid that is from solution phase to the solid phase. Adsorption actually describes a group of processes which include adsorption and precipitation reactions. Adsorption recently has become one of the alternative treatment techniques for surface water laden with heavy metals (Abasi *et al*., 2011). Basically, adsorption is the mass transfer process by which a substance is transferred from the liquid phase to a surface of a solid and becomes bound by physical or chemical interactions (Barakat, 2011).

2.4.1.1 Factors influencing the adsorption of heavy metals

Adsorption of heavy metals from aqueous solutions depends on a number of factors. Factors which were investigated in this study were: Ph, temperature, contact time, initial metal ion concentration and adsorbent dosage which are briefly discussed below.

2.4.1.1.1 Effects of adsorbent dosage

Adsorption of metal ions from aqueous solution is affected by the adsorbent dose. Such that as adsorbent dose increased the rate of adsorption also increased. Increasing the adsorption dosage increases the surface area which makes it possible for more metal ions to be adsorbed.

2.4.1.1.2 Effects of initial metal ion concentration

Initial metal ion concentration also affects adsorption. At low concentration of metal ion there is a high percentage removal of metal ions by the adsorbent, this is explained by the fact that as concentration increases there is saturation of the adsorbent sites leading to low metal uptake (Genson *et al*., 2012). Thus, increase in metal ion concentration leads to decrease in percentage removal of metal ions from aqueous solution.

2.4.1.1.3 Effects of temperature

Temperature also affects adsorption of metal ions. The percentage removal efficiency decreases with increase in temperature. At low temperature the adsorption capacity is very high which may imply that the adsorption of metal ions is exothermic

(Viraraghavan and Kapoor, 1995). In any chemical reaction, increasing temperature enables the equilibrium to be attained within a short time.

2.4.1.1.4 Effects of contact time

The effects of contact time on the removal of metals to reach equilibrium varies with the type of metals. Increase in time increases the more amount of metal gets adsorbed onto the surface of the adsorbent and surface available decreases. The adsorbate, normally forms a thin one molecule thick layer over the surface. When this monomolecular layer covers the surface, the capacity of the adsorbent is exhausted (Satya *et al*., 2012).

2.4.1.1.5 Effects of pH

The pH of solution significantly affects the adsorption capacity of the adsorbent by modifying its surface, availability of functional groups and overall properties (Iftekhar *et al*., 2018). Depending on a specific metal ion and its interaction with the adsorbent may enhance or diminish the adsorbent capacity on metal ion.

2.4.2 Application of Agricultural Wastes in Water Remediation

Prevention and remediation of water pollution is the main aim and objective of modern environmentalists. Different agricultural wastes have been used to develop the best adsorbents for removal of water pollutants (Dai *et al*., 2018). These agricultural wastes, include: crop residues, husks, shells, and peels as they are cheap, requires less energy, show high removal efficiency and are easily available. These wastes are mainly composed of polysaccharides (cellulose, hemicellulose), lignin and smaller amounts of pectin substances (Sun, 2010), which enhance their capacity to adsorb contaminants from water.

Several studies have demonstrated the effectiveness of agricultural wastes in removing heavy metals, dyes, and organic pollutants from aqueous solutions. For instance, rice husk, banana peel, coconut shell, and sugarcane bagasse have been reported to efficiently adsorb lead, cadmium, chromium, and methylene blue from wastewater (Nguyen et al., 2019; Kumar et al., 2020). Experimentally corn cob, stalk, grain and seedling have been used as adsorbent. It gives a better economy and has other properties

which are favourable for water purification. Corn is a fibrous material and consists of fibre like hemicelluloses, cellulose and lignin. The waste corn cob as a material possesses some filtration properties and excellent bio-adsorbent through activation process (Christica *et al*., 2018).

Agricultural wastes are also environmentally friendly alternatives to conventional adsorbents such as activated carbon, which are often expensive and require energy-intensive production processes. The use of these wastes not only provides a value-added application for biomass residues but also reduces environmental pollution caused by their disposal (Foo & Hameed, 2012). However, it has been found out that adsorption is one of the best methods for water pollution remediation because it is environmentally friendly, economical and efficient.

Moreover, the adsorption capacity of agricultural wastes can be enhanced through simple chemical or physical modifications, including acid or base treatment, carbonization, or impregnation with functional groups, which improve surface area, poe structure, and active binding sites (Gupta and Suhas, 2009). This versatility makes agricultural wastes a promising material for sustainable and cost-effective water treatment technologies.

2.4.3 Method of Preparation of Corn-cob Derived Carbon Powder

According to the method described by Jawad *et al*., 2018, corn-cob derived carbon powder can be prepared by a multi-step process involving dehydration, carbonization and activation. The corn-cobs are first dried and crushed then heated to high temperature (carbonization) to form a carbonize material. This material is then subjected to chemical activation using agents like KOH, nitric acid or physical activation using gases like carbon (iv) oxide. It is followed by washing and drying. In this study a modification of the method described by was done (Jawad *et al*., 2018).

2.4.4 Adsorption Kinetics

Adsorption kinetics describe the rate at which a solute (adsorbate) is transferred from the aqueous phase to the solid adsorbent. Both linear and nonlinear analyses are used to fit kinetic models, and goodness-of-fit criteria are applied to determine which model best represents the adsorption process (Musah *et al*., 2018).

2.4.4.1 Pseudo First Order Model

The pseudo-first-order model assumes that the rate of adsorption is proportional to the difference between the equilibrium adsorption capacity (q_e) and the amount adsorbed at time *t* (q_t):

$$\log(q_e - q_t) = \log(q_e) - \frac{k_1}{2.303} t \qquad eqn\ 1$$

where,

q_e = adsorption capacity at equilibrium (mg/g)

q_t = adsorption capacity at time t (mg/g)

k_1 = pseudo-first-order rate constant (1/min)

When the values of Log (q_e-q_t) are correlated linearly with t. The plot of Log (q_e-q_t) versus t gives a linear relationship from k_t and q_e can be determined from the slope and the intercept of the plot.

2.4.4.2 Pseudo Second Order Model

This model assumes that the rate of solute sorption is directly proportional to the number of available uptake sites on the adsorbent. The reaction depends on the quantity of solute attached to the surface of the adsorbent.

The adsorption kinetics rate equation for pseudo second order is expressed in linear form (Ademiluyi and Nze, 2016; Ebelegi *et al*., 2020).

$$\frac{t}{q_t} = \frac{1}{k_2\, q_e^2} + \frac{t}{q_e} \qquad eqn\ 2$$

where,

t = time/duration that has passed since the reaction began

q_e = adsorption capacity at equilibrium

q_t = adsorption capacity at time t

k_2 = pseudo-second-order rate constant (g/mg·min)

If the initial rate of adsorption, h ($mg.g^{-1}\cdot min^{-1}$) is defined as:

$$h = k_2 q_e^2 \qquad \text{eqn 3}$$

Where,

h = initial rate of adsorption

k_2 = pseudo-second-order rate constant (g/mg·min)

q_e = adsorption capacity at equilibrium

Then substituting *h* into equation 2 yields:

$$\frac{t}{q_t} = \frac{1}{h} + \frac{t}{q_e} \qquad eqn\ 4$$

Where,

t = time/duration that has passed since the reaction began

q_e = adsorption capacity at equilibrium

q_t = adsorption capacity at time t

h = initial rate of adsorption

The plot of [t/qt] and t in equation 4 gives a linear relationship whose slope and intercept can be used to determine q_e and k_2 respectively (Edet and Ifelebuegu, 2020)

2.4.5 Adsorption isotherms

Adsorption isotherms describe how solutes interact with adsorbents at equilibrium. Commonly used models include empirical isotherms such as Freundlich and Langmuir (Goldberg *et al*., 1993)

2.4.5.1 Freundlich adsorption isotherm

Unlike the Langmuir isotherm, this empirical model can be used for multilayer adsorption on heterogeneous sites. It assumes that the adsorption heat distribution and affinities toward the heterogeneous surface are non-uniform (Foo and Hameed, 2009). The mathematical model can be shown as

$$q_e = bC_e^{1/n} \qquad eqn\ 5$$

where,

b = adsorption capacity (L/g)

1/n = adsorption intensity or surface heterogeneity

q_e = adsorption capacity at equilibrium

C_e = equilibrium concentration of the adsorbate in solution

When 0 < 1/n < 1, adsorption is considered favourable. Unfavourable adsorption occurs when 1/n > 1 and is irreversible at 1/n = 1.

The linearized form can be written as

$$lnq_e = lnb + \frac{1}{n} lnC_e \qquad eqn\ 6$$

Where,

b = adsorption capacity (L/g)

1/n = adsorption intensity or surface heterogeneity

q_e = adsorption capacity at equilibrium

C_e = equilibrium concentration of the adsorbate in solution

A plot of ln q_e versus ln Ce produces a straight line with a slope = 1/n and intercept = ln b.

2.4.5.2 Langmuir Isotherm

The Langmuir isotherm was initially developed for gas–solid interaction but is also used for various adsorbents. It is an empirical model based on kinetic principles; that is, the surface rates of adsorption and desorption are equal with zero accumulation at equilibrium conditions (Elmorsi, 2011). Based on the following assumptions, (a) monolayer adsorption, (b) homogeneous sites, (c) constant adsorption energy, and (d) no lateral interaction between the adsorbed molecules, the Langmuir isotherm can be written as:

$$q_e = \frac{q_0 K_L C_e}{1 + K_L C_e} \qquad eqn\ 7$$

Where,

qo is the maximum amount of adsorbed surfactant in mg/g

KL is the Langmuir constant in L/mg.

q_e = adsorption capacity at equilibrium

C_e = equilibrium concentration of the adsorbate in solution

The linearized version of equation is

$$\frac{C_e}{q_e} = \frac{1}{K_L q_0} + \frac{C_e}{q_0} \qquad eqn\ 8$$

A plot between C_e/q_e versus Ce generates a straight line with a slope of $1/q_o$ and an intercept equals to $1/K_L q_o$

2.5 Analytical Procedure for Determination of Heavy Metals and Anions

2.5.1 Atomic Absorption Spectroscopy

Atomic absorption Spectroscopy (AAS) is one of the analytical techniques utilized for quantitative analysis of trace metals. The technique is applicable directly to some elements including some metalloids. This technique is essentially solution based with only very limited application for the direct analysis of solids or gases. AAS technique depends on the interpretation of atomic spectra and quantification interaction between atoms and energy, which causes electronic transitions (Welz and Sperling, 2008). Electrons within an atom can occupy only discrete levels. Electron transitions between such levels give rise to atomic spectra. When an atom is in its lowest energy level, it is said to be in its ground state. In their ground state, atoms absorb radiation of their specific wavelength and get excited to higher energy levels.

In a case of steady states m and n, associated with energies Em and En, where En > Em the transition m→n will result in the absorption of light of frequency v_{mn} which is given by the Plank's equation,

$$v_{mn} = \frac{E_n - E_m}{h} \qquad eqn\ 9$$

where,

h is the Plank's constant (6.626×10^{-34} J·s)

Em, En = energies of the ground and excited states, respectively

The transitions m →n is simulated by absorption of external radiation. This forms the integral part of atomic absorption. The relationship between the ground-state and excited state population at a given temperature is given by the Maxwell-Boltzman distribution (Welz and Sperling, 2008);

$$\frac{N_n}{N_m} = \frac{G_n}{G_m} exp\left(-\frac{E_n - E_m}{kT}\right) \qquad eqn\ 10$$

where,

Nm = Number of atoms in ground state

Nn = Number of atoms in the excited state,

Gn /Gm = ratio of statistical weights for ground and excited states,

Em– En= Energy of excitation,

k = Boltzmann constant (1.38×10^{-23} J/K),

T =Thermodynamic temperature.

From equation (2) above, it can be seen that the ratio Gn / Gm is dependent upon both the excitation energy and temperature T. Calculations show that only a small fraction of the atoms is excited, even under very favourable conditions, that is when the temperature is high and the excitation temperature low (Welz and Sperling, 2008). Absorption by atoms takes place within very narrow spectral regions of the order of hundredths of angstrom.

In the laboratory analytical experiments, absorptions involving the ground state are observed. These absorptions are normally referred to as resonance lines. The absorptions of most elements are simple in character and less prone to inter element interference than is flame emission spectroscopy (Welz and Sperling, 2008).

The degree of absorption of specific radiation a particular frequency by an atomic vapor is related to the path traversed and to the concentration of the absorbing atoms in the vapor. This is described by the Beer – Lambert law (Welz and Sperling, 2008). When incident radiation of power P0, passing through a solution of an absorbing species at concentration and path length b, and the emergent radiation has radiant power P, then absorbance is given by;

$$\mathrm{A} = \log\frac{\mathrm{P_0}}{\mathrm{P}} = \varepsilon \mathrm{bc} \qquad \text{eqn } 11$$

A = absorbance

a = absorptivity

b = path length in centimetres and

c = concentration

Absorbance is directly proportional to the concentration (Welz and Sperling, 2008) and thus by measuring absorbance, concentration can be determined. The relationship discussed is linear for small values of absorbance. Beer's law is obeyed over a wide range except at very high concentrations (Welz and Sperling, 2008).

2.5.2 Theory of UV-Visible Spectrophotometry

Spectrophotometry is a method to measure how much a chemical substance absorbs light by measuring the intensity of light as a beam of light passes through a sample solution. The basic principle is that each compound absorbs or transmits light of a certain range of wavelength (Perkampus, 2013). UV-visible spectrophotometer uses light over the ultraviolet range (185-400 nm) and visible range (400-700 nm) of electromagnetic radiation spectrum (Perkampus, 2013). A spectrometer produces a desired range of wavelength of light, first a collimator (lens) transmits a straight beam of light (photons) that passes through a monochromator (prism) to split it into several component wavelengths (spectrum). Then a wavelength selector transmits only the desired wavelengths. After the desired range of wavelength of light passes through the solution of a sample in cuvette, the photometer detects the amounts of photons that is absorbed and then sends a signal to a digital display (Perkampus, 2013).

CHAPTER THREE
MATERIALS AND METHODS

3.1 Study Site

Nguue spring is located in Tharaka-Nithi County, Maara sub-county, Mwimbi ward, Iruma location and Iruma sub-location with coordinates between latitude 00º 13´and 00º 6´ South and between longitude 37º 40´and 37º 46´ East. River Mutonga is shared among Meru County and Tharaka-Nithi County with coordinates between 00º 25´ and 00º 49´South and between longitude to 37º 56´ and 37º 13´ East. Tharaka-Nithi latitude County borders the Counties of Embu to the South and South West, Meru to the North and North East, Kirinyaga and Nyeri to the West and Kitui to East and South East. The County has two ecological zones that is the highland (upper zone) and the semi-arid (lower zone). "The highland region, comprising Maara and Chuka, experiences rainfall ranging from about 500 mm to approximately 2,200 mm in the lower Tharaka zone and in the Chogoria forest repectively, with the highland being highly suitable for agriculture. The temperature in the highland ranges between 14 ºC to 30 ºC. The soils in the study area are generally characterized by low clay content, low organic matter, poor biological activity, high acidity, and limited weatherable minerals, making them highly susceptible to erosion. Vegetation varies with altitude, where deciduous montane forests dominate the highland areas, while dry forests with shrub vegetation are more common in the low-lying zones. Agriculture remains the main economic activity, with both crop and livestock production being practiced. The climate supports the cultivation of diverse crops such as tea, coffee, maize, cowpeas, pigeon peas, tobacco, sorghum, millet, green grams, black beans, and bananas, among others. In contrast, the county is not well endowed with mineral resources, with sand, building bricks, and ballast being the most commonly exploited.

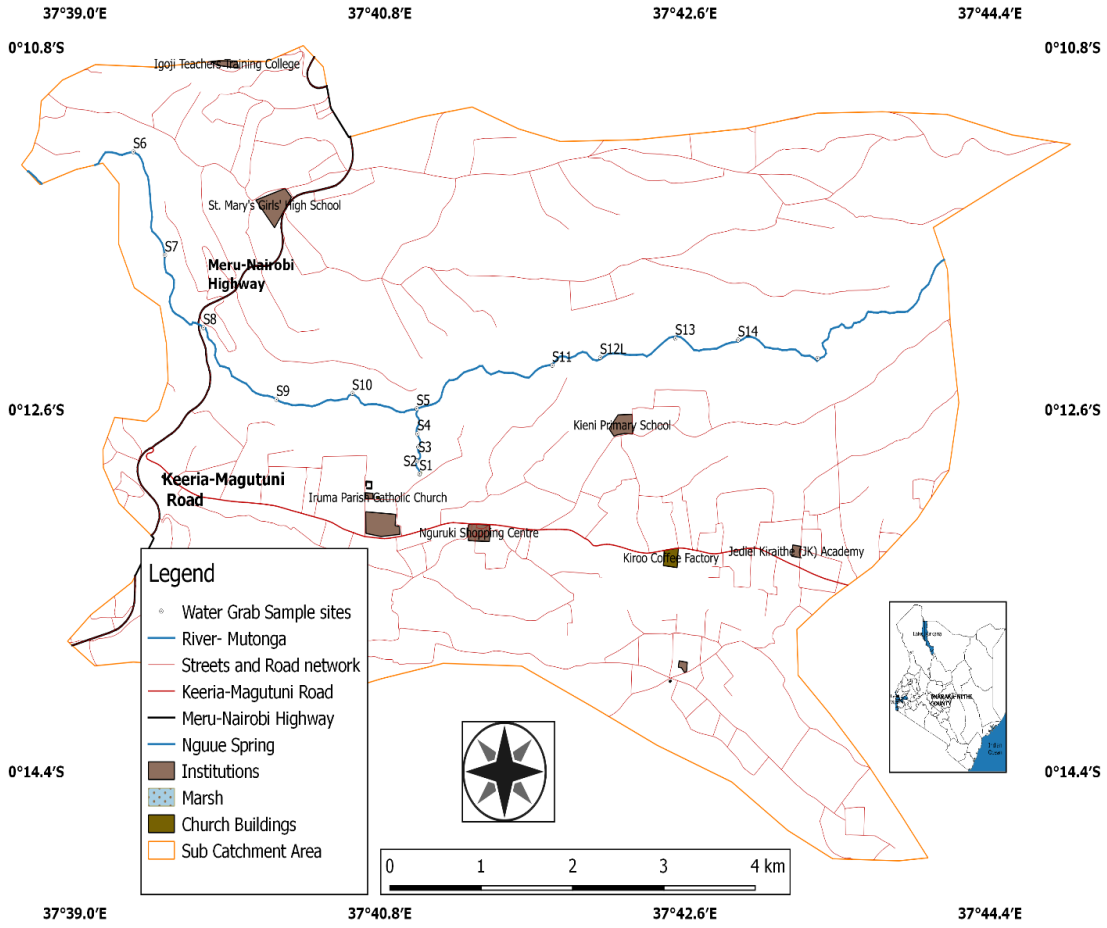

Figure 1: Map of Kenya showing Tharaka-Nithi County and location of Nguue spring and Mutonga river study area. High-resolution map showing river, spring, boundaries, scale bar and north arrow

3.2 Research Design

The study adopted a quasi-experimental research design to investigate the physico-chemical and microbial parameters of water samples, and adsorption characteristics of the corn-cob. This design was appropriate since it allowed for controlled laboratory experiments on adsorption parameters while utilizing field-collected samples. This design enabled the answering of research questions.

3.3 Chemicals and Materials

The chemicals that were used in the experiment were of high analytical purity which included: Nitric acid (68%, IndiaMART), Hydrochloric acid (35%, Loba chemie), Ammonium chloride (99%, Span chemie), Chloroform (99%, Pallar) Magnesium chloride (98%, Laba chemie), EDTA (99%, Sigma Aldrich), Ammonia aqueous

(25%w/w, Kenya Chemicals), deionized water (99%, Harris Chemical laboratories), Aluminium foil (Alu foil supplier), isopropanol (95%, Echem), Eosin Methylene Blue Agar, Levine(EMB, 99% , Himedia), Nutrient Agar (99%, Srichem), Lactose Broth (99%, Srichem), Brilliant Green Bile Broth 2% (99%, Biomark laboratories, India), Gram staining kit (Thermo Fischer scientific), Ethanol (99%, Merck), Potassium bromide(99%, Merck) Whatman filter paper No.1(Echem), Hydrazine sulfate (98%, Sigma Aldrich), Ammonium molybdate (99%, Rankem), Eriochrome Black T (99%, Sigma-Aldrich), pH 10 buffer (99%, Thermo Fisher Scientific) Phosphate dihydrogen orthophosphate (99%,Central Drug House ltd, India) and corn cobs (*Zea mays*) collected from rural area in Meru.

3.4 Data Collection

Water samples were collected from both the river and the spring in the study area during dry and wet seasons in the months of September and November 2024 respectively. Six sampling points were identified along the river and an equal number from the spring, with the sampling points being approximately five hundred metres apart. Primary data were generated from laboratory analyses of the collected samples. Physico-chemical and microbial properties were determined, and adsorption studies were conducted under varying experimental conditions guided by the independent variables.

3.4.1 Collection of Samples

Water was sampled using the standard methods for examination of water and wastewater (APHA, 2005). Water samples were collected in clear 500 ml polypropene bottles which was washed with one molar concentrated nitric acid rinsed with deionized water and preserved with a 0.2M nitric (v) acid to immobilize the metals against surface adsorption. Before collection of samples the bottles were then rinsed with sample water. There were six sampling points which were five hundred metres apart. Water samples were collected from the river and the spring from either side and at a depth of about 30 cm. Sampling of the spring and river was done during the dry and wet seasons in the months of September and November 2024 respectively. A random sampling was used to collect the spring and the river water in order to obtain a representative sample. Treated glass bottles were used to collect samples required for determination of dissolved oxygen.

Samples for microbial analysis were collected using sterile techniques to minimize contamination and maintain the integrity of the microbial community. The samples were packed in icebox and transported to Chuka University laboratory for analysis within 24 hours. The assortment of volumetric glassware used in the experiment was presterilized in autoclave at 121ºC for 15 minutes prior to analysis.

3.4.2 Physical Parameter Analysis

3.4.2.1 Determination of Water Temperature

Temperature was measured using a MKlab-900 multi-parameter meter (with a range of temp of -10 to 100 ºC). The temperature probe was immersed in water to a depth of 10 cm allowed to stabilize and temperature read in degrees Celsius (WHO, 2009).

3.4.2.2 Determination of water pH

Water pH was determined using a MKlab-900 multi-parameter meter with a temperature compensation of up to 25 ºC. The pH probe was immersed in water to a depth of 10 cm, allowed to stabilize and the pH read directly and recorded (APHA, 2005).

3.4.2.3 Determination of Water Electrical Conductivity

The electrical conductivity was examined using a MKlab-900 multi-parameter meter and temperature compensation of up to 25 ºC. The conductivity probe was immersed in water to a depth of 10 cm, allowed to stabilize and conductivity read in micro- Siemens per centimetre (µs/cm) (WHO, 2009).

3.4.2.4 Determination of Water Dissolved Oxygen (DO)

The dissolved oxygen was measured using a MKlab-900 multi-parameter meter. The DO probe was immersed in water to a depth of 10 cm while stirring the water. The readings were allowed to stabilize and dissolved oxygen read in mg/l (WHO, 2009).

3.4.2.5 Determination of Total Dissolved Solids in Water

TDS was determined with a MKlab-900 multi-parameter meter. The TDS probe was immersed in water to a depth of 10 cm while stirring the water. The readings were allowed to stabilize and total dissolved solids was read in ppm. (WHO, 2009).

3.4.2.6 Determination of Total Hardness in Water

The burette was filled with 0.01M EDTA solution. 50 ml of water samples was transferred into a 250 ml conical flask. 5 ml of Ammonia buffer was added followed by 2 drops of Eriochrome Black T indicator. The above content was titrated against EDTA solution in the burette. Endpoint was determined when colour changed from wine red to blue. Titration was repeated twice until concordant value was achieved. Total hardness was then estimated using the following expression.

$$\text{Total Hardness} = \frac{\text{Volume of EDTA consumed}}{\text{Volume of hard water taken}} \times 1000\text{ppm}$$

The results were interpreted as shown in Table 1

Table 1 Displaying interpretation of water hardness

Total hardness concentration in mg/l (ppm)	Interpretation
0-90	Soft
91-180	Medium Hard
181-270	Hard
>270	High Hardness

Source: (Mora, 2000)

3.4.3 Analysis of Cations

3.4.3.1 Digestion of Samples

Water samples intended to be analysed were prepared by filtering through Whatman No. 1 filter paper just before analysis and then preserved immediately to a pH < 2 by adding 1.5 ml concentrated nitric acid per litre to minimize precipitation that would occur and adsorption of cations on the walls of the container. The acidified samples were then refrigerated at approximately 4 ^{0}C to prevent change in the volume due to evaporation. The preserved water samples were digested in order to reduce the organic matter and convert metals associated with particulates into free form that can be analysed by Atomic Absorption Spectroscopy (AAS).

3.4.3.2 Elemental Analysis

The stock and the standard solutions of the cations (zinc and iron) were prepared using respective analytical grade soluble salts. The samples were then analysed by the standard calibration method using the AA-7000 Shimadzu- Atomic Absorption

Spectrophotometer (MTRD). The respective wavelengths were employed for determination of metals were Fe at 248.7 nm and Zinc at 213.9 nm.

3.4.4 Analysis of Anions

3.4.4.1 Analysis of Nitrates Using Spectrophotometric Method

The nitrate concentration in spring and river water samples were determined by UV spectrophotometric method, at a wavelength of 220 nm and 275 nm. The samples were treated by adding 1 ml of 1N HCl solution to a 50 ml clear sample and mixed thoroughly. The standard curve was prepared in the range of 0-7.0 mg/l nitrate by diluting to 50ml the following volume of working nitrate solution 0, 4, 8, 12, 16, 20, 24, 28 and 32 ml in 100 ml volumetric flask, 1.0 ml of 1N HCl solution was added to all the standards and the blank made up to mark and mixed thoroughly. Spectrophotometric measurement was done using UV Visible NIR spectrophotometer where the wavelength of 220 nm was set for reading of nitrate. It was set at zero with blank (distilled water and HCl). Absorbance was read with all standard solutions and blank at 220nm and at 275nm to determined interference due to dissolved organic matters. Then a standard curve was constructed by plotting absorbance against various nitrate concentrations and blank.

The UV Visible NIR spectrophotometer was set at zero with blank standard solution. Absorbance reading of samples was taken at 220nm wavelength and simultaneously at 275nm absorbance due to nitrate interference due to dissolved organic matter and distilled water was used as references.

3.4.4.2 Analysis of Phosphate

Phosphate concentration was determined by Molybdenum Blue Method and spectrophotometric method according to the standard method for examination of water and wastewater. The phosphate stock solution was prepared by weighing 1.3609g of potassium dihydrogen phosphate, in 1000 ml volumetric flask and distilled water added up to the mark. Phosphate standard solutions were prepared by serial dilution of stock solution ranging from 0.5-3.5 ppm. For ammonium molybdate, 1.7081g was accurately weigh and dissolved in 100ml warm distilled water to form a milky colouration. It was cooled and transferred in 250 ml volumetric flask and made up to the mark by double

distilled water. 0.125 g of hydrazine sulphate was accurately weighed and dissolved in a clean 100 ml volumetric flask and made up to the mark. The concentration of phosphate was determined with the help of calibration curve. To prepare a standard curve 20ml of standard solution (0.5-3.5 ppm) 10ml of ammonium molybdate and 4ml of hydrazine sulphate was was added in a clean 100 ml volumetric flask and using double distilled water the solution was made up to the mark . Then these flasks were kept for at least 30 minutes in a water bath for heating at 60 ℃. On heating, a blue colour was developed due to formation of phosphomolybdate complex and was cooled and the absorbance was measured using UV Visible NIR spectrophotometer at 860 nm. Distilled water was used as experimental blank solution. The analysis was carried out in triplicate (Pradhan and Pokharel, 2013).

Water samples were collected from the study site, and assigned serial number. Filtration of water samples was done using Whatmann-10 filter paper. In 40ml of water, 10ml of ammonium molybdate and 4ml of hydrazine sulphate was was added in a clean 100 ml volumetric flask and using double distilled water the solution was made up to the mark. Then these flasks were kept for at least 30 minutes in a water bath for heating at 60 ℃. On heating, a blue colour was developed due to formation of phosphomolybdate complex and was cooled and the absorbance was measured using UV Visible NIR spectrophotometer at 860 nm. Distilled water was used as experimental blank solution. The analysis was carried out in triplicate (Pradhan and Pokharel, 2013).

3.4.5 Microbial Analysis

3.4.5.1 Cultural Characterization

The microbial analysis was carried out using the Most Probable Number (MPN) technique. The working bench was disinfected by 70% ethanol before preparation of the culture medium. Lactose broth was prepared according to the manufacturer's instruction, covered in an Aluminium foil and sterilized in an autoclave at 121 ºC for fifteen minutes. The broth was then cooled in a water bath maintained at 60 ºC. Three sets of sterile test tube fitted with Durham's tube were prepared: one set containing 10 ml of double strength (DS) and two sets containing 10 ml of single strength (SS) broth each. Using sterile pipettes, 10 ml of water sample was transferred to each of the double strength broth tube. 1 ml of water samples was transferred to each of the three tubes of

one set of SS broth tube and in the remaining set of SS broth tube, 0.1 ml of water sample was transferred.

The tubes were incubated at 37 ºC in a Mermmett incubator for 24 hours and 44 ºC for faecal coliform and observed for gas production Gas production in in the Durham tubes and colour change in the broth form purple to yellow were used as indicators of positive results. Counts per 100 ml were calculated from MPN tables. Observations for gas production and colour change were made after both 24 and 48 hours. The number of positive tubes from each set was recorded and compared with standard charts to estimate the presumptive coliform count per 100 ml of the water sample. The MPN procedure was carried out in three steps: the presumptive test, confirmatory test and completed test.

Since microorganisms other than coliforms may also produce acid and gas from lactose fermentation, a confirmatory test was performed. A loopful of suspension from positive tubes was streaked onto Eosin Methylene Blue (EMB) agar plates, which were incubated at 37 ºC for 24 hours. Colonies exhibiting dark centres with a characteristic green metallic sheen were considered positive of the coliforms.

For the completed test, a suspected coliform colony from the EMB agar plate was inoculated into a tube with 3 ml of brilliant green bile broth with Durham's tube as well as onto the surface of nutrient agar slant. These were incubated at 37 ºC for 24 hours. Gas production in the broth confirmed coliform presence, and gram-staining was done on the nutrient agar slant to validate the bacterial identity.

3.4.5.2 Procedure for Gram staining

Gram staining was performed to differentiate bacterial isolates into Gram-positive and Gram-negative groups. Heat-fixed smears were first stained with crystal violet for 60 seconds, after which the excess stain was gently rinsed off with water. The smear was then treated with Gram's iodine solution for 60 seconds, serving as a mordant to form a crystal violet–iodine complex within the cells. Following rinsing with water, the smear was subjected to decolourisation using a mixture of ethanol and acetone applied dropwise until the runoff was clear, after which it was immediately rinsed to stop further

decolourisation. The smear was then counterstained with safranin solution for 60 seconds, rinsed again with water, and gently blotted dry using bibulous paper before microscopic examination (Popescu & Doyle, 1996).

3.5 Adsorption

3.5.1 Collection and Preparation of the Adsorbent

Corn-cobs (maize cobs), the raw material for adsorption studies, were sourced from rural area within Maara sub-county. The cobs were first cut into small pieces of approximately 2cm in length using a clean knife. The pieces were thoroughly washed with tap water followed by rinsing with distilled water to remove adhering dust, dirt and other extraneous matter. After cleaning, the maize cobs were sun-dried under ambient conditions until a constant weight was achieved, ensuring removal of surface moisture and preparing them for subsequent experimental procedures.

3.5.2 Carbonization Process

A total of 220 g of corn-cobs afforded 100g of charcoal, after thermal treatment in a furnace at 500 ℃ for 1 hour in absence of air, following the procedure described by Ademiluyi *et al*., (2007). The resulting charred material was then allowed to cool to room temperature before being transferred into a clean, airtight container for storage.

3.5.3 Chemical Activation

The carbonized material was crushed and sieved using 1.18 mm sieve mesh to obtain uniform particle sizes suitable for adsorption studies. The charred material was impregnated with 1M nitric acid in the ratio 2:3 and was soked for 24 hours. The soaked charr was stirred for 10 minutes for proper distribution of the acid. The impregnated charr was then subjected to heat treatment at 800 ºC for 1 hour, under limited oxygen conditions to enhance pore development and increase the surface area-to-volume ratio of the adsorbent. After thermal treatment, the activated carbon was cooled to room temperature and then washed thoroughly using distilled water to remove all traces of chmical agent. It was then stored in airtight containers for subsequent use. Nitric acid was selected as the activating agent since previous studies have shown its effectiveness in enhancing the adsorption capacity of carbon materials for metal ions (Ademiluyi and David-West, 2011).

3.5.4 Characterization of Maize Cob Powder

3.5.4.1 Structural Analysis Using X-Ray Diffraction Spectroscopy

The structural properties of the corn-cob carbon powder derived from maize cobs was analyzed using powder X-ray diffraction (XRD). Samples were ground into powder, loaded into glass-plate holders, and analyzed using a Rigaku Miniflex II desktop x-ray diffractometer. The diffraction patterns were obtained using Cu Kα (λ=1.540598 Å) radiation with a beam current of 15 mA and voltage of 30 kV. Data were collected over a scanning range of 10 ° to 80 ° at a scan speed of 2 ° min^{-1}, under operating conditions of 30kV and 15mA. The structures of the corn-cob were identified through a comparison of obtained diffraction data to standards from the Joint Committee on Powder Diffraction Standards (JCPDS).

3.5.4.2 Elemental Chemical Analysis using X-Ray Fluorescence Spectroscopy

The elemental composition of both activated and inactivated corn-cob carbon was determined using an X-ray fluorescence (XRF) spectrometer. The samples were first pulverized in air mode to ensure homogeneity before analysis. Instrument calibration was performed using the internal standard A750, an accessory provided with the equipment, and the detector was cooled by adding 2.5 litres of liquid nitrogen into the designated compartment.

Energy position checking on the A750 confirmed correct calibration, with the CuKα peak observed within 8.00-8.08 keV and the presence of SnLα, SnKα, AlKα and NiKα peaks validating the accuracy of the calibration process. For analysis, the pulverized samples were placed on the sample plate with the analysis face facing down, and the chamber was securely closed. After completion of the run, the results were displayed in the analysis window of the instrument, which provided both qualitative and quantitative data based on the detected spectra.

3.5.4.3 Determination of Adsorption Capacity

Metal ions, specifically iron and zinc, which are commonly found in surface water, were selected for this study. Different concentrations of these heavy metal ion solutions were prepared, and batch adsorption experiments were carried out using corn cob activated carbon. For each test, 100 mL of the mixed metal ion solution was treated

with 1 g of activated carbon, and the mixture was stirred to ensure proper contact. Adsorption was monitored at time intervals of 30, 45, 90, 120, 240, and 360 minutes until equilibrium was reached. At the end of each interval, the mixture was filtered through filter paper to remove residual carbon particles. The same procedure was repeated for various initial concentrations of the metal ion solutions, as well as for inactivated corn cob charcoal, in order to compare adsorption efficiency. From each filtrate, a 5 mL aliquot was diluted with 50 mL of 2% nitric acid, and the residual metal ion concentrations were analysed using an Atomic Absorption Spectrophotometer (AAS, Model 7000).

The adsorption capacity of the activated carbon at equilibrium was calculated using the following equation:

$$q_e = \frac{(C_0 - C_e)V}{m} \qquad \text{eqn 12}$$

where,

q_e = adsorption capacity at equilibrium (mg/g),

C_0 = initial concentration of metal ions (mg/L),

C_e = equilibrium concentration of metal ions (mg/L),

V = volume of the solution (L),

m = mass of the adsorbent (g)

3.5.5 Optimization of factors affecting dsorption of heavy metals

3.5.5.1 Optimization of Adsorbent Dosage

Effect of adsorbent dosage on adsorption of Zn^{2+} and Fe^{3+} was achieved by varying adsorbent dosage from 0.1 g, 0.2 g and 0.3 g for the all the adsorbent. 10mg/l of 50 ml solution was used for both metal ions. The mixture was shaken at a speed of 100 rpm for 1 hour and then centrifuged at a speed of 3800 rpm 20 min. The filtrate was decanted and analysed for remaining metal ions concentration using AAS.

3.5.5.2 Optimization of Metal Ion Concentration

The initial metal ion concentration for both Zn^{2+} and Fe^{3+} was varied using from 5, 10, 15, 20, 25 mg/l . 0.2 g of the adsorbent (corn-cob activated carbon and corn-cob charcoal), was added to 50 ml of the solution containing Zn^{2+} and Fe^{3+} at different concentration as stated above. The mixture was then shaken at a constant speed of 100

rpm for 1 hour. The smixture wa the centrifuged for 20 min at 3800 rpm and then decanted. The filtrate was then analysed for remaining metal ion concentration using AAS.

3.5.5.3 Optimization of Temperature

0.2g of the adsorbents were added to 10 mg/l to 50 ml of solution of both Zn^{2+} and Fe^{3+} solutions. The mixture was then shaken at a constant speed of 100 rpm for 1 hour. After the mixture was then centrifuged for 20 min at 3800 rpm and decanted. The filtrate was then analysed for remaining metal ions concentration using AAS.

3.5.5.4 Optimization of pH

A dosage amount of 0.2 g of corn-cob activated carbon and corn-cob charcoal was put in two different flasks. 50 ml of 10 mg/l solution of Zn^{2+} and Fe^{3+} ion at pH of 4, 6, 7, 8 and 10 was added. The mixture was then shaken for 1 hour at a constant speed of 100 rpm and then allowed to attain equilibrium. The mixture was centrifuged at a speed of 3800 rpm for 20 mins and decanted. The filtrate was analysed for remaining metal ions using AAS. The pH of solution was calibrated using pH meter with 50% concentrated nitric acid and sodium hydroxide solution.

3.5.5.5 Optimization of Contact Time

To determine equilibrium time for both Zn^{2+} and Fe^{3+}, batch experiment for both was carried out using two adsorbent corn-cob activated and corn-cob charcoal were used. 0.2 g of each adsorbent as mixed with 50 ml of solutions of both Zn^{2+} and Fe^{3+} at initial concentration 10 mg/l. The mixturewas then shaken at constant speed of 100 rpm for 1 hour at intervals aof 30 minutes for 120 minutes. The mixture was then centrifuged at a speed of 3800 rpm for 20 minutes. It was then decanted and the concentration of remaining metal ions was determined by AAS.

3.6 Data Analysis

The data obtained from the analysed physico-chemical and microbial parameters were summarized using descriptive statistics and presented in tables for clarity. These results were compared with the World Health Organization (WHO, 2010) and Kenya Bureau of Standards (KEBS, 2010) guidelines to determine compliance with acceptable limits.

Statistical analyses were performed using SAS software (Version 9.4). Analysis of variance (ANOVA) was employed to evaluate differences among treatments, and where significant differences were detected, mean separation was conducted using the Least Significant Difference (LSD) test at the 5% probability level. To assess seasonal variability, between the dry and wet seasons paired t-tests were applied at a 5% probability level. Prior to conducting ANOVA and t-tests, the underlying assumptions were verified. Normality of residuals was tested using the Shapiro–Wilk test, while homogeneity of variances was assessed using Levene's test. These checks ensured that the data met the assumptions required for valid parametric statistical inferences.

3.7 Ethical Consideration

Before the commencement of the research, ethical clearance was first obtained from the Chuka University Ethics Committee (CUEC) (Appendix I). Thereafter, a research permit was granted by the National Commission for Science, Technology and Innovation (NACOSTI) (Appendix II). To uphold research integrity, plagiarism and bias were strictly avoided, and all sources of information were duly acknowledged and cited in accordance with academic standards. Only original findings generated from this study are disseminated for purposes of knowledge sharing.

CHAPTER FOUR

RESULTS AND DISCUSSION

4.1 Physico-chemical and Bacteriological Parameter of Nguue Springs and River Mutonga in Dry and Wet season

4.1.1 Seasonal Variation in Physico-Chemical Parameters of River Mutonga and Nguue Springs

The physico-chemical characteristics of water samples collected from River Mutonga and Nguue Springs during the dry and wet seasons are presented in Tables 2 to 5, Appendices iii and iv .

Table 2 Physicochemical parameters for River Mutonga in dry season

Sample id	Temp (°C)	Ph	EC (µs)	TDS (mg/l)	DO (mg/l)	TH (mg/l)	Nitrates (mg/l)	Phosphates (mg/l)
M1	25.9±0	7.4±0.5	202±1	0.886±0.001	4.47±0.01	268±2	17.95±0	2.07±0
M2	26.0±0	7.1±0.001	182.6±0.1	0.869±0.001	3.5±0.01	216±2	16.57±0	2.10±0
M3	26.1±0	7.3±0.001	176±0.1	0.852±0.001	3.48±0.01	258±2	18.72±0	2.11±0
M4	26.4±0	7.3±0.001	173.3±0.1	0.848±0.001	3.32±0.01	176±2	19.35±0	1.95±0
M5	26.5±0	7.2±0.001	172.5±0.1	0.844±0.002	3.25±0.02	230±2	19.01±0	2.03±0
M6	26.6±0	7.1±0.003	170.8±0.1	0.838±0.001	3.19±0.01	190±2	19.05±0	2.12±0
Mean	26.25	7.23	179.53	0.856	3.535	223	18.442	2.063
SD	0.27	0.19	11.1	0.017	0.4460	34.29	1.033	0.064
KEBS 2015	-	6.5-8.5	2500	1500	-	500	10	2.2
WHO2022	-	6.5-7.4	400	<1000	>4	10-500	-	0.5

EC=Electrical conductivity, TDS= Total dissolved solids, DO= Dissolved oxygen, TH= Total hardness, SD= Standard deviation, M=Mutonga sampling points

In the dry season, River Mutonga recorded a temperature between 25.9-26.6 °C. The pH was in the range of 7.1-7.4 and this was in agreement within both (WHO, 2022) and (KEBS, 2015) permissible ranges (6.5–7.4 and 6.5–8.5, respectively). Electrical conductivity was (172.8-202 µS/cm) and total dissolved solids (0.838-0.886 mg/L) were considerably below the maximum allowable limits. Dissolved oxygen were in the range between 3.19-3.25 mg/l, however, was slightly lower than the WHO recommended minimum of 4 mg/L. Total hardness between 0.838-0.886 mg/L, falling within acceptable standards. Nitrate concentrations was between 16.57-19.35mg/L and exceeded the KEBS limit of 10 mg/L, while phosphate was between 1.95-2.12 mg/L slightly surpassed the WHO guideline of 0.5 mg/L but remained within KEBS limits (2.2 mg/L).

Nguue Spring during the dry season exhibited a temperature of 25.9-26.5 °C, (Table 3, Appendix iii). The pH was (5.21-6.58) was marginally below the WHO lower limit

(6.5) in sampling point N5, indicating slight acidity. Electrical conductivity was (147.6-193.6 µS/cm) and total dissolved solids (0.552-1.2 mg/L) were far below the permissible levels. Dissolved oxygen ranged between 2.61-6.24 mg/L, with sampling point N1 just above the WHO minimum. Total hardness was relatively low (58-160 mg/L), well within the acceptable range. Similar to Mutonga River, nitrate levels (16.83-19.47 mg/L) exceeded KEBS standards, while phosphate was (2.03-2.09 mg/L) was above the WHO threshold but within KEBS limits.

Table 3 Physicochemical parameters for Nguue spring in dry season

Sample	Temp (°C)	pH	EC (µs)	TDS (Mg/l)	DO (Mg/l)	TH (Mg/l)	NO_3^- (mg/l)	PO_4^{3-} (mg/l)
N1	26.4±0	6.08±0.01	193.6±1	1.2±0.001	6.24±0.01	124±2	19.47±0	2.09±0
N2	26.5±0	6.43±0.01	157.0±1	0.651±0.001	2.61±0.01	160±2	19.09±0	2.03±0
N3	26.5±0	6.38±0.01	149±1	0.640±0.001	4.39±0.01	60±2	16.83±0	2.07±0
N4	26.2±0	6.58±0.01	147.6±1	0.552±0.001	3.61±0.01	58±2	16.83±0	2.12±0
N5	26.0±0	5.21±0.01	181.3±1	0.806±0.001	2.62±0.01	159.32±	18.1±0	2.08±0
N6	25.9±0	6.20±0.01	185.6±1	0.83±0.001	4.62±0.01	157±2	18.6±0	2.04±0
Mean	26.25	6.690	174.28	0.7812	4.015	119.722	18.153	2.0717
SD	0.2588	0.4914	20.17	0.2318	1.381	48.94	1.124	0.033
WHO 2022	-	6.5-7.4	500	<1000	>4	10-500	45-100	0.5
KEBS 2015	-	6.5-8.5	2500	1500	-	500	10	2.2

EC=Electrical conductivity, TDS= Total dissolved solids, DO= Dissolved oxygen, TH= Total hardness, SD=Standard deviation, N= Nguue sampling piont

In the wet season, River Mutonga recorded a lower temperature of (21 °C) compared to the dry season (Table 4, Appendix iv). The pH was (5.973-6.288) fell below both WHO and KEBS permissible ranges 6.5-7.4 and 6.5-8.5 respectively, indicating increased acidity in sampling point M1. Electrical conductivity (57.2-60.4 µS/cm) and total dissolved solids (31.3-36.6 mg/L) were markedly lower than in the dry season, reflecting dilution effects of rainfall. Dissolved oxygen was (8.72-8.92 mg/L) increased substantially and was well above the WHO minimum standard 4.0 mg/l. Total hardness decreased to (87.3-122) mg/L but remained within permissible limits. Nitrate levels dropped to (7.25-12.35) mg/L, now falling within KEBS standards which is 10 mg/l, while phosphates was (2.01-2.29 mg/L) remained above WHO limits (0.5 mg/l) but acceptable under KEBS (2.2mg/l).

Table 4 Physico-chemical parameters of river Mutonga in wet season

Sample	Temp (ºC)	Ph	EC (µs)	TDS (Mg/l)	DO (Mg/l)	TH (Mg/l)	NO_3^- (mg/l)	PO_4^{3-} (mg/l)
M1	21±0	5.973±0.001	57.2±0.1	36.1±0.1	8.72±0.01	108±1	9.15±0	2.01±0
M2	21±0	6.080±0.001	57.6±0.1	32.5±0.1	8.91±0.01	87.3±1	7.25±0	2.02±0
M3	21±0	6.033±0.001	58.1±0.1	31.3±0.1	8.87±0.01	120±1	7.98±0	2.24±0
M4	21±0	6.259±0.001	58.8±0.1	34.9±0.1	8.83±0.01	96±1	9.02±0	2.27±0
M5	21±0	6.280±0.001	59.2±0.1	33.5±0.1	8.873±0.01	122±1	11.67±0	2.26±0
M6	21±0	6.288±0.001	60.4±0.1	34.43±0.1	8.92±0.01	116±1	12.35±0	2.29±0
Mean	21	6.152	58.55	33.788	8.854	108.2	9.57	2.182
SD	0	0.14	1.17	1.73	0.073	13.97	2.03	0.13
WHO 2022	-	6.5-7.4	500	<1000	>4	10-500	45-100	0.5
KEBS 2015	-	6.5-8.5	2500	1500	-	500	10	2.2

EC=Electrical conductivity, TDS= Total dissolved solids, DO= Dissolved oxygen, TH= Total hardness, SD= Standard deviation, M=Mutonga sampling points

Nguue Spring in the wet season showed a temperature of 20.5-21 °C (Table 5, Appendix iv). The pH was(4.210-5.724) was consistently below both WHO and KEBS ranges, suggesting acidic conditions. Electrical conductivity was (37.8-55.6 µS/cm) and total dissolved solids (27.7-59.5 mg/L) decreased compared to the dry season, reflecting rainwater dilution. Dissolved oxygen was (8.58-8.86 mg/L) was significantly elevated and met WHO standards. Total hardness was (22.6-84 mg/L) remained within permissible limits. Nitrate concentration was (7.8-14.65 mg/L) was marginally above the KEBS guideline, while phosphate was (1.95-2.23 mg/L) exceeded WHO standards but was acceptable under KEBS.

Table 5 Physico-chemical parameters of Nguue spring in wet season

Sample	Temp (ºC)	Ph	EC (µs)	TDS (Mg/l)	DO (Mg/l)	TH (Mg/l)	NO_3^- (mg/l)	PO_4^{3-} (mg/l)
N1	21±0	5.231±0.001	55.6±0.2	32.5±0.1	8.86±0.01	84±2	7.8±0	2.04±0
N2	21±0	5.588±0.001	51.6±0.2	29.9±0.1	8.83±0.01	64±2	9.39±0	2.11±0
N3	21±0	5.561±0.001	51.2±0.2	27.7±0.1	8.78±0.01	64±2	9.21±0	1.95±0
N4	20.5±0	5.724±0.001	45.5±0.2	57.5±0.1	8.72±0.01	22.6±2	9.14±0	2.23±0
N5	20.5±0	4.344±0.001	38.7±0.2	59.5±0.1	8.61±0.01	32.0±2	14.65±0	2.03±0
N6	20.5±0	4.210±0.001	37.8±0.2	58.6±0.1	8.58±0.01	42±2	13.28±0	2.01±00
Mean	20.75	5.110	46.73	44.28	8.731	51.4	10.58	2.062
SD	0.274	0.666	7.333	15.67	0.115	23.13	2.718	0.097
WHO 2022	-	6.5-7.4	500	<1000	>4	10-500	45-100	0.50
KEBS 2015	-	6.5-8.5	2500	1500	-	500	10	2.20

EC=Electrical conductivity, TDS= Total dissolved solids, DO= Dissolved oxygen, TH= Total hardness, SD= Standard deviation, N=Nguue spring sampling points

Overall, results show that both River Mutonga and Nguue Springs experience seasonal variations in physico-chemical parameters. Higher temperatures, electrical conductivity, and nitrate levels were observed in the dry season, while pH decreased and dissolved oxygen increased in the wet season. Importantly, nitrate and phosphate concentrations often exceeded WHO (2022) thresholds, raising potential concerns for water quality and public health. Moreover, the results showed clear seasonal variation in the measured physico-chemical parameters of water quality, with most parameters exhibiting higher mean values during the dry season compared to the wet season (Figure 2). This suggests that seasonal changes influenced the concentration and distribution of these parameters, potentially due to reduced dilution effects and increased evaporation during the dry period. The observed trends highlight the importance of considering seasonal dynamics when assessing water quality status. The results obtained were in agreement with those reported by Adongo *et al*., 2022.

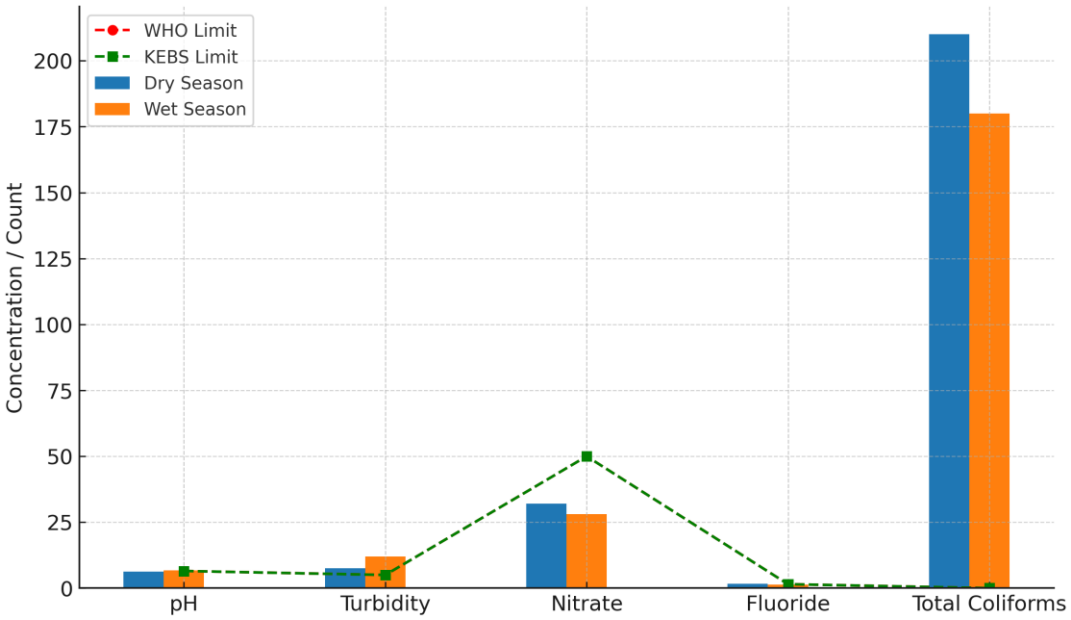

Figure 2: Seasonal variation in selected physico-chemical water quality parameters, comparing dry and wet seasons. Bars represent mean values.

The physico-chemical characteristics of River Mutonga and Nguue Spring revealed notable seasonal variations that can be attributed to differences in seasonal conditions and hydrological processes. Water temperature was significantly higher during the dry season compared to the wet season, a trend explained by the influence of direct solar radiation, reduced water volumes, and general atmospheric conditions. Elevated water

temperature is known to reduce the solubility of dissolved gases, particularly carbon dioxide, thereby influencing taste and other water chemistry parameters (Karunakaran *et al*., 2019). The lower temperatures recorded in the wet season were likely due to cooler weather conditions and rainfall input, consistent with findings by Ekhaise and Anyansi (2005).

The pH values demonstrated marked spatial and seasonal differences. Where in dry season samples from River Mutonga fell within the permissible KEBS (2015) and WHO (2022) limits, Nguue Spring recorded slightly acidic values in both seasons, with acidity becoming more pronounced in the wet season. This was likely due to increased dissolution of carbon dioxide forming carbonic acid, which releases hydrogen ions and lowers pH. Similar observations of reduced pH during the wet season have been reported in other studies (Alexis *et al*., 2017). Acidic waters pose the risk of pipe corrosion and mobilization of toxic metals such as lead, cadmium, and zinc, raising concerns for long-term domestic use (Buridi and Gedala, 2014).

Electrical conductivity (EC) and total dissolved solids (TDS) were consistently higher in the dry season and declined in the wet season, primarily due to dilution effects from increased rainfall and surface runoff. This pattern reflects seasonal variability in ionic concentrations, as reduced water volumes in the dry season concentrate salts and other dissolved substances. The recorded electrical conductivity and total dissolved solids values were all below WHO and KEBS permissible limits, indicating that both sources are relatively poor conductors of electricity due to low ionic content (Basavaranja *et al*., 2011).

Dissolved oxygen (DO) levels showed an inverse trend, being lower in the dry season and substantially higher in the wet season. Warmer water holds less oxygen, while rainfall and enhanced turbulence in the wet season promote aeration and oxygen saturation (Rahman *et al*., 2021; Subehi *et al*., 2024). The dry season values in River Mutonga fell below WHO minimum standards, suggesting potential ecological stress and reduced capacity for aquatic life support.

Total hardness also exhibited seasonal variability, with higher concentrations in the dry season and lower values during the wet season. Hardness in River Mutonga was classified as “hard” in the dry season and “medium hard” in the wet season, while Nguue Spring ranged from “medium hard” to “soft.” The seasonal decrease reflects dilution and lower leaching of calcium and magnesium ions during the wet season (Rahman *et al*., 2021).

The study revealed seasonal variation in nitrate concentration, with higher levels recorded during the dry season compared to the wet season in both Mutonga River and Nguue Spring. The elevated nitrate concentrations during the dry season is attributed to reduced dilution from surface runoff, leading to the accumulation of pollutants from agricultural activities and other anthropogenic inputs (Sharma and Bhattacharya, 2017). Conversely, the wet season recorded significantly lower nitrate concentrations due to increased runoff, which enhances dilution and reduces pollutant concentration. Elevated nitrate levels are a public health concern, particularly for infants, and contribute to eutrophication by encouraging algal blooms that diminish water quality (Ward *et al.,* 2018).

Phosphate concentrations showed an opposite seasonal trend compared to nitrate, with higher levels recorded during the wet season and lower levels during the dry season. This increase during the wet season may be explained by runoff from agricultural fields, leaching of pit latrines and septic systems, which wash phosphorus-rich materials into water bodies (Contreras *et al*., 2024). The results suggest that phosphate concentrations in both Mutonga River and Nguue Spring were slightly below KEBS permissible limits, indicating relatively lower contamination compared to nitrates. However, even moderate phosphate levels are ecologically significant since phosphorus is a limiting nutrient in aquatic ecosystems. Elevated phosphate concentrations can accelerate eutrophication, leading to algal blooms, hypoxia, and loss of biodiversity (Amorim and Moura, 2021). Potential sources of phosphorus contamination in the study sites include agricultural fertilizer application, wastewater discharge, and leaching from onsite sanitation systems, which are common in rural settings (Contreras *et al*., 2024). Therefore, phosphate pollution management should focus on controlling agricultural runoff through best management practices, improving sanitation infrastructure, and

enhancing wastewater treatment systems to reduce nutrient loading into water resources.

Overall, the discussion confirms that physico-chemical parameters in both River Mutonga and Nguue Spring are strongly influenced by seasonal hydrological dynamics. Elevated temperatures, ionic concentrations, and hardness dominate the dry season, whereas the wet season is characterized by dilution, lower pH, and improved oxygenation. These findings are consistent with global literature and highlight the need to integrate seasonal considerations into water quality monitoring and management.

4.1.2 Heavy Metal Concentrations (Zinc and Iron) in Nguue Spring and River Mutonga across Seasons

The concentrations of zinc and iron in River Mutonga and Nguue Spring showed notable variations between the dry and wet seasons. In River Mutonga, zinc levels were relatively low during the dry season, ranging between 0.1233-0.14 mg/L, while iron concentrations was 1.0333-1.1767 mg/L (Table 6, Appendix v).

Table 6 Heavy metal concentration in River Mutonga in dry and wet season

Sample id	Dry season		Wet season	
	Zinc(mg/l)	Iron(mg/l)	Zinc(mg/l)	Iron(mg/l)
M1	0.1333	1.0333	1.9458	2.5593
M2	0.1233	1.1	2.6298	2.7537
M3	0.1267	1.0933	1.6375	1.1025
M4	0.14	1.1767	2.4668	2.4025
M5	0.13	1.1133	2.5332	2.5215
M6	0.1267	1.1533	2.678	2.5575
Mean	0.13	1.1117	2.3168	2.3162
SD	0.0060	0.0502	0.4236	0.6052
KEBS 2015	5.0	0.3	5.0	0.3
WHO 2022	5.0	0.3	5.0	0.3

In concentration of zinc were below but within the permissible limits set by KEBS (2015) and WHO (2022). Iron concentration exceeded the permissible standards of KEBS and WHO. However, during the wet season, zinc concentrations increased markedly to a range of 1.6375-2.678 mg/L, and iron concentrations also rose to 1.1025-2.7537 mg/L. Although zinc remained within the recommended limits, iron concentrations exceeded the maximum permissible limit of 0.3 mg/L under both dry

and wet conditions, indicating potential contamination risks from this metal. Similarly, in Nguue Spring, zinc and iron concentrations during the dry season were relatively low, with values ranging between 0.11-0.1867 mg/L and 1.0-1.9 mg/L, respectively (Table 7, Appendix v).

Table 7 Heavy metal concentration in Nguue spring in dry and wet season

Sample id	Dry season		Wet season	
	Zinc(mg/l)	Iron(mg/l)	Zinc(mg/l)	Iron(mg/l)
N1	0.11	1.0	8.9155	6.4151
N2	0.1533	1.17	9.3430	4.2815
N3	0.18	1.1533	8.91	7.8080
N4	0.1833	1.1667	1.5915	2.3075
N5	0.14	1.14	2.3487	1.7828
N6	0.1867	1.19	2.3569	2.4589
Mean	0.1587	1.1367	5.5776	4.1756
SD	0.0303	0.0690	3.8239	2.4651
KEBS 2015	5.0	0.3	5.0	0.3
WHO 2022	5.0	0.3	5.0	0.3

As with River Mutonga, iron levels consistently exceeded the KEBS and WHO standard of 0.3 mg/L during the dry season. In contrast, the wet season revealed sharp increases in heavy metal levels, with zinc ranging between 1.5915-9.3430 mg/L, with N1,N2 andN3 slightly above the allowable limit of 5.0 mg/L, and iron was between 1.7828-7.8080 mg/L, far surpassing the permissible threshold. These elevated concentrations suggest that the wet season significantly influences heavy metal loading in both water sources, potentially due to surface runoff, soil erosion, and leaching of metals from surrounding catchments.

Overall, the results indicate that while zinc and iron concentrations remain relatively low and within acceptable limits during the dry season, both River Mutonga and Nguue Spring experience a substantial increase in heavy metal levels during the wet season. The iron concentrations are consistently above permissible limits across both seasons and sites, while zinc levels exceed standards in Nguue Spring during the wet season. This pattern highlights seasonal and site-specific differences in heavy metal pollution, with Nguue Spring being more vulnerable to wet season contamination than River Mutonga.

The elevated concentrations of zinc and iron during the wet season in both River Mutonga and Nguue Spring can largely be attributed to enhance surface runoff, soil erosion, and leaching processes triggered by increased rainfall. Runoff from agricultural land, leaching from pit latrines and domestic effluents often mobilizes heavy metals into surface and groundwater, leading to higher contaminant loads during periods of intense precipitation (Ali *et al*., 2019). In particular, the higher zinc concentrations observed in Nguue Spring, which exceeded WHO (2022) guidelines during the wet season, may reflect site-specific vulnerability linked to land-use practices, localized anthropogenic activities, and reduced dilution capacity in spring waters compared to larger rivers.

Although zinc is an essential trace element, elevated concentrations in drinking water can pose health risks, including nausea, vomiting, and long-term gastrointestinal effects (ATSDR, 2005). More importantly, the iron levels recorded across both sites and seasons consistently surpassed the permissible limit of 0.3 mg/L set by WHO (2022) and KEBS (2015). While iron is physiologically important as a micronutrient, excessive concentrations impart undesirable organoleptic qualities such as metallic taste, discoloration, and turbidity, which can compromise water acceptability for domestic use (WHO, 2017). The presence of elevated iron in both dry and wet seasons suggests possible geogenic sources, including weathering of iron-bearing rocks, but the seasonal increase implies that anthropogenic inputs, such as corrosion of metal infrastructure or wastewater discharge, may also be contributing factors (Asfaw, 2022).

The observed seasonal differences align with findings from other studies in sub-Saharan Africa, which report higher heavy metal contamination during wet periods due to stormwater mobilization and reduced filtration capacity of soils under saturated conditions (Asfaw *et al*., 2018). The fact that Nguue Spring exhibited more severe contamination than River Mutonga highlights the susceptibility of groundwater-fed systems to pollution when recharge occurs rapidly through fractured rock or poorly protected catchments. This underscores the importance of protecting spring recharge zones from direct anthropogenic impacts such as farming, pit latrines, and informal waste disposal.

Overall, the consistently elevated iron concentrations and the exceedance of zinc limits in Nguue Spring during the wet season raise significant concerns regarding water safety for human consumption. These findings emphasize the need for continuous monitoring, implementation of low-cost treatment options such as aeration and filtration, and improved watershed management practices to minimize heavy metal contamination risks in rural water supplies.

4.1.3 Seasonal Variations and Correlations of Physico-Chemical Parameters in River Mutonga and Nguue Spring

The analysis of variance (ANOVA) revealed clear seasonal and spatial differences in the physicochemical parameters of River Mutonga and Nguue Spring. During the dry season, most parameters, including pH, electrical conductivity (EC), total dissolved solids (TDS), dissolved oxygen (DO), total hardness (TH), zinc (Zn), and iron (Fe), varied significantly across the sampling stations ($p < 0.05$), while temperature showed no significant differences and remained relatively stable, ranging between 25.9 and 26.6 °C (Table 8, Appendix vi).

Table 8 Seasonal Physico-Chemical Characteristics of Nguue Springs and River Mutonga - Dry Season

Station	Temp	Ph	EC	TDS	DO	TH	Zn	Fe
M1	25.9^{g}	7.36^{a}	202^{a}	0.886^{b}	4.47^{c}	268^{a}	0.133^{cd}	1.033^{cd}
M2	26.0^{f}	7.13^{ab}	182.6^{d}	0.869^{c}	3.50^{f}	216^{bc}	0.123^{cd}	1.1^{abc}
M3	26.1^{e}	7.32^{ab}	176.0^{f}	0.852^{d}	3.48^{g}	258^{ab}	0.127^{cd}	1.093^{bcd}
M4	26.4^{c}	7.29^{ab}	173.3^{g}	0.848^{e}	3.32^{g}	176^{cd}	0.140^{cd}	1.18^{ab}
M5	26.5^{b}	7.19^{ab}	172.5^{h}	0.844^{f}	3.25^{h}	230^{ab}	0.130^{cd}	1.113^{abc}
M6	26.6^{a}	7.11^{b}	170.8^{i}	0.838^{g}	3.19^{i}	190^{cd}	0.127^{cd}	1.153^{ab}
N1	26.4^{c}	6.08^{e}	193.6^{b}	1.20^{a}	6.24^{a}	124^{e}	0.110^{d}	1.000^{d}
N2	26.5^{b}	6.43^{c}	157.0^{j}	0.651^{i}	2.61^{j}	160^{de}	0.153^{bc}	1.17^{ab}
N3	26.5^{b}	6.38^{cd}	149^{k}	0.640^{j}	4.39^{d}	60^{f}	0.180^{ab}	1.153^{ab}
N4	26.2^{d}	6.58^{c}	147.6^{l}	0.552^{k}	3.61^{e}	58^{f}	0.183^{ab}	1.167^{ab}
N5	26.0^{f}	5.21^{f}	181.3^{e}	0.806^{h}	2.62^{j}	159.33^{de}	0.140^{cd}	1.140^{ab}
N6	25.9^{g}	6.20^{de}	185.6^{c}	0.838^{g}	4.62^{b}	157^{de}	0.187^{a}	1.19^{a}
Mean	26.25	6.690	174.28	0.8187	3.774	171.36	0.144	1.124
R^2	1	0.973	0.999	0.999	0.999	0.886	0.764	0.624
CV	-	2.019	0.173	0.1259	0.377	17.348	12.34	5.073
LSD	-	0.2288	0.5103	0.0017	0.0241	50.339	0.0302	0.097
P-value	.0001	0.0001	0.0001	0.0001	0.0001	0.0001	0.0002	0.0158

[a]Mean followed by same letters are not significantly different at $\alpha = 0.05$.

The pH ranged from 5.21 at station N5 to 7.36 at M1, with the notably low pH at N5 likely influenced by elevated dissolved CO_2 forming carbonic acid. Dissolved oxygen levels varied widely, from 2.61 mg/L at N2 to 6.24 mg/L at N1, highlighting differences in aeration and organic matter decomposition among sites. Similarly, EC and TDS were highest at M1 (202 µS/cm and 0.886 g/L, respectively) and lowest at N4 (147.6 µS/cm and 0.552 g/L), reflecting variations in ionic concentration. Total hardness also showed site-specific variation, ranging from 58 mg/L at N4 to 268 mg/L at M1. Zinc levels were generally low (0.110–0.187 mg/L) but still varied significantly across stations. Iron concentrations, however, were consistently elevated at all sites, ranging between 1.0 and 1.19 mg/L, and exceeded the WHO and KEBS permissible limits of 0.3 mg/L, suggesting potential effects on water taste and odour.

In contrast, the wet season presented distinct trends. While temperature remained uniform (20.5–21.0 °C) with no significant spatial variation, other parameters, including pH, EC, TDS, TH, zinc, and iron, varied significantly across stations ($p < 0.05$) (Table 9, Appendix vii).

Table 9 Seasonal Physico-Chemical Characteristics of Nguue Springs and River Mutonga – Wet Season

Station	Temp	pH	EC	TDS	DO	TH	Zn	Fe
M1	21.0^{a}	5.973^{f}	57.2^{f}	36.1^{d}	8.72^{e}	108^{c}	1.95^{j}	2.5593^{e}
M2	21.0^{a}	6.080^{d}	57.6^{e}	32.5^{h}	8.91^{a}	87.3^{e}	2.63^{e}	2.7537^{d}
M3	21.0^{a}	6.033^{e}	58.1^{d}	31.3^{i}	8.87^{b}	120^{a}	1.64^{k}	1.1025^{l}
M4	21.0^{a}	6.259^{c}	58.8^{c}	34.9^{e}	8.83^{c}	96^{d}	2.47^{g}	2.4025^{i}
M5	21.0^{a}	6.280^{b}	59.2^{d}	33.5^{g}	8.873^{b}	122^{a}	2.53^{f}	2.5215^{g}
M6	21.0^{a}	6.288^{a}	60.4^{a}	34.43^{f}	8.92^{a}	116^{b}	2.68^{d}	2.5275^{f}
N1	21.0^{a}	5.231^{j}	55.6^{g}	32.5^{h}	8.86^{b}	84^{f}	8.92^{b}	6.4151^{b}
N2	21.0^{a}	5.588^{h}	51.6^{h}	29.9^{j}	8.83^{c}	64^{g}	9.34^{a}	4.2815^{c}
N3	21.0^{a}	5.561^{i}	51.2^{i}	27.7^{k}	8.78^{d}	64^{g}	8.91^{c}	7.8080^{a}
N4	20.5^{b}	5.724^{g}	45.5^{k}	57.5^{c}	8.72^{e}	22.6^{j}	1.59^{l}	2.3073^{j}
N5	20.5^{b}	4.344^{k}	38.7^{l}	59.5^{a}	8.61^{f}	32.0^{i}	2.35^{i}	1.7828^{k}
N6	20.5^{b}	4.210^{l}	37.8^{m}	58.6^{b}	8.58^{g}	42^{h}	2.36^{h}	2.4589^{h}
Mean	20.875	5.6309	52.64	39.03	8.79	79.83	3.95	3.2459
R^2	1.000	0.9998	0.9998	0.9999	0.9943	0.9992	1.00	1.00
CV	-	0.0203	0.2361	0.2844	0.1178	1.5431	-	-
LSD	-	0.0019	0.2105	0.188	0.0175	2.0859	-	-
p-value	0.0001	0.0001	0.0001	0.0001	0.0001	0.0001	0.0001	0.0001

[a]Mean followed by same letters are not significantly different at $\alpha = 0.05$.

The pH values were markedly lower compared to the dry season, ranging from 4.21 at N6 to 6.29 at M6, with acidic conditions particularly pronounced at N5 and N6. Both EC and TDS decreased substantially relative to the dry season, with the lowest values observed at N5 (38.7 µS/cm, 59.5 mg/L) and the highest at M6 (60.4 µS/cm, 34.4 mg/L). Dissolved oxygen levels were consistently high across all sites (8.58–8.92 mg/L), reflecting enhanced mixing and aeration during the rainy period. Total hardness decreased significantly, ranging from 22.6 mg/L at N4 to 122 mg/L at M5, indicating dilution effects from increased water volumes. Heavy metal concentrations, however, increased sharply during the wet season. Zinc concentrations ranged from 1.59 mg/L at N4 to 9.34 mg/L at N2, with the mean values in Nguue Spring slightly exceeding the WHO permissible limit of 5 mg/L. Iron concentrations were even more elevated, ranging from 1.78 mg/L at N5 to 7.81 mg/L at N3, all well above acceptable standards, raising concern about the quality of the water.

When comparing the two seasons, several clear patterns emerged. Temperatures were higher in the dry season (around 26 °C) than in the wet season (around 21 °C). pH declined in the wet season, with some stations, especially N5 and N6, recording strongly acidic conditions. EC, TDS, and total hardness were consistently higher in the dry season, likely due to evaporation and solute concentration effects, whereas DO levels were elevated in the wet season, reflecting rainfall-driven aeration. Zinc and iron concentrations were significantly higher in the wet season, suggesting mobilization of metals from soils, rocks, and anthropogenic sources via surface runoff. Across both seasons, iron consistently exceeded WHO and KEBS permissible limits, while zinc exceeded limits in Nguue Spring during the wet season, underscoring persistent and seasonally aggravated heavy metal contamination in the study sites.

The physico-chemical parameters for dry season revealed most parameters, including pH, electrical conductivity (EC), total dissolved solids (TDS), dissolved oxygen (DO), total hardness (TH), zinc (Zn), and iron (Fe), varied significantly across the sampling stations. While temperature showed no significant differences and remained relatively stable (Table 8, Appendix vi). The consistent temperature suggests a relatively uniform climatic condition on these stations (Cloutier *et al*., 2017).

The notably low pH at N5 is likely influenced by elevated dissolved CO_2 forming carbonic acid which releases hydrogen ions and lowers pH. (Alexis *et al*., 2017). The significant differences ($p<0.05$) are indicated by different letters. The coefficient variation (Cv) for pH was 2.019%, indicating low variability and suggesting consistent condition in the spring and river. The LSD test showed significant differences ($p<0.05$) between pH levels of different stations in spring and river.

Similarly, electrical conductivity was highest at M1 (202 µS/cm) and lowest at N4 (147.6 µS/cm), reflecting variations in ionic concentration primarily due to reduced water volumes in the dry season concentrate salts and other dissolved substances. The recorded electrical conductivity in both sources are relatively poor conductors of electricity due to low ionic content (Basavaranja *et al*., 2011). The significant differences ($p<0.05$) are indicated by different letters. The coefficient variation (Cv) for electrical conductivity was 0.173%, indicating low variability and suggesting consistent ionic concentration in the stations. The LSD test showed significant differences ($p<0.05$) between the electrical conductivity levels of different stations.

Similarly, total dissolved solids TDS were highest at M1 (0.886 g/L) and lowest at N4 (0.552 g/L), reflecting variations in ionic concentration. Total dissolved solids (TDS) were consistently higher in the dry season primarily due to reduced water volumes which concentrate salts and other dissolved substances (Basavaranja *et al*., 2011). N6&M6 were not statistically different ($p<0.05$) as were indicated by similar letters. The significant differences ($p<0.05$) are indicated by different letters. The coefficient variation (Cv) for TDS was 0.1259%, indicating low variability and suggesting consistent ionic concentration in the stations. The LSD test showed significant differences ($p<0.05$) between the TDS levels of different stations.

Dissolved oxygen DO levels varied widely, with higher dissolved oxygen at N1 while lower dissolved oxygen levels at N2, highlighting differences in aeration and organic matter decomposition among sites. Warmer water holds less oxygen (Rahman *et al*., 2021; Subehi *et al*., 2024). M3&M4 and N5&N2 showed no significant differences ($p<0.05$) indicating similar aeration and organic matter decomposition. The significant differences ($p<0.05$) are indicated by different letters. The coefficient variation (Cv) for

DO was 0.377%, indicating low variability in the stations. The LSD test showed significant differences ($p<0.05$) between the DO levels of different stations.

Total hardness TH also showed site-specific variation, with the lowest at N4 and the highest at M1. This reflects on dilution and lower leaching of calcium and magnesium ions (Rahman *et al*., 2021). Stations with similar letters showed no significant differences ($p<0.05$). The coefficient variation (Cv) for TH was 17.348%, indicating high variability in the stations. The LSD test showed significant differences ($p<0.05$) between the TH levels of different stations.

Zinc levels were generally low (0.110–0.187 mg/L) but still varied significantly across stations ($p<0.05$) with the lowest at N1 and the highest at N6. Although zinc is an essential trace element, elevated concentrations in drinking water can pose health risks, including nausea, vomiting, and long-term gastrointestinal effects (ATSDR, 2005). There was no significant difference ($p < 0.05$) between stations with similar letters. The coefficient variation (Cv) for zinc concentration was 12.34%, indicating high variability in the stations. The LSD test showed significant differences ($p < 0.05$) between the zinc levels of different stations.

Iron concentrations, however, were consistently elevated at all sites, with the highest at N6 and the lowest at N1. 1.0 and 1.19 mg/L, and exceeded the WHO and KEBS permissible limits of 0.3 mg/L, suggesting potential effects on water taste and odour. The elevated concentrations of iron in stations can largely be attributed to enhance surface runoff, soil erosion, and leaching processes. Runoff from agricultural land, septic systems, and urban effluents often mobilizes heavy metals into surface and groundwater, leading to higher contaminant loads during periods of intense precipitation (Ali *et al*., 2019). While iron is physiologically important as a micronutrient, excessive concentrations impart undesirable organoleptic qualities such as metallic taste, discoloration, and turbidity, which can compromise water acceptability for domestic use (WHO, 2017). The presence of elevated iron in dry season suggests possible geogenic sources, including weathering of iron-bearing rocks (Asfaw, 2022). The coefficient variation (Cv) for iron concentration was 5.073%,

indicating low variability in the stations. The LSD test showed significant differences ($p<0.05$) between the iron levels of different stations.

Significant variations were observed among physico-chemical across the stations in wet season (table 9), for most parameters, including pH, electrical conductivity (EC), total dissolved solids (TDS), dissolved oxygen (DO), total hardness (TH), zinc (Zn), and iron (Fe), varied significantly across the sampling stations. While temperature showed no significant differences and remained relatively stable (Table 9). The consistent temperature suggests a relatively uniform climatic condition on these stations (Cloutier *et al*., 2017).

The notably low pH at N6 is likely influenced by elevated dissolved CO_2 forming carbonic acid which releases hydrogen ions and lowers pH. (Alexis *et al*., 2017). Acidic waters pose the risk of pipe corrosion and mobilization of toxic metals such as lead, cadmium, and zinc, raising concerns for long-term domestic use (Buridi and Gedala, 2014). The significant differences ($p<0.05$) are indicated by different letters. The coefficient variation (Cv) for pH was 0.0203%, indicating low variability and suggesting consistent geochemical condition in the spring and river. The LSD test showed significant differences ($p<0.05$) between pH levels of different stations in spring and river.

Similarly, electrical conductivity was highest at M6 (60.4 µS/cm) and lowest at N6 (37.8 µS/cm), reflecting variations in ionic concentration primarily due to dilution effects from increased rainfall and surface runoff. The recorded electrical conductivity in both sources are relatively poor conductors of electricity due to low ionic content (Basavaranja *et al*., 2011). The significant differences ($p<0.05$) are indicated by different letters. The coefficient variation (Cv) for electrical conductivity was 0.2361%, indicating low variability and suggesting consistent ionic concentration in the stations. The LSD test showed significant differences ($p<0.05$) between the electrical conductivity levels of different stations. Similarly, total dissolved solids TDS were highest at N5 (59.5 g/L) and lowest at N3 (27.7 g/L), reflecting variations in ionic concentration. Total dissolved solids (TDS) were consistently higher in the wet season primarily due to increased surface runoff which concentrates dissolved substances

(Basavaranja *et al*., 2011). N1&M2 were not statistically different ($p < 0.05$) as were indicated by similar letters. The significant differences ($p < 0.05$) are indicated by different letters. The coefficient variation (Cv) for TDS was 0.2844%, indicating low variability and suggesting consistent ionic concentration in the stations. The LSD test showed significant differences ($p<0.05$) between the TDS levels of different stations.

Dissolved oxygen DO levels varied slightly, with highest dissolved oxygen at M6 while lowest dissolved oxygen levels at N6, highlighting differences in aeration and organic matter decomposition among sites. Rainfall and enhanced turbulence in the wet season promote aeration and oxygen saturation (Rahman *et al*., 2021; Subehi *et al*., 2024). Stations with similar letters (table4.8) showed no significant differences ($p < 0.05$) indicating similar aeration and organic matter decomposition. The significant differences ($p < 0.05$) are indicated by different letters. The coefficient variation (Cv) for DO was 0.1178%, indicating low variability in the stations. The LSD test showed significant differences ($p < 0.05$) between the DO levels of different stations.

Total hardness TH also showed site-specific variation, with the lowest at N4 and the highest at M5. This reflects on increased rainfall results dilution and lower leaching of calcium and magnesium ions (Rahman *et al*., 2021). Stations with similar letters showed no significant differences ($p < 0.05$). The coefficient variation (Cv) for TH was 1.5431%, indicating low variability in the stations. The LSD test showed significant differences ($p<0.05$) between the TH levels of different stations.

Zinc levels were generally high in wet season compared to dry season (1.59-9.34 mg/L) and varied significantly across stations ($p < 0.05$) with the lowest at N4 and the highest at N2. Although zinc is an essential trace element, elevated concentrations in drinking water can pose health risks, including nausea, vomiting, and long-term gastrointestinal effects (ATSDR, 2005). There was a significant difference ($p < 0.05$) between stations with different letters.

Iron concentrations, however, were consistently elevated at all sites, with the highest at N3 and the lowest at M3. 1.0 and 7.81 mg/L, and exceeded the WHO and KEBS permissible limits of 0.3 mg/L, suggesting potential effects on water taste and odour.

The elevated concentrations of iron in stations can largely be attributed to enhance surface runoff, soil erosion, and leaching processes. Runoff from agricultural land, septic systems, and urban effluents often mobilizes heavy metals into surface and groundwater, leading to higher contaminant loads during periods of intense precipitation (Ali *et al*., 2019). While iron is physiologically important as a micronutrient, excessive concentrations impart undesirable organoleptic qualities such as metallic taste, discoloration, and turbidity, which can compromise water acceptability for domestic use (WHO, 2017). The presence of elevated iron in dry season suggests possible geogenic sources, including weathering of iron-bearing rocks (Asfaw, 2022). There was a significant difference ($p<0.05$) between stations with different letters.

4.1.4 Assessment of Total Coliforms in Nguue Springs and River Mutonga

Total coliforms were detected at all sampling points in both Nguue Springs and River Mutonga, indicating widespread microbial contamination. Counts were generally higher in the wet season compared to the dry season, due to enhanced surface runoff carrying contaminants into the water sources, with the highest value recorded at N5 (>1100 MPN/100ml) during the wet season and the lowest at M3 (11 MPN/100ml) in the dry season (Table 10). Notably, *E. coli* was detected at sites M2, N3, and N4, as indicated by the characteristic green metallic sheen on EMB agar, suggesting feacal contamination. All measured total coliform counts exceeded the KEBS and WHO recommended limit of 10 MPN/100ml, demonstrating that the water at these sources is unsuitable for human consumption (KEBS,2015, WHO,2022).

The microbial quality of spring and river water was assessed by enumerating total coliform bacteria, which are widely used as indicator organisms for water contamination by feacal matter. The results showed that total coliform counts increased significantly during the wet season, likely due to enhanced surface runoff carrying contaminants into the water sources. Furthermore, water from three sampling points, M2, N3, and N4, was found to contain *Escherichia coli*, as evidenced by the characteristic green metallic sheen on EMB agar. High total coliform counts may indicate the presence of other enteric microorganisms in addition to coliforms. The

presence of *E. coli* and other pathogenic bacteria renders the water unsafe for human consumption and poses significant public health risks (Alotaibi, 2009; WHO, 2011).

Table 10: Seasonal variation of total coliforms in Nguue Springs and River Mutonga relative to KEBS guidelines

Sample ID	MPN per 100ml in wet season	MPN per 100ml in dry season	KEBS 2010
M1	36	29	10
M2	1100	460	10
M3	14	11	10
M4	43	38	10
M5	36	27	10
M6	460	240	10
N1	460	290	10
N2	43	36	10
N3	460	210	10
N4	1100	460	10
N5	>1100	1100	10
N6	460	150	10

Similar studies conducted in other parts of Kenya have also reported the presence of total and faecal coliforms in water sources intended for drinking and domestic use (Sila, 2019). According to KEBS and WHO guidelines, drinking water should not exceed 10 MPN/100ml total coliforms and must have no detectable faecal coliforms. Therefore, the results indicate that water from Nguue Springs and River Mutonga is microbiologically contaminated beyond recommended limits and constitutes a potential health hazard to the surrounding communities.

4.2 Structural Properties and Elemental Composition of Adsorbent

4.2.1 X-ray Diffraction Patterns for Corn-cobs Activated Carbon and Corn-cob Charcoal

The corn-cob charcoal and activated carbon was obtained after calcination of dry corn-cobs at 500ºC. The corn-cob activated carbon was activated with 2M nitric acid. The patterns in figure 3 and 4 show that both corn cob charcoal and activated carbon were essentially amorphous. Amorphous substances generally have a higher surface area and more active sites compared to their counter part due to lack of a regular order structure. This creates a more heterogenous and complex surfaces with more defects and undercoordinated atoms can interact with adsorbate molecules. There was a major

broad peak at 2θ (15-30) this shows a significant peak shift to the right at 2θ (18-30) as the crystal size is greater due to activation (Sagayaraj *et al*., 2020). This study is in agreement to study reported by Yuwita *et al*., 2020 in structural, morphological and group analysis of corn-cob powder, that also shows low crystallinity and amorphous structure of corn cob.

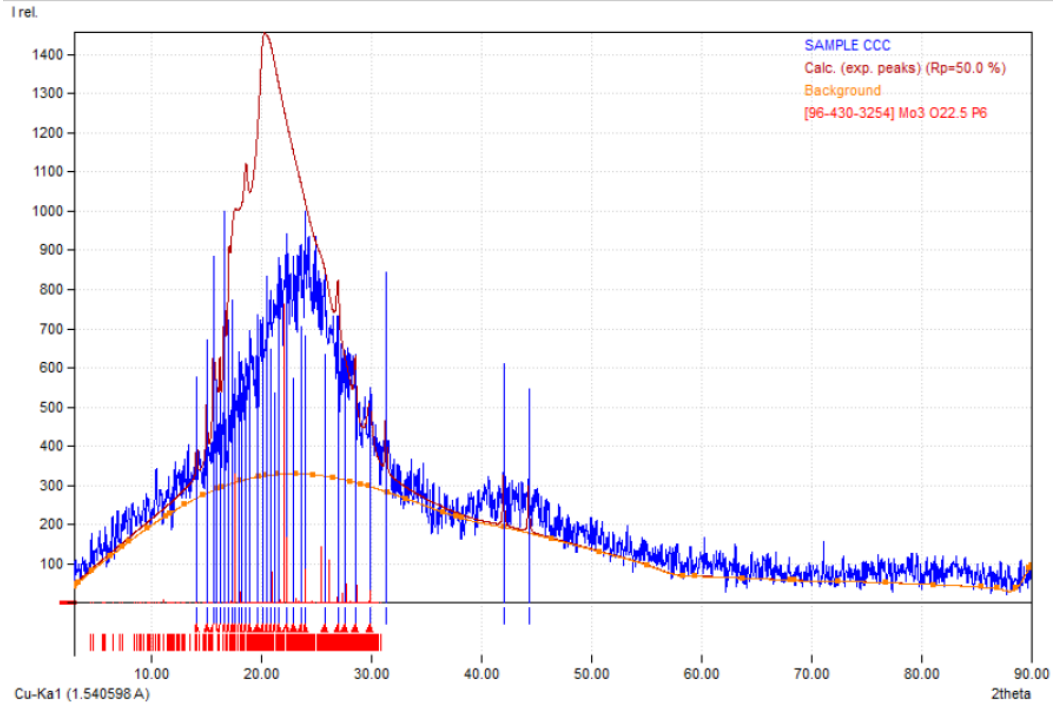

Figure 3 XRD diffraction patterns of corn-cob activated carbon

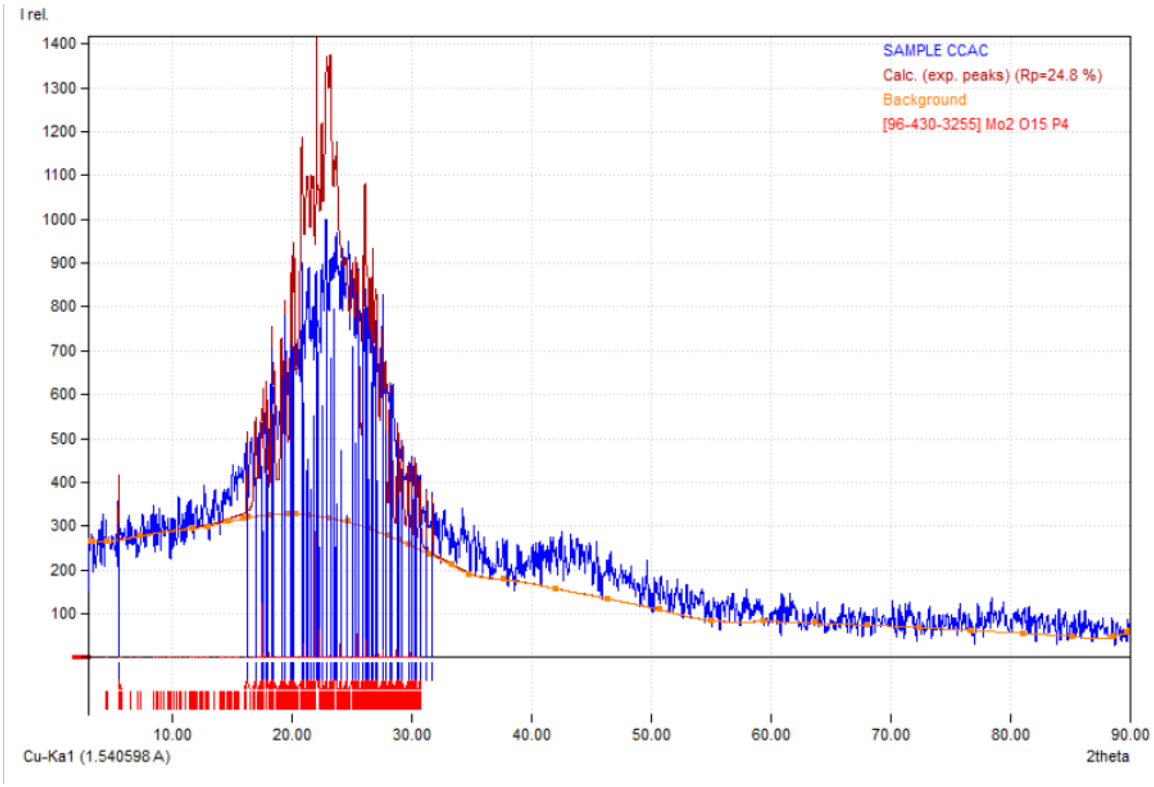

Figure 4 XRD diffraction patterns of corn-cob charcoal

4.2.2 Elemental Composition of Corn-Cob Ash before and after Activation

The percentage composition of major elements in corn-cobs ash was analysed using X-ray fluorescence (XRF). The results are presented in Table 11 and 12 for activated and inactivated (charcoal) ash, respectively.

Table 11 Elemental composition of corn-cob activated carbon ash

Compound	K_2O	Fe_2O_3	SiO_2	CaO	P_2O_5	TiO_2	MnO	CuO	SO_3
% oxide	72.950	9.262	8.080	4.760	3.344	0.740	0.683	0.102	0.080

Table 12 Elemental composition of corn-cob charcoal ash

Compound	K_2O	Fe_2O_3	SiO_2	CaO	P_2O_5	MnO
% oxide	75.140	7.712	7.417	5.991	3.264	0.476

The findings of the study shows that activated carbon ash contained nine oxides, including trace amounts of TiO_2 (0.740%), CuO (0.102%) and SO_3 (0.080%) (Table 11), which were not detected in the inactivated charcoal ash (Table 12). This indicates that the activation process introduced or enhanced the detectability of these oxides.

Chemical activation introduces Oxygen containing functional group such as carbonyl (COOH) and phenolic (OH) group.

When comparing the two forms, both activated and inactivated ash contained K_2O, Fe_2O_3, SiO_2, CaO, P_2O_5, and MnO as the dominant oxides. Potassium oxide (K_2O) was the most abundant element in both samples, with slightly higher content in charcoal (75.140%) than in activated carbon (72.950%). Conversely, the relative proportions of Fe_2O_3 (9.262% vs. 7.712%) and SiO_2 (8.080% vs. 7.417%) were higher in activated ash compared to charcoal, suggesting that activation concentrated certain oxides. Overall, the results show that activation not only alters the oxide composition of corn-cob ash but also introduces additional trace elements (Ti, Cu, and S) that were absent in the inactivated form.

Titanium oxide with 0.740%, copper (ii) oxide with 0.102% and Sulphur (vi) oxide with 0.080% were present in ash of corn-cob activated carbon but absent in corn-cob charcoal. The ash also contained potassium oxide, iron (iii) oxide, silica, calcium oxide, phosphorous (v) oxide and manganese (ii) oxide in both charcoal and activated carbon. The percentage composition of oxides of potassium in charcoal was 75.140% while in activated carbon was 72.950%. The percentage composition of oxides of silica, iron, calcium, phosphorous and manganese decreased in charcoal. The elemental component become more concentrated after activation process. The results demonstrate that activation modified both the composition and diversity of oxides in corn-cob ash. The appearance of TiO_2, CuO, and SO_3 exclusively in the activated carbon suggests that activation enhanced mineral release or improved the sensitivity of oxide detection. Similar observations have been reported in studies on other biomass ashes, where activation increased the range of detectable trace elements (Areti *et al*., 2024).

Potassium oxide was the predominant component in both samples, in line with earlier reports that highlight K_2O as a major constituent of agricultural biomass ashes due to the high potassium content of plant tissues (Pérez-Santín *et al*., 2021; Oloyede *et al*., 2023). Although K_2O decreased slightly after activation, Fe_2O_3 and SiO_2 were relatively more concentrated in the activated sample. This may be attributed to the volatilization of light elements and restructuring of mineral phases during activation,

which increases the relative proportion of non-volatile oxides (Pérez-Santín et al., 2021). The consistent presence of CaO and P_2O_5 in both ash types indicates the potential use of corn-cob ash as a calcium and phosphate-rich additive in agricultural and environmental applications. Moreover, the additional oxides detected in activated ash may enhance its catalytic and adsorptive properties, thereby widening its applicability in environmental remediation and material development. Thus, activation resulted in both quantitative and qualitative changes in ash composition, reducing the relative dominance of K_2O while enhancing the concentration of Fe_2O_3 and SiO_2 and introducing trace oxides. These changes are significant for the potential functional applications of corn-cob ash.

4.3 Batch Adsorption, Kinetics and Isotherms of Zinc and Iron Using Corn Cob Activated Carbon and Corn Cob Charcoal

4.3.1 Effect of Contact Time on Zinc Adsorption Using Corn Cob Activated Carbon and Corn Cob Charcoal

The impact of contact time on zinc (Zn^{2+}) adsorption using corn-cob activated carbon (CCAC) and corn-cob charcoal (CCC) was determined for 120 minutes as shown in figure 5. CCC had a sharper adsorption efficiency rise from 81.10% at time 30 minutes to 91.63% after 60 minutes, with high adsorption rates of above 90% in the rest of the intervals. CCAC, in contrast, started higher at 90.16% and gradually dropped at 20-40 minutes, and a sharp rise was observed at 60 mins before dropping to 88.28% after 120 minutes, after reaching 91.58% after 90 minutes. The increase in % adsorption was due to presence of higher number of unoccupied active sites. The equilibrium was achieved at 90 mins and thereafter a decline in adsorption capacity observed as a result of supersaturating of active sites and desorption as time prolonged. The trend shows that CCC reaches equilibrium sooner in time and achieves steady adsorption capacity, while CCAC is subjected to marginal desorption or saturation after prolonged exposure. Abdel-Shafy et al. (2022), appraised the adsorption of aqueous media of Zn^{2+}, Cd^{2+}, and Ni^{2+} ions using activated carbon from corncob waste. The maximum adsorption capacities of 95.4%, 93.6%, and 92.1% for the Zn^{2+}, Cd^{2+}, and Ni^{2+} ions, respectively, were achieved after 6 hours of contact time.

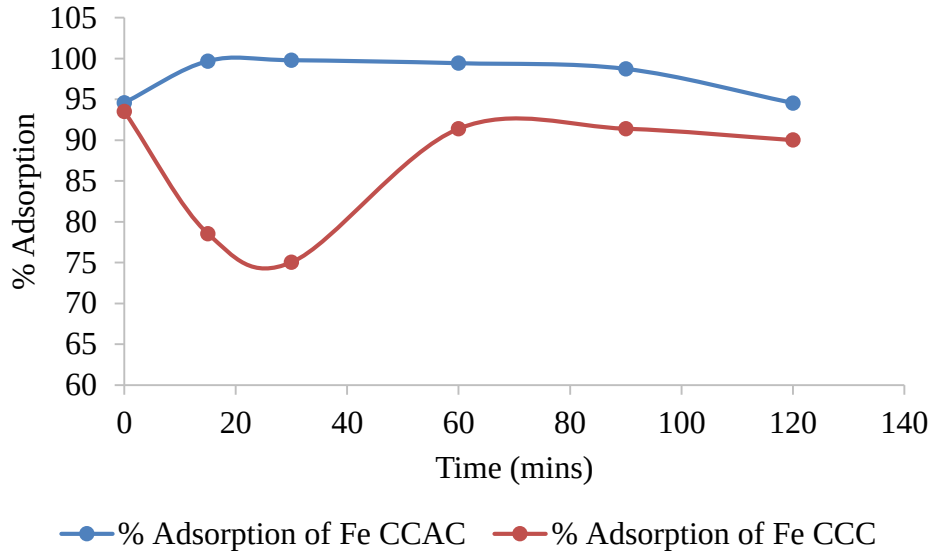

Figure 5: Effect of contact time on adsorption of Zn using corn cob activated carbon and corn cob charcoal

Liu *et al*. (2021), investigated mercury (Hg^{2+}) adsorption using modified corn-cob activated carbon and the equillibrium adsorption capacity of 184.76 mg/g was achieved at a contact time of 120 minutes. Similarly, Ungureanu et al. (2023), also included a critical review of low-cost adsorbents. Corn husk biochar adsorbed 99.66% of Pb^{2+}, 92.36% of Ni^{2+}, and 96.01% of Cu^{2+} within 90 minutes of contact time. Raut et al. (2021), also performed a comparative study with corncob and coconut-shell activated carbon. Optimized contact time of 60 minutes resulted in 92.6% of Zn^{2+}, 91.4% of Cu^{2+}, and 89.3% of Cd^{2+} elimination for corncob carbon. The study indicates that metal absorption is strongly regulated by means of particle size and surface area. Lala *et al*. (2023), also aimed for the elimination of Ni^{2+} with the employment of maize cob-activated carbon. The equillibrium, was achieved at a contact time of 120 m.

inutes, with 97.13%, which shows that corn-based carbons are successful for removal of divalent cations with different ionic radii. Adebayo et al. (2015), used maize cob activated carbon for the removal of Mn^{2+} and Co^{2+} ions from solution. Adsorption was maximum after 120 minutes, achieving 91.3% (Mn^{2+}) and 89.7% (Co^{2+}) this was a result of high number of active sites. Ismail (2021), used functionalized corn husk carbon for the adsorption of Ni^{2+}, Pb^{2+}, and Cu^{2+}. Adsorption efficacies achieved were 87% for Ni^{2+}, 80% for Pb^{2+}, and 79% for Cu^{2+} at 95 minutes for lead and 125 minutes for nickel and copper. The study concluded that acid-functionalization improved

surface polarity and ion exchange capacity. The maximum adsorption periods within the 60-90 minutes range agree for biomass adsorbents in this study. High (>90%) removal efficiencies of CCAC and CCC also attest to the viability of adsorbents from corn cob for sustainable and cheap uses in zinc-polluted wastewater treatment.

4.3.2 Effect of Initial Concentration on Adsorption of Zn using Corn Cob Activated Carbon and Corn Cob Charcoal

The effect of initial zinc (Zn^{2+}) concentration on the effectiveness of adsorption was examined for the adsorbents corn-cob activated carbon (CCAC) and corn-cob charcoal (CCC) for initial concentrations of 5–25 ppm as shown in figure 6. The results show that the adsorbents performed well in low concentrations, with the same adsorbent performance of 90.52% for 5 ppm. With a higher concentration of 10 ppm, the two adsorbents improved in performance, with CCC registering 94.69% and CCAC 92.31%. For 15 ppm, CCC had the best performance of 97.68%, whereas CCAC had 90.88%. For concentrations above 15 ppm, CCAC had a downward trend in adsorbent performance, down to 87.59% for 20 ppm and 85.78% for 25 ppm. CCC also showed a downward trend after 15 ppm, down to 95.82% for 20 ppm. The results show that CCC not only adsorbs zinc better than CCAC for high concentrations but also had better stability for increased levels of zinc loading. The adsorption would be explained through the saturation of active sites for elevated concentrations of zinc. In the initial instances, with increased numbers of adsorptive sites in comparison to numbers of zinc ions, CCC and CCAC adsorb best. However, when the concentration of zinc rises, the fixed number of adsorbent accessible active sites is not enough for the adsorbate for full sorption capacity, so the percentage of adsorption falls. CCC adsorbs better than CCAC, most likely due to larger surface, volume of the pore, and increased number of effective adsorbent functional groups for the complexing of the Zn^{2+} ions.

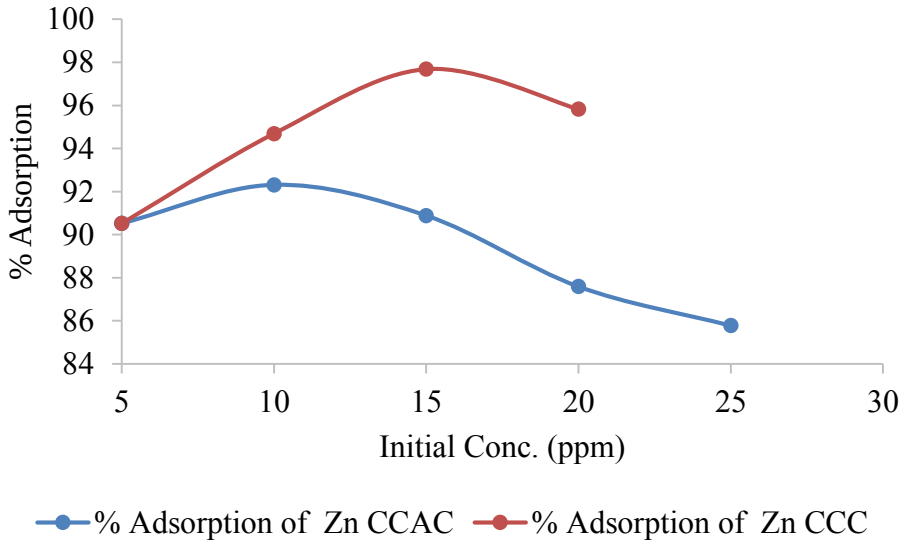

Figure 6: Effect of initial concentration on adsorption of Zn using corn cob activated carbon and corn cob charcoal

A study conducted by Abdel-Shafy *et al*. (2022), found that with corncob-activated carbon, adsorption of the metals reached 98.15% for Zn^{2+}, 100% for Cd^{2+}, and 100% for Ni^{2+} when the concentration was 2 ppm, but dropped gradually to 8.7%, 24% and 21% for zinc, cadmium and nickel respectively when the concentration increased to 10 mg/l because of site saturation. Similarly, Raut et al. (2021), studied adsorption of Zn^{2+}, Cu^{2+}, and Cd^{2+} using biomass-derived activated carbon and registered maximum removal at 10–15 ppm: 92.6% for Zn^{2+}, 91.4% for Cu^{2+}, and 89.3% for Cd^{2+}. Adsorption efficiency decreased above 20 ppm in accordance with the effect of saturation and overlapping of adsorbate ions on the adsorbent surface. Ungureanu et al. (2023), examined numerous agricultural adsorbents and reinforced that optimal adsorption of Zn^{2+} tended to happen within the 10–20 ppm range, averaging above 90% removal, whereas high concentrations triggered a sharp fall except when surface area or modification was enhanced.

Ismail (2021), tested functionalized corn husk activated carbon and achieved 99.8% adsorption for Ni^{2+}, 94.8% for Pb^{2+}, and 99.7% for Cu^{2+} with initial concentrations of 10, 16 and 12 ppm respectively. These levels resulted in 5–10% declines in effectiveness in higher concentrations. This was due to competition for adsorption sites and pore diffusion resistance when more than one ion was introduced. Lala *et al*. (2023), studied the adsorption of nickel through maize cob carbon and achieved maximum

performance of 97.61% for Ni^{2+} for 9.85 ppm, followed by decreases for concentrations greater than 10 ppm. This is directly related to the present study, showing that CCC performed better than CCAC in retaining adsorption capacity with increasing concentrations.

4.3.3 Effect of Temperature on Adsorption of Zn using Corn Cob Activated Carbon and Corn Cob Charcoal

Effect of temperature on adsorption effectiveness of Zn (II) with corn-cob activated carbon (CCAC) and corn-cob charcoal (CCC) is presented in figure 7, Appendix viii. The two adsorbents had high adsorption effectiveness of more than 94% in the temperature range 25 to 55°C, with CCAC attaining a maximum of 95.6% at 45°C before consistently declining down to 92.8% at 55°C. CCC, being lower in maximum adsorption (95.2%), proved, however, to be temperature-stabler in profile. The implication is that adsorption of Zn onto CCAC and CCC is elevated with temperature to an optimum through heightened diffusion kinetics but decreased through desorption as a result of diminished binding affinity with high-temperature use, in concordance with exothermic adsorption characteristic.

These findings are in agreement with research conducted by Fertu *et al*. (2022), who investigated the biosorption of Pb(II), Cd(II), and Zn(II) from aqueous solution using low-cost sorption soybean waste and soybean biomass. Adsorption of Zn attained the optimum value of 95.4% at 45°C, Pb achieved 96.7%, and for Cd, 93.2% was achieved. Temperature was found to significantly influence the transport of metal ions, and they improved sorption before desorption mechanisms dominated high-temperature conditions.

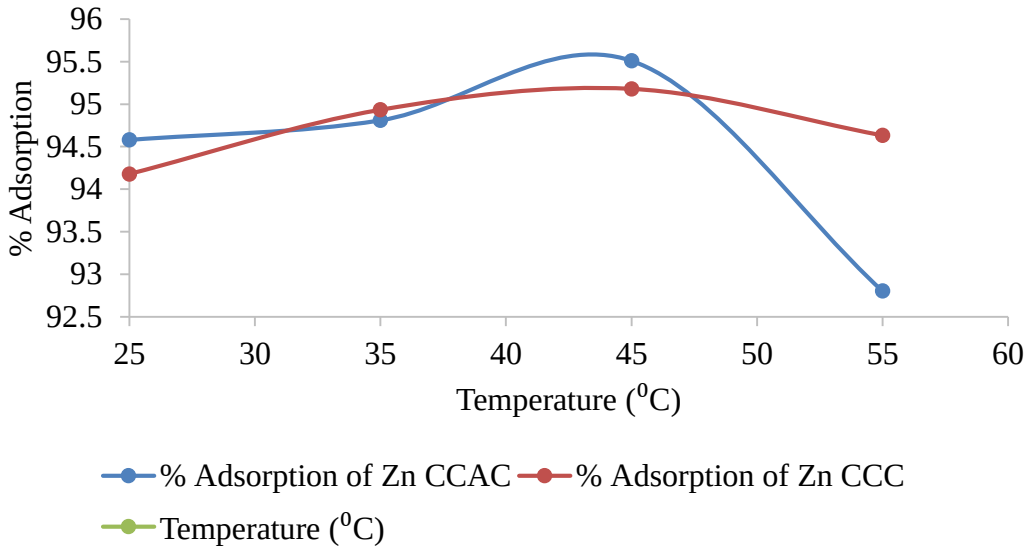

Figure 7: Effect of temperature on adsorption of Zn using corn cob activated carbon and corn cob charcoal

Moreover, Loganathan *et al*. (2025), investigated a hybrid stormwater filtration medium of biomass-derived adsorbents and demonstrated 69.3% adsorption capacities for Zn(II), 27.4% for Cu(II), 77% for Ni(II), and 36.3% for Pb(II) for a 20-hour column test conducted at 40°C using alumina-based composite media. These findings are in agreement with those for CCC and CCAC, verifying that the adsorption of Zn using bio-derived substrates is optimal in the 35–45°C temperature range in general. These studies confirm that Zn adsorption in water phases using adsorbents from biomass commonly shows an endothermic-to-exothermic transition in that adsorbability is favored up to a thermal threshold. CCAC's better adsorbent performance compared to CCC, most notably in elevated temperature conditions, is likely attributed to greater surface contact and porosity exposure that the activation treatment offers, a general outcome that is consistently supported in the researches cited.

4.3.4 Effect of pH on Adsorption of Zn using Corn Cob Activated Carbon and Corn Cob Charcoal

The adsorption behavior of the Zn(II) ions with pH using corn-cob activated carbon (CCAC) and corn-cob charcoal (CCC) shows discernible patterns as shown in figure 8, Appendix viii. The two adsorbents record increasing adsorption with pH in the acidic through slightly acidic-neutral pH range, with maximum within the pH range 5–6. CCC records a maximum of 96.6% elimination of Zn when the pH is 6, while CCAC had

96.1% maximum at the same pH. After this, the two adsorbents record declining efficiency, attaining 93.2% (CCC) and 93.0% (CCAC) for pH 10. This trend is explained in terms of competition of hydrogen ions and the metal ions when the pH is low and precipitation of the zinc hydroxide when the pH is high, therefore declining availability for adsorption. Similar pH-dependent properties have been reported by Tahoon *et al*. (2020), study on the adsorption of Zn, Pb, Cu, and Cd using pectin-based bio-nanomaterials. Optimal adsorption for these metal pollutants was 96.2% for Zn when the pH was 6, 97.5% for Pb when the pH was 5.5, 95.3% for Cu when the pH was 5.5, and 93.8% for Cd when the pH was 6. The results were attributed to the balance of protonation-deprotonation of the adsorbent surface, affecting electrostatic interaction with divalent ions.

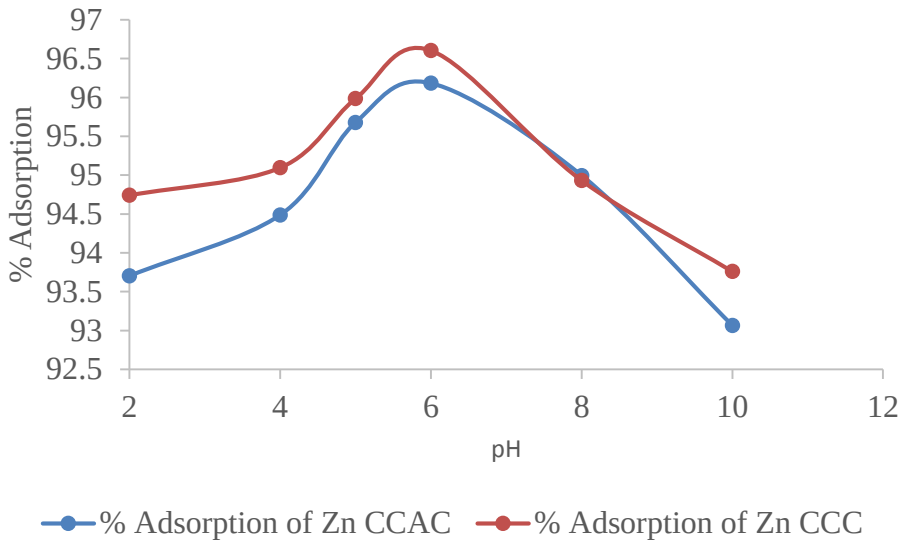

Figure 8: Effect of pH on adsorption of Zn using corn cob activated carbon and corn cob charcoal

4.3.5 Effect of adsorbent dose on adsorption of Zn using Corn Cob Activated Carbon and Corn Cob Charcoal

The experimental data on the adsorption of Zn using corn cob activated carbon (CCAC) and corn cob charcoal (CCC), is presented in figure 9, Appendix viii. The removal efficiency of zinc increased with the increase in adsorbent dosage from 57.9% at 0.025 g for CCAC to 80.3% at 0.05 g and 46.4% at 0.025 g to 74% at 0.05 g for CCC. The maximum adsorption of zinc by CCAC was 94 percent with a dosage of 0.1 g, whereas CCC attained its peak at 93 percent at the same dosage. Above 0.1 g, the capacity to

adsorb Zn ions declines progressively in both adsorbents, as a result of particles aggregation leading to a decrease in the surface area and active sites available. The better adsorption capacity of the CCAC relative to CCC at each dosage level can be ascribed to chemical activation that resulted in more porosity and surface area and therefore the increased number of functional groups and active binding sites of the material. The adsorption at low dosage steadily increases mainly due to the increasing availability of active sites. Nonetheless, the descending curve is as expected in many adsorption measurements, where the use of too much adsorbent results in the overlapping or covering of active sites and thereby a weakened overall performance.

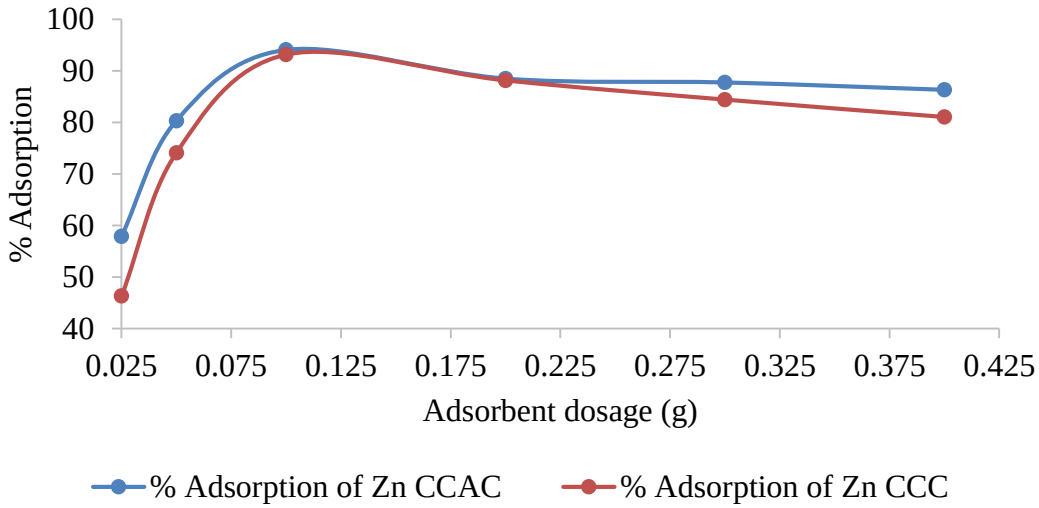

Figure 9: Effect of adsorbent dose on adsorption of Zn using corn cob activated carbon and corn cob charcoal

These results are consistent with Liu *et al.* (2021), studied the adsorption of mercury using modified corn cob activated carbon and discovered that the maximum removal was achieved with 100 mg of adsorbent dose. Micro-mesoporous activated carbon from corn husks was utilized for removal of hexavalent chromium ions and the optimum adsorption was achieved at 1 g/L adsorbent dosage, further increase led to particle agglomeration and pore clogging which decreased the removal capacity (Ammar *et al.*, 2021). Removal of Cd^{2+}, Ni^{2+}, and Zn^{2+} using corn cob and granular activated corn cob from aqueous solutions increased when dosage was adjusted from 0.1 -2.0 g and percent efficiencies of 53.87 % to 100 % for cadmium, 45.87 % to 100 % nickel, and 55.55 % to 100 % zinc using corn cob were reported. The adsorption efficiencies using granular activated corn cob were 69.83 % to 100 % cadmium, 81.97 % to 100 % nickel, and

51.22 % to 100 % zinc, the results confirm the increase of active adsorption sites as dosage is increased (Abdel-Shafy *et al*., 2022).

4.3.6 Effect of contact time on adsorption of Fe using Corn Cob Activated Carbon and Corn Cob Charcoal

The adsorption of iron (Fe) onto corn-cob activated carbon (CCAC) and corn-cob charcoal (CCC), was studied in relation contact time, and the results presented in figure 10, Appendix viii. In the initial time, 30 minutes, CCAC presented 94.6% of adsorption efficiency, increasing significantly to 99.7% in 60 minutes and 99.8% in 90 minutes. The performance was nearly stabilized in the range of 90 minutes with 98.74%, then declined a bit to 94.56% in 120 minutes. These results indicate that CCAC achieves equilibrium fast and with high efficiency, highlighting the presence of high numbers of active binding sites and good attraction of Fe ions. CCC, however, showed a different adsorption pattern. Although the initial relative efficiency was high, 93.51%, there was a notable drop down to 78.54% after 30 minutes and then dropped down to 75.04% after 60 minutes. Despite that, its adsorption performance increased after 30 minutes, and the relative efficiency was 91.42% after 60 and 90 minutes. The relative efficiency stabilized back to 90.03% after 120 minutes. The adsorption pattern shows that CCC may undergo slower diffusion or surface functional group rearrangement, therefore taking longer before adsorption performance is achieved, but ultimately close to the adsorption capability of CCAC. The lagged peak and later stabilization of CCC may also be due to the necessity of time for penetration through the pores and for the complexation processes of the Fe ions.

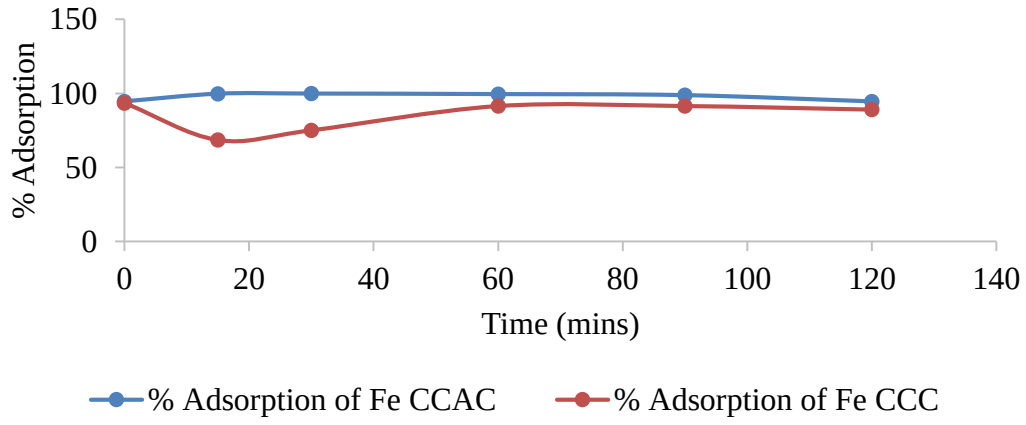

Figure 10: Effect of contact time on adsorption of Fe using corn cob activated carbon and corn cob charcoal

Various research from the literature support these results, a study conducted by Onyekwere *et al*. (2024), used modified corncob for the adsorption of Ni^{2+} from wastewater, obtaining maximum adsorption capacities of 86%, with equilibrium reached in 120 minutes. The adsorption of Fe, Cu, and Mn was achieved at a contact time of 60 minutes with efficiencies of 29.9mg/g, 1.4 mg/g and 8.9 mg/g respectively using one-stage microwave-assisted activarted carbon from Langsat peel raw material (Ni'Mah *et al*., 2023). Similarly, Marin (2022), studied the use of maize stalks in the removal of copper, lead,nickel, cadmium, iron and chromium in synthetic wastewater and the equillibrium was attained at 60 minutes, with efficiencies of 0.052 mg/g Cu^{2+}, 0.024 mg/g Pb^{2+}, 0.042 mg/g Ni^{2+}, 0.050 mg/g Cd^{2+}, 0.056 mg/g Fe^{3+} and 0.063 mg/g Cr^{3+} which correlates CCC results of the current study.

Vafakhah *et al*. (2014), recorded adsorption of Cu^{2+} onto native corn-cob, chemically modified corn-stalk and corn stalk adsorbents from electroplating effluents. Equillibrium adsorption capacities of Cu^{2+} were 0.08 mg/g for corn stalk, 0.17 mg/g modified corn stalk and 0.125 mg/g for corn-cob were achieved at 60, 80 and 120 minutes respectively. Their research confirms the swift and effective adsorption abilities of corncob material for metal ions, as is the case in this research. Nilavazhagi and Felixkala (2021), investigated the adsorption of Fe^{2+} using chemically, physically and chemically-physically activated Jamun fruit seeds. The CAJFS and PCAJFS attained equillibrium at 30 minutes while PAJFS at 60 minutes. These research findings concur that in spite of different biomass sources and activation procedures, the adsorbents based on corncob always have high potential for the adsorption of iron.

4.3.7 Effect of initial concentration on adsorption of Fe using Corn Cob Activated Carbon and Corn Cob Charcoal

The effect of initial concentration on adsorption of Fe using corn-cob activated carbon (CCAC) and corn-cob charcoal (CCC) is shown in figure 11, Appendix viii. The adsorption performance increases with higher initial metal ion concentration, peaks in the optimal range of 10–15 ppm, and then is decreased because adsorbent surface sites become filled. The maximum adsorption attained was 88.6% for CCAC at 15 ppm and 89.2% for CCC at 10 ppm. Though CCAC is in activated form and would therefore be expected to give better performance, CCC actually gave better performance to some degree in the lower concentrations, but CCAC showed greater adsorption in the higher

concentrations because of better structure of the pore spaces and active sites developed through activation.

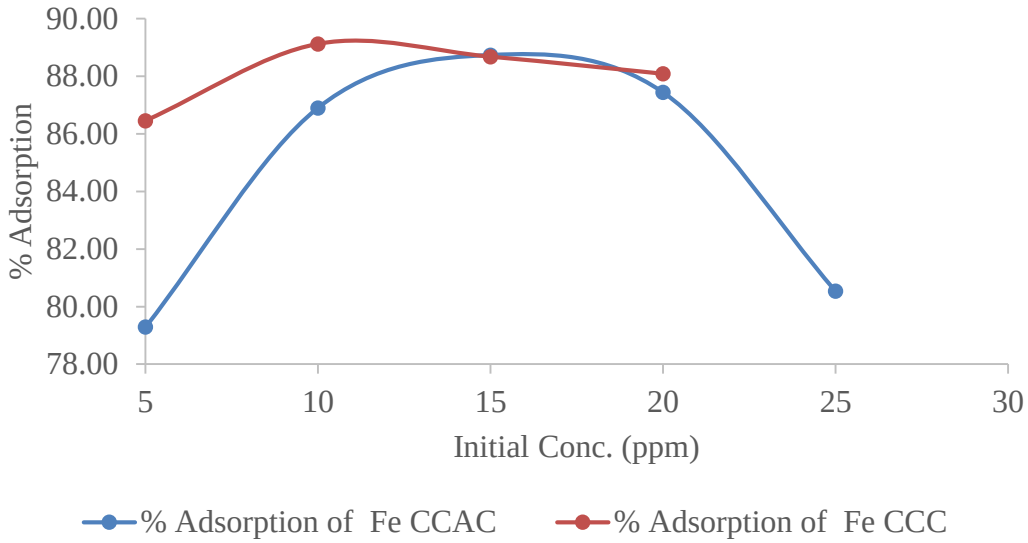

Figure 11: Effect of initial concentration on adsorption of Fe using corn cob activated carbon and corn cob charcoal

These findings are in accordance with previous research involving similar biomass-derived adsorbents. Eletta *et al*. (2023), investigated a mesoporous composite activated carbon from Tithonia diversifolia stalk and Theobroma cacao pod for the adsorption of Pb (II) and Fe (II) simultaneously. They adsorbed 99.7% and 98.7% of Fe (II) and 99.5% and 98% of Pb (II) at 25 ppm concentration and showed that adsorption decreased after this concentration due to the saturation of the pores, in accordance with the decrease registered for CCAC and CCC after 20 ppm concentration. Wang e*t al*. (2023), also examined biomass-activated carbon from crop waste. They achieved 99.76% removal of chromium in the best concentration of 15 ppm of Fe-loaded magnetic activated carbon. The high efficiency was because of better surface reactivity and magnetic separations. The result, despite being higher than the adsorbents of the corn cob, used more advanced means of modification. Sharma et al. (2023), review on biochar from activated biomass from egg shell and java plum seeds demonstrated 78-87% adsorption effectiveness of arsenic at 20 ppm, with the optimum performance being preserved in a larger concentration range due to the homogeneous pore structure and hydrophilic surfaces. Similarly, Giri *et al*. (2012), used Eichhornia crassipes root-activated carbon and the percentage adsorption of Cr (VI) increased from 77% at 10

ppm to 92.24% at 100 ppm which showed potential for use in the decentralized wastewater treatment process.

4.5.8 Effect of temperature on adsorption of Fe using Corn Cob Activated Carbon and Corn Cob Charcoal

The experimental results for the effect of temperature on adsorption of iron using corn cob activated carbon (CCAC) and corn cob charcoal (CCC) are presented in figure 4.11, Appendix vi. The CCAC adsorption efficiency increases from 85.9% when the temperature is 25 °C to a peak of 88.9% when the temperature is 40 °C and then shows a sharp decline to 82.3% at 55 °C. Conversely, CCC is subjected to a greater, less variable adsorption efficiency in the temperature range, spanning from 93.6% when the temperature is 25 °C to 89.8% at 55 °C. This implies that even though CCC demonstrates better baseline performance as well as thermal stability, CCAC is more thermally sensitive, because of the degradation of the porous structures or the alterations of the surface chemistry when high-temperature conditions are employed. The decrease in adsorption after equilibrium was attained resulted from reduced binding affinity and the potential for desorption.

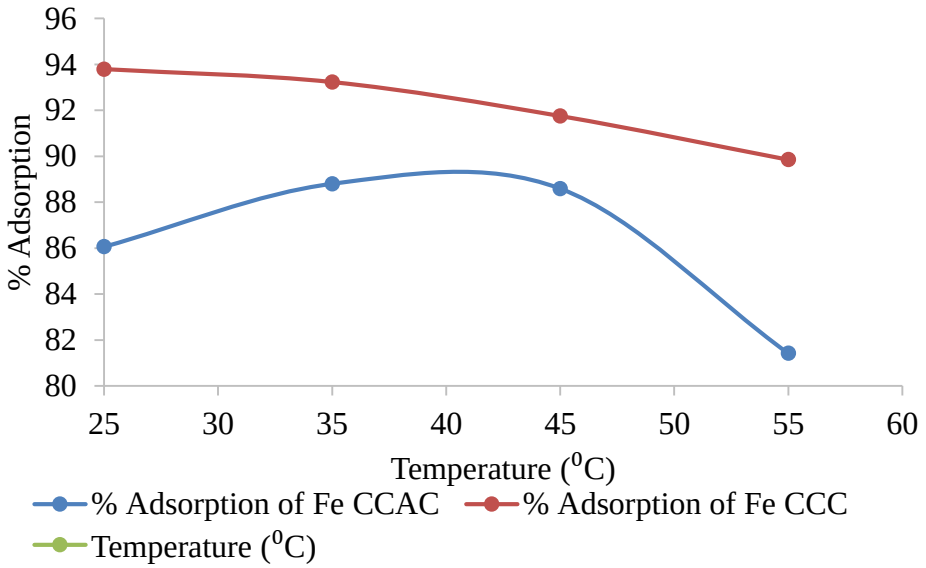

Figure 12: Effect of temperature on adsorption of Fe using corn cob activated carbon and corn cob charcoal

These findings are correlates with El-Bendary and Mahanna (2021), study that examined the adsorption of Fe (III) using modified activated carbon from corn cob and

luffa sponge, and they achieved 91.7% adsorption efficiency at 30 °C, but the adsorption fell when the temperature increased because of lower electrostatic attraction among the Fe ions and adsorbent surface. Also, Adebayo *et al*. (2015) studied the adsorption thermodynamics of Mn (II) and Co (II) onto maize cob activated carbon and achieved optimum sorption at 70 °C, above this temperature the adsorption declined because of the variation in the thermodynamic favorability and breakdown of the newly formed bonds between adsorbate ions and adsorbent surface groups. In general, the variation in thermal stability and adsorbency of CCAC and CCC points towards the structural and chemical differences in surface functionality, adsorbent preparation, and thermal resistance.

4.3.9 Effect of pH on adsorption of Fe using Corn Cob Activated Carbon and Corn Cob Charcoal

The influence of pH on adsorption onto corn cob activated carbon (CCAC) and corn cob charcoal (CCC) is shown in figure 13, Appendix viii. CCAC adsorption mildly rised from 84.1% for pH 2 to a maximum of 86.5% for pH 6, then declines to 80.7% for pH 10. CCC adsorption was generally higher, with 94.0% for pH 2, maximum 96.0% for pH 6, and declined to 92.4% for pH 10. These findings suggest weakly acidic conditions to be optimum for the two adsorbents, with CCC being superior in performance and pH stability in the range of study. The trend is attributed to the change in the surface charge and speciation of the Fe ions within pH levels. The lower removal percentage at pH 2 was due to competition of H^+ with Fe (II) ions for active sorption sites. The decrease recorded above pH 6 resulted from precipitation of the Fe (II) ions and supersaturation of available active sites.

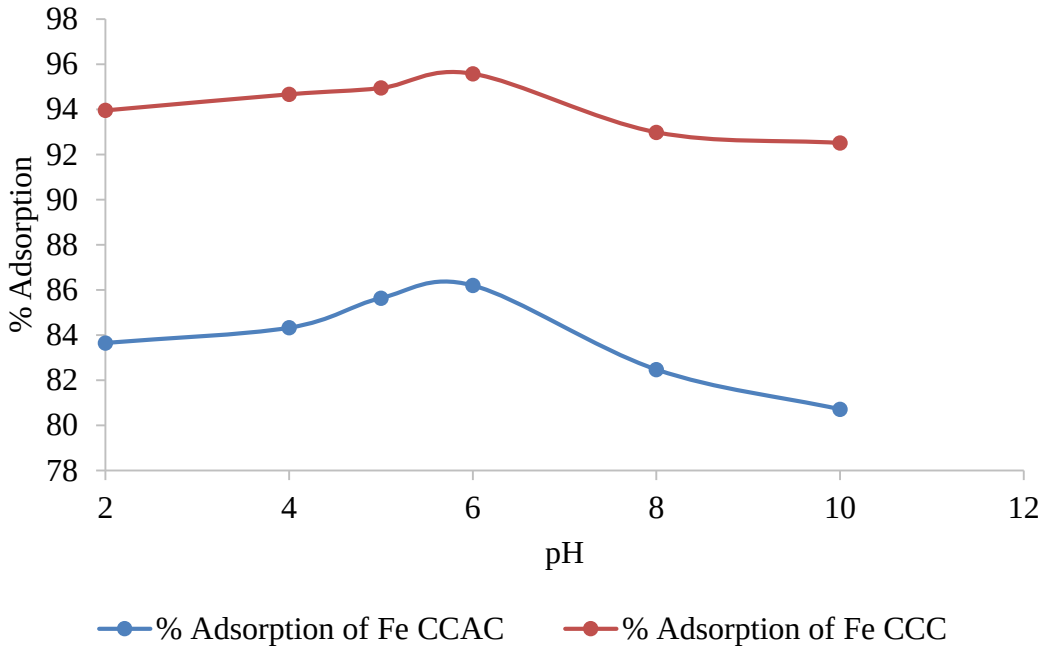

Figure 13: Effect of pH on adsorption of Fe using corn cob activated carbon and corn cob charcoal

These findings are in good agreement with El-Bendary and Mahanna (2021), study that demonstrated the maximum adsorption of Fe(III) in the form of the modified corn cob activated carbon occurred at pH 8, with 94.5% effectiveness, but decreased for lower and higher pH levels due to the competition of protons and precipitation, respectively. Activated charcoal made from corn cobs adsorbed 75.44% of Fe and 56.52% of Mn at optimum pH 4, but this decreased at higher pH due to hydroxide precipitation interrupting the bioavailability of Fe and Mn for adsorption (Viviani and Yanopa, 2023). Correspondingly, Areti *et al*. (2024), produced composite activated carbon from corn cob and banana peel for the adsorption of Cr(VI) and registered adsorption decreased from 96% at pH 2 to 28% at pH 10, then decline was attributed to specaition of chromium at different pH values. Ajala *et al*. (2023), used maize cob activated carbon for adsorbing Fe(II) and achieved 94.5% maximum removal when the pH was 6.3, but the adsorption reduced to 86.0% if the pH is 9.0. The low adsorption in high pH was associated with the precipitation of the $Fe(OH)_3$ and repulsive surface charge effects. Lastly, these studies collectively confirm the present findings, which show that pH significantly influences adsorption performance, and mildly acidic pHs (more so pH 6) are optimal for the removal of Fe using adsorbents made of corn cob. The relative better

adsorption performance of CCC compared to CCAC is likely the result of the difference in the structure of the pores, the surface functional group, and the surface area.

4.3.10 Effect of adsorbent dose on adsorption of Fe using Corn Cob Activated Carbon and Corn Cob Charcoal

The effect of adsorbent dosage on adsorption of iron (Fe) onto activated carbon of corn cob (CCAC) and charcoal of corn cob (CCC) is shown in figure 14, Appendix viii. Increase in dosage from 0.025 g to 0.1 g, led to higher Fe adsorption efficiency for CCAC and CCC to 90%. This increment can be explained by presence of increased active sites and surface area to bind the Fe ions. Nevertheless, above 0.1 g, the adsorption efficiency decreases, due to aggregation of adsorbent particles, causing a decrease in the actual surface area and active sites, and potentially a saturation effect. Compared to CCC at higher doses, CCAC reveal a little less adsorption capacity which could be attributed by various differences in the surface chemistry and porosity. The initial increase in adsorption for both materials agrees to the hypothesis that the ideal dosage brings the maximum availability of binding sites, whereas the too high dosage brings more inter-particle interference and site overlap, which diminishes its performance.

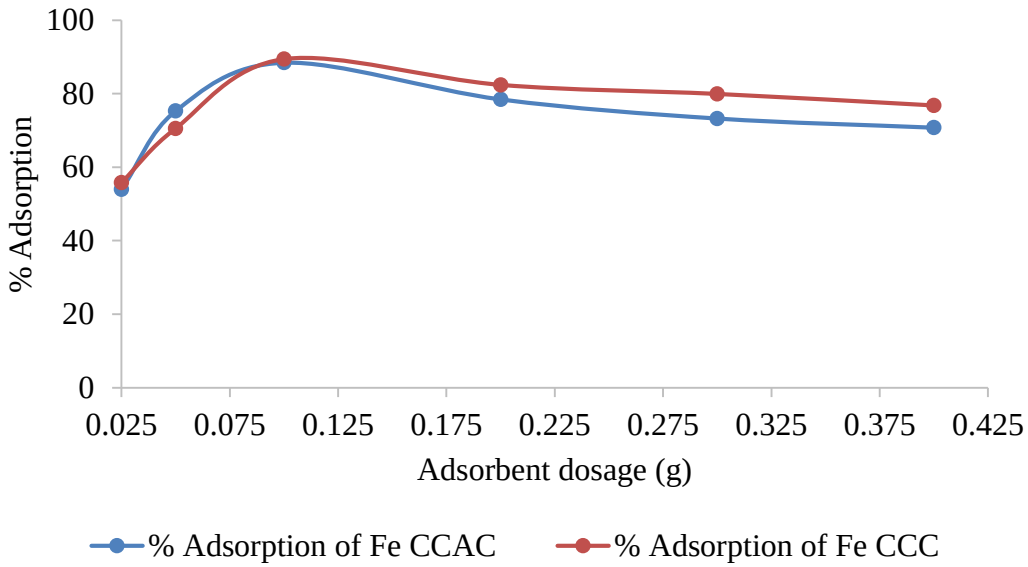

Figure 14: Effect of adsorbent dose on adsorption of Fe using corn cob activated carbon and corn cob charcoal

Similar results are mentioned by El-Bendary and Mahanna (2021), study that examined the removal of Fe(III) with activated carbon of corn cob and luffa sponge and found

that the adsorption efficiency was the highest at the lowest dose of 0.1 g and declined with subsequent dose increase because of agglomeration factors. Likewise, Viviani and Yanopa (2023), used corn cobs as the primary producer of activated charcoal in the removal of Fe and Mn, where the highest Fe adsorption was 70.14% at 1 g, and 41.6% for Mn at 0.5 g subsequently decreased with an increase in dosage. Kamel *et al*. (2025) also confirmed that adsorption capacity decreases with excessive dosage. When they used corn-cob based activated carbon in removing Cr (VI) and Ni (II), and 99.2% of Cr (VI) was removed with 0.289 g and 98.7% Ni (II) wit with 0.94 g dosage, and elevated dosages exhibited lower efficiency because of site overlapping.

Liu *et al*. (2021), produced modified corn cob activated carbon and used it to remove mercury ions and determined that the most suitable dosage was 100 mg. An additional dose addition decreased removal efficiency because of active site clustering. Similarly, Younes *et al*. (2021), applied corn cobs holding nano-zero valent iron to eliminate Cd(II), and achieved 90% elimination with a dosage of 0.01 g, and subsequent weaker performance was reported at higher dosages. Areti *et al*. (2024), used a biochar synthesized with corn cob composites to remove Cr (VI) and achieved an adsorption efficiency of 97.92 percent at the optimal dosage of 0.4 g. The compatibility of these results with the present research supports the vitality of maximizing the adsorbent dose to obtain maximum adsorption capacity.

4.3.11 Pseudo first and second order kinetics of Fe using Corn Cob Charcoal

The kinetic data for the adsorption of Fe using corn cob charcoal (CCC) indicate that the process conforms more closely to the pseudo-second-order kinetic model than the pseudo-first-order model as shown in table 13 (Appendix x, figure 15 and 16, appendix xi,). In the pseudo-first-order model, the rate constant K_1 was $0.024\ min^{-1}$ with an equilibrium adsorption capacity Qe of 2.25 mg/g and a correlation coefficient R^2 of 1.00. Conversely, the pseudo-second-order model yields a higher rate constant K_2 of 0.1289 g/mg·min, a slightly greater Qe of 2.33 mg/g, and a correlation coefficient R^2 of 0.99638. Although the R^2-value for the pseudo-first-order model appears perfect, the slight overestimation of Qe in the second-order model and its compatibility with chemisorption mechanisms suggest it better captures the rate-limiting step involving electron sharing or exchange between Fe ions and active sites. Igwe and Abia (2007)

studied Fe(II), Co(II), and Cu(II) adsorption on maize cob and noted that pseudo-second-order kinetics best described the data across all metals, with Fe(II) adsorption achieving R^2=1.002 for Co, Fe 1.008 and Cu 0.9994, supporting the chemisorptive mechanism observed with CCC

Table 13: Pseudo first and second order constants for corn cob charcoal

Pseudo first order			Pseudo second order		
K_1	Qe	R^2	K_2	Qe	R^2
0.024min^{-1}	2.25mg/g	1	0.1289g/mg.min	2.33mg/g	0.99638

The results of Alam et al. (2024), revealed that corn-cob biomass-derived magnetic activated carbon for the removal of dyes, also evidencing its predictive ability for heterogeneous systems of adsorption. Onyekwere et al. (2024), also assayed modified corn cob bioadsorbents for Ni ions and found that pseudo-second-order kinetics most fit of R^2=0.994.

4.3.12 Pseudo first and second order kinetics of Fe using corn cob activated carbon

The pseudo 1st and 2nd order kinetics of CCAC for adsorption of Fe are presented in table 14, Appendix x, figure 17 & 18 in Appendix xi. Pseudo-first-order kinetics yielded a rate constant K_1 of 0.037 min^{-1}, an equilibrium adsorption capacity Qe of 2.495 mg/g, and correlation coefficient R^2 of 0.97795. In comparison, pseudo-second-order kinetics yielded superior fit with higher correlation coefficient of 0.9989 and rate constant K_2 of 0.4056 g/mg·min and an equilibrium adsorption capacity Qe of 2.386 mg/g. Although the pseudo-first-order kinetics achieved a fair correlation, the higher value of R^2 in the pseudo-second-order kinetics suggests that the rate-limiting step entails chemisorption processes involving the exchange or sharing of electrons between the adsorbent and the Fe ions.

Table 14: Pseudo first and second order constants for corn cob activated carbon

Pseudo first order			Pseudo second order		
K_1	Qe	R^2	K_2	Qe	R^2
0.037min^{-1}	2.495mg/g	0.97795	0.4056g/mg.min	2.386mg/g	0.9989

This behaviour aligns with Adebayo *et al*. (2015), study on Co (II) and Mn (II) adsorption using maize cob activated carbon and obtained a pseudo-second-order model fit with R^2=0.968 and 0.997 respectively, reinforcing the predictive strength of

the model in metal ion adsorption systems. Putranto *et al*. (2022), investigated the methylene blue adsorption over corn cob activated carbon and followed the pseudo-second-order kinetics with K_2 of 0.0119, Qe=18.904 and correlation coefficient of 0.998 as compared to first order model with 0.959. The information, asserts that analogous kinetic behaviour applies to dyes and metal ions alike based on the accessibility of functional groups and surface charge state.

4.3.13 Pseudo first and second order kinetics of Zn using Corn Cob Activated Carbon

Pseudo-first-order and pseudo-second-order models were used to determine the adsorption kinetics of zinc (Zn) on corn cob activated charcoal (CCAC), data is shown in table 15, Appendix x and figure 19 and 20 in Appendix xi. The results indicate that the pseudo-second-order mechanism of kinetics provides a better explanation of the adsorption process. The pseudo-first-order model had a small rate constant K_1 of 0.008 min^{-1}, an equilibrium adsorption capacity Q_e of 2.2895 mg/g, and a relatively average correlation coefficient R^2 of 0.76332. The pseudo-second-order model, on the other hand, achieved a much higher value of correlation coefficient of 0.99937 with a rate constant K_2 of 1.169 g/mg·min and an equilibrium capacity Q_e of 2.229 mg/g. The almost perfect correlation suggests that the chemisorption via valence forces or exchange of electrons is the rate-controlling step during the zinc adsorption on CCAC.

Table 15: Pseudo first and second order constants for corn cob activated carbon

Pseudo first order			Pseudo second order		
K_1	Qe	R^2	K_2	Qe	R^2
0.008min^{-1}	2.2895mg/g	0.76332	1.169g/mg.min	2.229mg/g	0.99937

These findings are consistent with Igwe *et al*. (2011), study that applied maize cob for Zn(II) adsorption and observed that the pseudo-second-order model had superior correlation ($R^2 = 0.9998$) and better agreement with experimental Q_e than the first-order model, underscoring the reliability of the model for Zn (II) sorption from aqueous media. Yusop *et al*. (2022) investigated Zn (II) adsorption using coconut shell activated carbon and found similar kinetic behaviour, with the second-order model yielding Q_e = 1.01 mg/g, K_2 = 1.04 g/mg·min, and R^2 = 0.95, illustrating that the model is broadly applicable to bio char-derived adsorbents regardless of biomass source.

4.3.14 Pseudo first and second order kinetics of Zn using Corn Cob Charcoal

The pseudo first and second order kinetics data for adsorption of zinc onto CCC is shown in table 16, Appendix x and figure 21 and 22, Appendix xi. Adsorption kinetics of zinc (Zn) on corn cob charcoal (CCC) evidently show that the pseudo-second-order kinetic model provides a better depiction of the sorption process than the pseudo-first-order model. The pseudo-first-order parameters give a rate constant K_1 of 0.0119 min^{-1} and an equilibrium adsorption capacity Q_e of 2.2908 mg/g; however, the correlation coefficient R^2 is very small and unsatisfactorily low at 0.18981. This small value of R^2 suggests a weak fit and implies that the model is unable to properly describe the mechanism of Zn adsorption on CCC. In contrast, the pseudo-second-order model has a much larger rate constant K_2 of 4.67 g/mg·min and an equilibrium capacity Q_e of 2.2715 mg/g with a perfect correlation coefficient value of 0.99998. This implies that the adsorption follows chemisorption behaviour involving the sharing of electrons or valence bond interactions between the Zn ions and the functional groups located on the surface of the CCC.

Table 16: Pseudo first and second order constants for corn cob charcoal

Pseudo first order			Pseudo second order		
K_1	Qe	R^2	K_2	Qe	R^2
0.0119min^{-1}	2.2908mg/g	0.18981	4.67g/mg.min	2.2715mg/g	0.99998

These results are consistent with findings with Ahmed et al. (2022) study that explored corn-cob carbon for Zn(II), Cd(II), and Ni(II) removal and reported that Zn adsorption followed pseudo-second-order kinetics with Q_e = 0.3 mg/g, K_2 = 7.09 g/mg·min, and R^2 = 0.989, further confirming the chemical nature of Zn binding onto corn-based carbons. Similarly, Tejada-Tovar et al. (2021), study that evaluated Cd(II) adsorption onto corn cob-derived biomass, found that pseudo-second-order kinetics described the data better, yielding Q_e = 294.07 mg/g and R^2 = 0.98, supporting the current findings that chemisorption is the primary mechanism.

4.3.15 Freundlich and Langmuir Isotherm for Zn using Corn-cob Activated Charcoal

The adsorption of zinc on corn-cob activated charcoal (CCAC) was successfully represented using the Freundlich and Langmuir isotherm models as presented in table 17, Appendix x and figure 23 and 24, Appendix xi. The Freundlich model resulted had

KF=2.35 mg/g and intensity parameter n = 1.387 with a correlation coefficient R^2 = 0.9359, indicating favorable multilayer adsorption on a heterogeneous surface. The value of n > 1 implies that the adsorption is efficient and desirable. Conversely, the Langmuir isotherm assuming monolayer coverage on a surface with finite, uniform adsorption sites resulted in a maximum adsorption capacity Qmax = 10.11 mg/g, Langmuir constant KL=0.3239 L/mg, and a slightly lower correlation coefficient of R^2 = 0.88149. This suggests that while the Langmuir model provides a reasonable description, the Freundlich model offers a more accurate representation in this case.

Table 17: Freundlich and Langmuir isotherm constants for Zn using corn-cob activated charcoal

Freundlich isotherm			Langmuir isotherm		
KF	n	R^2	Qmax	KL	R^2
2.35mg/g	1.387	0.9359	10.11mg/g	0.3239L/mg	0.88149

Abdel-Shafy *et al*. (2022), reported that Zn (II) adsorption on granular activated corn-cob carbon fit best with the Langmuir model, with R^2=0.96, compared to a freundlich model fit of R^2=0.534, which indicated monolayer adsorption process. Okafor et al. (2015), examined adsorption of Pb (II) using maize cob-derived carbon and also observed superior fitting to the Langmuir model, with R^2=0.98 confirming homogeneous surface interactions as opposed to this study. Adebayo et al. (2015) conducted studies using maize cob activated carbon for Mn (II) and Co (II) and found that the Langmuir model gave the best fit for the metals with R^2=0.915, and 0.925 respectively compared to freundlich model with R^2=0.887 and 0.864. The difference from the results of this study is attributed to different surface groups on the adsorbent after modification. Alzaydien (2010), similarly demonstrated Zn (II) preference for heterogeneous surfaces using modified corn cob, with a stronger correlation R^2=0.99 compared to the Langmuir model R^2=0.98.

4.3.16 Freundlich and Langmuir isotherm for Zn using Corn-cob Charcoal

The adsorption of zinc on corn-cob charcoal (CCC) was successfully represented using the Freundlich and Langmuir isotherm models as presented in table 18, Appendix x and figure 25&26, Appendix xi. The Freundlich model offers a better fit to the experimental data than the Langmuir model. The Freundlich isotherm gave a large adsorption capacity constant KF= 116.84 mg/g and an intensity factor n = 0.1634 with a correlation

coefficient of R^2 = 0.9497. Conversely, the Langmuir model yielded a monolayer adsorption capacity Qmax= 0.4386 mg/g, a Langmuir constant KL= 1.561 L/mg, and a lower correlation coefficient R^2 = 0.85515, suggesting that the monolayer adsorption assumption is less appropriate for this system.

Table 18: Freundlich and Langmuir isotherm constants for Zn using corn-cob charcoal

Freundlich isotherm			Langmuir isotherm		
KF	n	R^2	Qmax	KL	R^2
116.84mg/g	0.1634	0.9497	0.4386mg/g	1.561L/mg	0.85515

Ahmed *et al*. (2022) used corn-cob carbon and observed that the Langmuir model yielded Qmax = 0.08 mg/g and KL =1.3 L/mg with R^2=0.97, while the Freundlich model provided KF=0.185mg/g, n=1.42n = 7.2, and R^2 = 0.205, indicating favorable adsorption onto a homogeneous surface as opposed to this study. Similarly, Tejada-Tovar *et al*. (2021), study that evaluated Cd(II) adsorption onto corn cob-derived biomass, found that Langmuir model described the data better, with R^2 = 0.98, supporting monolayer adsorption on homogeneous sites.

4.3.17 Freundlich and Langmuir isotherm for Fe using Corn Cob Activated Carbon

The freundlich and Langmuir isotherm for adsorption of iron (Fe) onto corn-cob activated charcoal (CCAC) data is presented in table 19, Appendix x (figure 27&28, Appendix xi). Freundlich isotherm model gave a KF = 1.1498 mg/g and an intensity factor n = 0.5826 with a correlation coefficient of R^2 = 0.90703. Conversely, the Langmuir model gave a maximum monolayer adsorbency Qmax = 3.692 mg/g, a Langmuir constant KL = 0.2435 L/mg, and a smaller correlation coefficient R^2 = 0.51623, proving that assumptions of monolayer coverage do not adequately represent the interaction of Fe with the CCAC surface. Thus, the experimental data was best suited to freundlich model implying that heterogeneous surfaces and different binding energies of the CCAC adsorbent controlled the process.

Table 19: Freundlich and Langmuir isotherm constants for Fe using corn cob activated carbon

Freundlich isotherm			Langmuir isotherm		
KF	n	R^2	Qmax	KL	R^2
1.1498mg/g	0.5826	0.90703	3.692mg/g	0.2435L/mg	0.51623

Study conducted by El-Bendary and Mahanna (2021) demonstrated that activated carbon synthesized from corn cobs and luffa sponge removed Fe (III) effectively, following Freundlich behaviour with correlation coefficient of 0.993 and 0.882 for the two adsorbents, outperforming the Langmuir model. In contrast, Adebayo *et al*. (2015) reported that Mn (II) and Co (II) adsorption using maize cob activated carbon better fitted the Langmuir model, with R^2=0.915 and 0.925, although the Freundlich model also showed a reasonable fit with R^2=0.887 and 0.864 respectively. Yu *et al*. (2020), also applied corn-cob activated carbon for the removal of roxarsone and was found to obey Langmuir isotherm with good accuracy R^2=0.9991 compared to freundlich isotherm with R^2=0.8491 and a surface heterogeneity index (n < 1) indicative of non-uniform sites. These findings confirm multilayer and monolayer adsorption can occur onto activated corn-cob.

4.3.18 Freundlich and Langmuir isotherm for Fe using Corn-cob Charcoal

The Freundlich and Langmuir isotherms experimental data for the adsorption of Fe onto corn-cob charcoal (CCC) is presented in table 20, Appendix x and figure 29 & 30, Appendix xi. The Freundlich constants are KF = 1.8034 mg/g and n = 0.9063, and the correlation coefficient is strong, R^2= 0.97692. The Langmuir, however, gave the highest monolayer adsorption capacity of Qmax= 30.497 mg/g and the Langmuir constant, KL = 0.0556 L/mg, yet with a rather low correlation coefficient of R^2 = 0.16216, indicating that the model does not fit well. The adsorption of Fe onto CCC was best described by freundlich model indicating multilayer adsorption took place on heterogeneous surfaces of the adsorbents with different binding energies

Table 20: Freundlich and Langmuir isotherm constants for Fe using corn-cob charcoal

Freundlich isotherm			Langmuir isotherm		
KF	n	R^2	Qmax	KL	R^2
1.8034mg/g	0.9063	0.97692	30.497mg/g	0.0556L/mg	0.16216

The findings correlates with Vafakhah *et al*. (2014), study on removal of copper (II) ions from electroplating effluent using corn-cob, which reported best fit in freundlich isotherm with R^2=0.999 compared to Langmuir with R^2=0.972. Contrary to this study adsorption of Fe (II) using raw jamun fruit seeds followed Langmuir isotherm with R^2=0.9904 as opposed to freundlich isotherm with R^2=0.896 indicating monolayer

adsorption onto adsorbent surfaces (Nilavazhagi and Felixkala, 2021). Removal of cadmium from wastewater using corn cobs had better fit into Langmuir isotherm R^2=0.99 while freundlich isotherm reported a lower value of 0.94 (Younes *et al*., 2021). The difference in results from this study is attributed to surface functional groups retained on the adsorbent surface as a result of thermal and acid treatment during the synthesis of the adsorbents.

CHAPTER FIVE

SUMMARY, CONCLUSION AND RECOMMENDATION

5.1 Summary

Water resources are essential for life and globally over 5 billion inhabitants are dependent on ground water and surface water system. The degradation of water resources is a much studied phenomena and can be caused by natural processes, human activities as well as considerable chemical compounds due to industrial revolution. Water quality depends on it physicochemical and biological parameters. Due to increased anthropogenic activities has led to changes in pH, temperature and essential and non-essential trace metals in water rendering it unfit for human use. Various techniques have been developed to remove contaminants from water but are expensive and environmentally unfriendly.

5.2 Conclusion

This study focused mainly on determination of physico-chemical and bacteriological properties of Nguue spring and river Mutonga and evaluation of corn cob carbon powder as a low cost adsorbent. The prepared adsorbents were then evaluated for their characterization and adsorption properties by using zinc and iron as model pollutant in aqueous solution. The empirical data generated on the physicochemical and microbial quality of water from Nguue Spring and River Mutonga, adds to the existing body of knowledge in environmental and analytical chemistry. In addition, it advances the application of locally available biomass, specifically maize cobs, in water remediation. Both River Mutonga and Nguue Springs experience seasonal variations in physico-chemical parameters. Batch adsorption experiments are affected by pH, initial concentration, dosage, temperature and contact time. Adsorption process was described by Freundlich adsorption isotherms and Pseudo secnd order kinetics.

5.3 Recommendations of the Study

The following recommendation were made from the study:

i. Periodic monitoring of physicochemical properties especially for parameters like zinc, iron, nitrates and phosphates since they pose health concerns after bioaccumulation.
ii. The level of microbiological contamination in the study area pose a health concern hence need for intervention by county government to put measures in

place to curb anthropogenic activities that amount to contamination and proper solid waste management to safeguard drinking water to consumers.

iii. Corn cob activated carbon and corn cob charcoal can be used as a low-cost adsorbent material for removal of zinc and iron from surface and contaminated water.

5.4 Recommendations for Further Research

The following recommendation were made for future study:

i. Extension of this work can be done by determination of colour, turbidity, manganese and sulphates in Nguue spring and River Mutonga to be done.
ii. Assessment of waterborne diseases affecting residents who consume water from Nguue spring and River Mutonga.
iii. Extension of this work can be done to cover entire stream and spring.
iv. Future work can be done on other rivers and springs in the neighbourhood.

REFERENCES

Abd-Elhamad, A.I and Aly, H.F. (2018). Removal of Fe (III) from Aqueous Solution Using Thiosalcyclic Acid as an Efficient and Novel Adsorbent. *Egypt. J. Chem* 61(4) 617-627

Abdel-Shafy, H. I., Hefny, M. M., Ahmed, H. M., and Abdel-Haleem, F. M. (2022). Removal of cadmium, nickel, and zinc from aqueous solutions by activated carbon prepared from corncob-waste agricultural materials. *Egyptian Journal of Chemistry*, *65*(3), 677–687

Adebayo, G., Adegoke, H., Jamiu, W., Balogun, B., and Jimoh, A. (2015). Adsorption of Mn (II) and Co (II) ions from aqueous solution using Maize cob activated carbon: Kinetics and Thermodynamics Studies. *Journal of Applied Sciences and Environmental Management*, *19*(4), 737–748

Ademiluyi, F.T and Nze, J.C. (2016). Sorption characteristics for multiple adsorption of heavy metal ions using activated carbon from Nigerian bamboo. *Journal of Material Science and Chemical Engineering*, 4, 39-48

Ademiluyi, T. and David-west, E.O. (2011). Effects of chemical activation on adsorption of heavy metals using activated carbon from waste materials, *Journal of Nigerian society of chemical engineers*, 6,74-209

Ademiluyi, T., Gumus, R., Adenji, S.M. and Jasem, O.T. (2007). Effects of process condition on characterisation of activated carbon from waste Nigerian Bamboo, *Journal of Nigerian society of chemical engineers*, 24,1-2

Ajala, L. O., Ali, E. E., Nnachi, E. O., and Onwukeme, V. I. (2023). Design of locally sourced activated charcoal filter from maize cob for wastewater decontamination: An approach to fight waste with waste. *Physical Sciences Reviews*, *8*(8), 1213–1232

Ajamal, M., Rao, R., Anwar, S., Ahamad, J. and Alunad, R. (2003). Adsorption studies on rice husk. *Removal and Recovery of Cd (II) from wastewater*. *Bioresource Technology*, 86, 147-149

Akhtar, N., Ishak, M.,Ahmad, M., Umar, K., Yusuff, M.M., Anees, M., Qadir, A., Almanasir, Y.A. (2021). Modification of the Water Quality Index (WQI) Process for Simple Calculation Using the Multi-Criteria Decision-Making(MCDM) Method: A Review. Water 13, 905

Alam, S., Ilyas, M., Ullah, S., ur Rahman, N., Zahoor, M., Umar, M. N., and Ullah, R. (2024). Fabrication of magnetic activated carbon from corn-cob biomass for the removal of acidic dyes from wastewater. *Desalination and Water Treatment*, *317*, 100049

Aldrich. Suggestion for cleaning glasswares. Corning, 2009. AL-228 Technical Bulletin. 6000N.Teutonia Ave., Milwaukee, WI 53209

Alexis. B.N., Periyasamy. S., Amandine, L., Patience. N., Jean. P.O., Alphonse, M., Crispin. K.M., Josue. I.M., Pius. T.M., and John. P. (2017). Seasonal variability of water quality by Physicochemical Indexes and traceable Metals in Suburban area in Kikwit Democratic Republic of Congo. *International Soil and Water Conservation Research*, 5(2), 158-165

Ali, H., Khan, E., and Ilahi, I. (2019). Environmental chemistry and ecotoxicology of hazardous heavy metals: Environmental persistence, toxicity, and bioaccumulation. Journal of Chemistry, 2019, 6730305. https://doi.org/10.1155/2019/6730305

Alotaibi, E.S. (2009). Bacteriological assessment of urban water sources in Khamis Mushait Governorate, south western Saudi Arabia. *International Journal of Health Geographics*, 8(16)

Alzaydien, A. (2010). Surface Characterization, Isotherm Modeling and Thermodynamics of Zn (II) Adsorption onto Modified Corncob. *Jordan Journal of Chemistry (JJC)*, *5*(3), 253–270

Amit, B. and Monicha, A.K. (2006). Conventional and non-conventional adsorbents for removal of pollutants from water. *Journal of Indian Chemical Technology*, 13, 203-217

Ammar, N. S., Fathy, N. A., Ibrahim, H. S., and Mousa, S. M. (2021). Micro-mesoporous modified activated carbon from corn husks for removal of hexavalent chromium ions. *Applied Water Science*, *11*(9), 154

Amorim, C. A., and Moura, A. d. N. (2021). Ecological impacts of freshwater algal blooms on water quality, plankton biodiversity, structure, and ecosystem functioning. Science of the Total Environment, 758, Article 143605. https://doi.org/10.1016/j.scitotenv.2020.143605

Anyamene, N.C and Osiagu, D. (2014). Bacteriological analysis of sachet water sold in Akwa Metropolis Nigeria, *International Journal of Agriculture and Biosciences*, 3,120- 122

APHA (1999) Standard Methods for the Examination of Water and Wastewater. 20th Edition, American Public Health Association/American Water Works Association/Water Environment Federation, Washington DC

APHA (2005) Standard Methods for the Examination of Water and Wastewater. 21st Edition, American Public Health Association/American Water Works Association/Water Environment Federation, Washington DC

APHA (2012) Standard Methods for the Examination of Water and Wastewater. 22nd Edition, American Public Health Association/American Water Works Association/Water Environment Federation, Washington DC

Areti, H. A., Jabesa, A., Muleta, M. D., and Emana, A. N. (2024). Adsorptive performances and valorization of green synthesized biochar-based activated carbon from banana peel and corn cob composites for the abatement of Cr(VI) from synthetic solutions: Parameters, isotherms, and remediation studies. Biomass Conversion and Biorefinery. Heliyon, 10(13), Article e33811. https://doi.org/10.1016/j.heliyon.2024.e33811

Areti, H. A., Jabesa, A., Muleta, M. D., and Emana, A. N. (2024). Adsorptive performances and valorization of green synthesized biochar–based activated carbon from banana peel and corn cob composites for the abatement of Cr (VI) from synthetic solutions: Parameters, isotherms, and remediation studies. *Heliyon*, *10*(13)

Arismendi, I., Johnson, S. L., and Dunham, J. B. (2022). Climate change and freshwater ecosystems: Impacts across multiple scales. Freshwater Biology, 67(1), 3–16. https://doi.org/10.1111/fwb.13815

Asfaw, E. D., Argaw, M., and Elias, E. (2018). Spatial and seasonal variation in physicochemical parameters and heavy metals in Awash River, Ethiopia. Applied Water Science, 8(1), 177. https://doi.org/10.1007/s13201-018-0803-x

Asfaw, M. D. (2022). Effect of seasonal variation on the levels of heavy metals and physicochemical parameters of borehole water in Woreillu Town, Amhara. Applied Water Science, 12(6), 128. https://doi.org/10.1007/s13201-022-01648-5

Assirey, E. A., and Altamimi, L. R. (2021). Chemical analysis of corn cob-based biochar and its role as water decontaminants. *Journal of Taibah University for Science*, *15*(1), 111-121

Babel, S. and Kurniawan, T.A. (2002). Low-cost adsorbents for heavy metals uptake from contaminated water. *Journal of Hazardous Materials*, 97, 219-243

Barakat, M.A. (2011). New trends in removing heavy metals from industrial wastewater. *Arabian Journal of Chemistry*, 4, 361-377

Bayou, J., Rwiza, M, J., and Mtei, K. M. (2023). Applicability of bio-adsorbent synthesized from maize/corn plant residues for heavy metals removal from aquatic environment: an insight review

Beechie, T., Imaki, H., Greene, J., Wade, A., Wade, A., Wu, H., Pess, G. (2013). Restoring salmon habitat for changing climate. *River Res Appl* 29, 936-960

Benaisa, S., Arhoun, B., Villen, G. M. El mail, R., Gomez, L.C., Rodriguez, M and Jose, M (2022). Kinetics, Equilibrium and Thermodynanics studies on Fe^{3+} Removal from Aqueous Solutions by chemically Modified Brown Algae. *Iran. J. Chem. Eng.* 41(7) 2022

Bhat, N. A., et al. (2020). Agricultural intensification and its impact on groundwater quality: A case study. Environmental Science and Pollution Research, 27(8), 8240–8252. https://doi.org/10.1007/s11356-019-07232-3

Burudi,K.R and Gedala, R.K (2014). Study on determination of physicochemical parameters of groundwater in industrial area of pydibheemavaram, Vizianagaram District, Andhrapradesh, India. *Austin Journal of Public Health and Epidemiology* 1(2) 1-2

Centers for Disease Control and Prevention. (2024). Germs that can contaminate tap water. https://www.cdc.gov/drinking-water/causes/germs-that-can-contaminate-tap-water.html

Chen, J.Z., Tao, X.C., Xu, J., Zhang, T. and Liu, Z.L. (2005). Biosorption of lead, cadmium and mercury by immobilized *Microcystis aeruginosa* in a column. *Process Biochemistry*, 40, 3675-3679

Chigor, V.N., Umoh, V.J., Okuofu, C.A., Ameh, J.B., Igbinosa, E.O., Okoh, A.I. (2012). Water quality assessment: Surface water sources used for drinking and irrigation in Zaria, Nigeria are a public health hazard. *Environ Monit Assess*. 184, 3389–3400.

Christica, I. and Muchlisyam, R.J. (2018). Activated carbon utilization from corn cob (*Zea mays*) as a heavy metal adsorbent in industrial waste. *Asian Journal of Pharmaceutical Research and Development* 6(5), 1-4

Contreras, E., Jurado-Ezqueta, M., Pimentel, R., Serrano, L., Hidalgo, C., Jiménez, A., and Polo, M. J. (2024). Assessment of seasonal and annual patterns in phosphorus content in a monitored catchment through a partitioning approach based on hydrometeorological data. Environmental Research, 242, 117501. https://doi.org/10.1016/j.envres.2023.117501

Dai, Y., Sun, Q., Wang, W., Lu, L., Liu, M., Li, J.,Yang, S., Sun, Y., Zhang, K. and Xu, J. (2018). Utilization of agricultural waste as adsorbent for removal of agricultural waste as adsorbent for the removal of contaminants: A review. *Chemosphere* 211, 235-253

Dara, S. and Mishra, D. (2011). A textbook of Environmental Chemistry and pollution control. New Delhi: Chad and company ltd

Dargie, H and Nigus, G (2021). Groundwater quality assessment of Chilanchil a bay watershed: the case of Bahir-Dar city waste disposal site. *Journal of Environmental Engineering and Landscape Management* 29(2) 123-134

Dodds, W. K., and Smith, V. H. (2016). Nitrogen, phosphorus, and eutrophication in streams. Inland Waters, 6(2), 155–164. https://doi.org/10.5268/IW-6.2.909

Ebelegi, A.N., Ayawei, N. and Wankasi, D. (2020). Interpretation of adsorption thermodynamics and kinetics. *Open Journal of Physical Chemistry*, 10, 166-182

Edet, U.A. and Ifelebuegu, A.O. (2020). Kinetics, isotherms and thermodynamic modelling of the adsorption of phosphate from model wastewater using recycled brick waste. *Processes*, 8(665), 1-15

El-Bendary, N., and Mahanna, H. (2021). High-performance removal of iron from aqueous solution using modified activated carbon prepared from corn cobs and luffa sponge. *Desalination and Water Treatment*, *213*, 348–357

Eletta, O. A., Ayandele, F. O., and Ighalo, J. O. (2023). Adsorption of Pb (II) and Fe (II) by mesoporous composite activated carbon from Tithonia diversifolia stalk and Theobroma cacao pod. *Biomass Conversion and Biorefinery*, *13*(11), 9831–9840

EPA. (2012). *Cyanobacteria and Cyanotoxins*: Information for drinking water systems United State Environmental Protection Agency: Washington, DC, USA

Esalah, J.O., Weber, M.E. and Vera, J.H. (2000). Removal of lead, cadmium and zinc from aqueous solution by precipitation with sodium di-(n-octyl) phosphinate. *Canadian Journal of Chemical Engineering*, 78, 948-954

Eureka, F (2024). Effects of High TDS on Health and Home Appliances, India. Retrieved online on Friday 26/07/2025

Feng, N. and Guo, X. (2012). Characteristics of adsorptive capacity and mechanisms on adsorption of copper, lead and zinc modified orange peels. *Journal of Transactions of Nonferrous Metal Society of China*, 22, 1224-1231

Fergusson, J.E. (1990). The Heavy Elements: Chemistry, Environmental Impact and Health Effects, Pergamon Press; Oxford, UK, 614

Fertu, D. I., Bulgariu, L., and Gavrilescu, M. (2022). Modeling and optimization of heavy metals biosorption by low-cost sorbents using response surface methodology. *Processes*, *10*(3), 523

Foo, K. Y and Hameed, B. H. (2010). Insights into the Modeling of Adsorption Isotherm Systems. *Chem. Eng. J.* 156 (1), 2–10. 10.1016/j.cej. 2009.09.013. [DOI] [Google Scholar]

Fred, A.O (2003). Heavy metals concentrations and burden in the bivalves (*Anadara senilia* (Senilis) *Crassostrea tulipa* and *Perna perna*) from lagoons in Ghana: Model to describe mechanism of accumulation/ excretion. *African Journal of Biotechnology* 2(9), 280-287

Gaber, E., Yahia, A. and Abdulrahim, A. (2012). Cadmium and lead Biosorption by *Chlorella vulgaris*. Sixteenth International Water Technology Conference, IWTC, Instanbul, Turkey.

Gadd G.M. (2007). Biosorption: Critical review of scientific rationale, environmental importance and significance for pollution treatment. *J. Chem. Technol. Biotechnol.* 84, 13–28

Gangil. R, Tripathi. R, Patyal. A, Dutta. P and Mathur.K.N, (2013). Bateriological evaluation of packaged bottle water sold at Jaipur city and its public health significance, *Veterinary World*, 6(1), 27-30

Gardiner, K. W. (2013). Flame photometry. *Physical Methods in Chemical Analysis* 3, (3)219

Gebrewold, B. D., Kijjanapanich, P., Rene, E. R., Lens, P. N., and Annachhatre, A. P. (2019). Fluoride removal from groundwater using chemically modified rice husk and corn cob activated carbon. *Environmental Technology*

Giri, A. K., Patel, R., and Mandal, S. (2012). Removal of Cr (VI) from aqueous solution by Eichhornia crassipes root biomass-derived activated carbon. *Chemical Engineering Journal*, *185*, 71–81

Gray, J. (2004). Conductivity analyzer and their application in: lehi RD (ed). Environmental instrumentation and analysis. Wiley Handbook, New York 491-510

Hasan, I. (2018). Water Quality Assessment: A Case Study of the Jhenai River in Bangladesh. *RA J. Appl. Res.* 4, 1884–1888

Hiscock, K.M. and Bense, V.F. (2014). *Hydrogeology: Principle and Practice*. 2nd Edition,Wiley Black Science Publisher, Hoboken, NJ

Huang, C.C., Su, C.C., Hsieh, J.L., Iseng, C.P., Lin, P.L.and Chang, J.S. (2003). Polypeptides for heavy metal biosorption: *Capacity and specificity of two heterogenous Mer proteins*. *Enzyme Microbial Technology,* 33, 379-385

Idibie, O.C., Oviojie, O.E., Isalar, O.F and Emoghene, A.O. (2018). Comparative microbial analysis of borehole water and other sources of water in Benin metropolis, Edo state. *Journal of environmental science and public health*, 2, 232-242

Iftekhar, A., Rahman, M., and Ullah, M.F. (2018). Factors affecting adsorption of dyes from aqueous solution. *Journal of Environmental Chemical Engineering*, 6(2), 2384-2396

Igwe, J and Abia, A. (2003). Maize cob and husk as adsorbents for removal of Cd, Pb and Zn ions from wastewater. *The Physical Sci*, 2, 83-94

Igwe, J., Abia, A., and Sonde, C. (2011). Pseudokinetics and intraparticle diffusion models for sorption of Zn (II), Cd (II) and Pb (II) ions onto maize cob. *ABSU Journal of Environ. Sci. and Technol*, *1*, 25–36.

Igwe, J.C. and Abia, A. (2006). A bioseperation process for the removal of heavy metals from wastewater using adsorbent. *Journal of African Biotechnology*, 5, 1167-1179

Isikwe, M.O and Chikezie, A. (2014) Quality assessment of various sachet water brands marketed in Bauchi Metropolis of Nigeria. *International Journal of Advances in Engineering and Technology,* 6, 2489-2495

Ismail, M. S. (2021). *Removal of Heavy Metal Ions from Local Battery Recycling Wastewater Using Functionalized Corn Husk Derived Activated Carbon*

Izah, S. C., and Ogwu, M. C. (2025). Modelling solutions for microbial water contamination in the Global South for public health protection. Frontiers in Microbiology, 16, 1504829. https://doi.org/10.3389/fmicb.2025.1504829

Jacob, J.M., Karthik, C., Saratale, R.C., Kumar, S.S., Prabakar, D., Kadirvelu., K and Pugazhendhi, A. (2018). Biological Approaches to Tackle Heavy Metal Pollution: A Survey of literature. J. Environ. Manag. 217, 56-70

Jaramillo, J., Gomez, S.V. and Alvareza, P.M. (2009). Enhanced adsorption of metal ions onto functionalized granular activated carbons prepared from cherry stones. *Journal of Hazard Matter*, 161, 670-676

Jay. M, Loessner. J and Golden. A (2005) Modern Food Microbiology 7th ed. New fYork: *Springer Science/Business Media Inc*

Johnson, A. B., and Brown, C. D. (2019). Chemical characterization of mineral water stream. *Journal of Environmental Chemistry*, 42(3), 145-160.

Johnson, D.L, Ambrose, S.H, Basett, T.J, Bowen, M.L, Crummey, D.E, Isaacson, J.S, Johnson, D.N., Lamb, P., Saul, M and Winternelson, A.E. (1997).'Meaning of Environmental Terms. *Journal of Environmental Quality* 26(3), 581-589

Johnson, D.L., Ambrose, S.H., Bassett, T.J., Bowen, M.L., Crummey, D.E., Isaacson, J.S., Johnson, D.N., Lamb, P., Saul, M. and Winter-Nelson, A.E. (1996) Meanings of Environment Terms. *Journal of Environmental Quality*, 26, 581-589.

Jones, E. F., and Smith, G. H. (2019). Anthropogenic influences on mineral waters in a stream:*Nitrate contamination. Environmental Science and Pollution Research*, 26,17, 16975-16989.

Kataria, H.C., Quershi, H.A., Labal, S.A. and Shandilya, A.K. (1996). Assessment of water quality of Kolar reservior in Bhopal (MP). *Pollution Research* 15(2), 191-193

Kaushal, S. S., et al. (2021). Freshwater salinization syndrome on a continental scale. Proceedings of the National Academy of Sciences, 118(1), e2025163118. https://doi.org/10.1073/pnas.2025163118

Kenya Bureau of Standards. (2015). Drinking water—Specification (KS EAS 12:2014). KEBS.

Khatri, N. and Tyagi, S. (2014). Influences of natural and anthropogenic factors on surface and groundwater quality in rural and urban areas. *Front. Life Sci*, 8, 23–39

Kumar, A., et al. (2021). Monitoring water quality for sustainable development: Recent advances and future directions. Science of the Total Environment, 774, 145785. https://doi.org/10.1016/j.scitotenv.2021.145785

Kurniawan, T.A., Chan, G.Y.S., Lo, W.H. and Babel, S. (2006). Physico-chemical treatment techniques of wastewater laden with heavy metals. *Journal of Chemical Engineering*, 118, 83-89

Kuyucak, N. and Volesky, B. (1990). Biosorption of heavy metals. CRC press, Boca Raton 173

Laar, C., Akiti, T.T., Brimah, A.K., Fianko, J.R., Osae, S., Osei, J. (2011a). Hydrochemistry and isotopic composition of the Sakumo Ramjar site Res. *Journal of Environmental Earth science,* 3(2), 14-152

Laar, C., Akiti, T.T., Brimah, A.K., Fianko, J.R., Osae, S., Osei, J. (2011b). Determination of heavy metals in the black-chin tilapia from Sakumo region. Ghana. Res *Journal of Environmental Earth science,* 3, 8-13

Lala, M. A., Olomowewe, Z. O., Adeniyi, A. T., and Giwa, A. (2023). Maize cob-derived activated carbon as an adsorbent for the removal of nickel (II) cation from aqueous solution: Optimization and kinetic studies. *Arab Journal of Basic and Applied Sciences*, *30*(1), 573–582

Laurent, P. (2005). Household drinking water systems and their impact on people with weakened immunity, MSF-Holland, Public Health Department

Liang, S., Guo, X.Y., Feng, N.C. and Tian, Q. (2009). Application of orange peel xanthate for the adsorption of lead ions from aqueous solution. *Journal of Hazardous Materials*, 170, 425- 429

Liang, Z., Li, X., Zhang, W. (2018*).* High-throughput sequencing reveals microbial community and functional gene changes of biofilm in a simulated drinking water distribution system with chlorination. *Science Total Environment,* 615, 906–913

Liu, Y., Xu, X., Qu, B., Liu, X., Yi, W., and Zhang, H. (2021). Study on adsorption properties of modified corn cob activated carbon for mercury ion. *Energies*, *14*(15), 4483

Loganathan, P., Kandasamy, J., Ratnaweera, H., and Vigneswaran, S. (2025). The Incorporation of Adsorbents with Contrasting Properties into the Soil Substrate for the Removal of Multiple Pollutants in Stormwater Treatment for the Reuse of Water—A Review. *Water*, *17*(13), 2007

MacDonald, A.M and Calow, R.C. (2009). Developing Groundwater for Secure Rural Water Supplies in Africa. *Desalination*, 248, 546-556

Maisa, T., Wanyonyi, A and Shisia, S (2022). Physico-chemical parameters and levels of nutrients during wet and dry season along river Ewaso Narok, Laikipia county, Kenya. *Journal of Science and Applied Technology* 1(2): ISSN 22791-1926

Marin, N. M. (2022). Maize stalk obtained after acid treatment and its use for simultaneous removal of Cu2+, Pb2+, Ni2+, Cd2+, Cr3+ and Fe3+. *Polymers*, *14*(15), 3141

McDowell, R. W., Luo, D., Pletnyakov, P., Upsdell, M., and Dodds, W. K. (2025). Anthropogenic nutrient inputs cause excessive algal growth for nearly half the world's population. Nature Communications, 16, Article 1830. https://doi.org/10.1038/s41467-025-57054-8

Miretzky, P., Saralegui, A. and Cirelli, A.F. (2006). Simultaneous heavy metal removal mechanism by dead macrophytes, *Journal of Chemosphere*, 62, 247-254

Mohamed, M.E and Gehad, G.M. (2017). Adsorption of copper(II) and zinc(II) ions from aqueous solution by activated carbon derived from halophytes (*Suaeda maritime*). *Desalination and Water Treatment*, 94, 198-210

Morales, R., *et al*. (2021). Dissolved oxygen dynamics in rivers: Drivers and ecological consequences. Aquatic Sciences, 83, 22. https://doi.org/10.1007/s00027-021-00787-w

Musah, M., Yisa, J., Suleiman, M.A.T., Mann, A., Shaba, E.Y. and Aliyu, A. (2018). Kinetics and isotherms studies of adsorption of Cr6+, Mn2+ and Cd2+ ions onto chemically modified Bombax buonopozense calyx. *Biological and Environmental Sciences Journal for Tropics*, 15(1), 28-34

Nagaraju, A., Thejaswi, A., Sreedhar, Y. (2016). Assessment of Groundwater Quality of Udayagiri area, Nellore District, Andhra Pradesh, South India Using Multivariate Statistical Techniques. *Earth Sci. Res. J.* 20, 1

Nahyan,A.S. (2012) Keynote Address. World Future Energy Summit 2012, Abu Dhabi, UAE

Ni'Mah, L., Juliastuti, S. R., and Mahfud, M. (2023). One-stage microwave-assisted activated carbon preparation from Langsat peel raw material for adsorption of iron, manganese and copper from acid mining waste. *Communications in Science and Technology*, *8*(2), 143–153

Nilavazhagi, A., and Felixkala, T. (2021). Adsorptive removal of Fe (II) ions from water using carbon derived from thermal/chemical treatment of agricultural waste biomass: Application in groundwater contamination. *Chemosphere*, *282*, 131060

Ogwu, M.C., Pamela, B.O., Dare, A.F., Ovuru, K.F. and Iyiola, A.O. (2024). Traditional and conventional water treatment methods: a sustainable approach. In Water Crises and Sustainable Management in the Global South 461-486. Singapore: Springer Nature

Okafor, J., Agbajelola, D., Peter, S., Adamu, M., and David, G. (2015). Studies on the adsorption of heavy metals in a paint industry effluent using activated maize cob. *Journal of Multidisciplinary Engineering Science and Technology*, *2*(2), 39–46

Oko, O. O., *et al*. (2020). Spatio-temporal variation of pH and alkalinity in streams impacted by urbanization. Environmental Earth Sciences, 79(21), 1–13. https://doi.org/10.1007/s12665-020-09202-w

Okoh, A.I., Odjadjare, E.E., Igbinosa, E.O., Osode, A.N. (2007). Wastewater treatment plants as a source of microbial pathogens in the receiving watershed. *Africa Journal of Biotechnology*. 6(29), 32–44

Okoro, I.E., Oriaku, C.I. and Ejike, E.N. (2007). Lead characterization of street dust in some cities in Southern Nigeria. *Journal of Research in Applied Science*, 2, 39-43

Oloyede, O. B., Akinyosoye, O. E., Balogun, R. A., and Akande, J. O. (2023). Utilization of agricultural residue ash as a solid green heterogeneous base catalyst for biodiesel production. Engineering Reports, 5(8), e12585.

Oludairo. O and Aiyedun. J (2016) Contamination of commercially packaged sachet water and the public health implications: an overview, *Bangladesh Journal of Veterinary Medicine* 13(2), 73-81

Omunyala, A. (2017) *Suitability of Athi river water for irrigation within Athi river town and its environments*, South Eastern Kenya University (unpublished Masters' Thesis)

Onyekwere, O., Hambali, H., Macaulay, F., Haruna, A., Ayinla, L., Ogundokun, P., Sulayman, I., Oyelade-Akinsola, O., & Hayes, A. (2024). Modified corn cob adsorbent for heavy metal removal from wastewater. *Savannah Journal of Science and Engineering Technology*, *2*(02), 33–40

Opara, A.U and Nnodium, J. (2014). Prevalence of bacteria in bottle and sachet water sold in Owerri metropolis *International Journal of Science Innovation and Discoveries* 4, 117- 122

Pérez-Santín, E., Maqueda, C., Gallardo-López, B., and Agrela, F. (2021). Chemical and mineral composition of ashes from biomass combustion and their potential reuse in construction materials. International Journal of Environmental Science and Technology, 18(5), 1001–1012.

Perkampus, H. H. (2013). *UV-VIS Spectroscopy and its Applications*. Springer Science & Business Media

Popescu, A. and Doyle, R.J. (1996). The Gram stain after more than a centuary. *Biotech Histochem*, 71(3), 14-51

Pradhan, S and Pokher, M.R. (2013) Spectrophotometric determination of phosphate in sugarcane juice, fertilizer, detergent and water sample by molybdenum blue method. *Scientific world*,11(11), 58-62

Purev, O., Park, C., Kim, H., Myung, E., Choi, N., and Cho, K. (2023). Spirulina platensis immobilized alginate beads for removal of Pb (II) from aqueous solutions. *International Journal of Environmental Research and Public Health*, *20*(2), 1106

Putranto, A., Ng, Z. W., Hadibarata, T., Aziz, M., Yeo, J. Y. J., Ismadji, S., and Sunarso, J. (2022). Effects of pyrolysis temperature and impregnation ratio on adsorption kinetics and isotherm of methylene blue on corn cobs activated carbons. *South African Journal of Chemical Engineering*, *42*(1), 91–97

Rabalais, N. N., et al. (2020). Gulf of Mexico hypoxia: Past, present, and future. Limnology and Oceanography Bulletin, 29(2), 71–78. https://doi.org/10.1002/lob.10435

Rahman, A., Jahanara, I and Jolly, Y.N (2021). Assessment of physico-chemical properties of water and their seasonal variation in an urban river in Bangladesh, *Water Science and Engineering* 14(2) 139-148

Rajiv, P., Rajeshwari, S., and Venckatesh, R. (2021). Agricultural waste materials as biosorbents for the removal of heavy metals and dyes from wastewater: A review. Environmental Nanotechnology, Monitoring and Management, 16, 100502. https://doi.org/10.1016/j.enmm.2021.100502

Raut, E. R., Thakur, A. B., and Chaudhari, A. R. (2021). *Review on toxic metal ions removal by using activated carbon prepared from natural biomaterials*. *1913*(1), 01209

Sen, T. K. (2023). Agricultural solid wastes based adsorbent materials in the remediation of heavy metal ions from water and wastewater by adsorption: a review. *Molecules*, *28*(14), 5575.

Servais P, Billen G, Goncalves A, Garcia, A.T. (2007). Modelling microbiological water quality in the Seine river drainage network: past, present and future situations. *Hydrology and Earth System Science*, 11, 1581–92

Sharma, R.C., Singh, N., Chauhan, A. (2016). The influence of physicochemical parameters on phytoplanktons distribution in a head water stream of Garhwa Himalaya: a case study. *Egypt J Aquat*, 42(1), 11-21

Sharma, S., and Bhattacharya, A. (2017). Drinking water contamination and treatment techniques. *Applied Water Science*, 7(3), 1043–1067. https://doi.org/10.1007/s13201-016-0455-7

Sharma, S., Devi, A., and Bhattacharyya, K. G. (2023). Nickel-titanium dioxide-Fuller's earth nanocomposites: Synthesis, characterization and application as a photocatalyst in aqueous methylene blue degradation under visible light irradiation. *Inorganic Chemistry Communications*, *151*, 110550

Sharma, V., Walia, Y. K., and Kumar, A. (2015). Assessment of Physico Chemical Parameters for Analysing Water: A. *A Review J Biol Chem Chron*, *2*(1), 25-33

Sila, O.N. (2019). Physico-chemical and bacteriological quality of water sources in rural setting: a case study of Kenya, Africa. *Scientific African*, 2, e00018

Sillanpää, M., Ncibi, M. C., and Matilainen, A. (2018). Advanced oxidation processes for the removal of natural organic matter from drinking water sources: A comprehensive review. Journal of Environmental Management, 208, 56–76. https://doi.org/10.1016/j.jenvman.2017.12.009

Singh, M. R., and Gupta, A. (2016). Water pollution-sources, effects and control. *Centre for Biodiversity, Department of Botany, Nagaland University*, 1-16

Singh, S., Kapoor, D., Khasnabis, S., Singh, J., and Ramamurthy, P. C. (2021). Mechanism and kinetics of adsorption and removal of heavy metals from wastewater using nanomaterials. *Environmental Chemistry Letters*, *19*(3), 2351–2381

Singh, A., Sharma, A., Verma, R. K., Chopade, R. L., Pandit, P. P., Nagar, V., ... and Sankhla, M. S. (2022). Heavy metal contamination of water and their toxic effect on living organisms. In *The toxicity of environmental pollutants*. IntechOpen.

Steffii, F., Brendan, M and Erin, N (2003). Nitrate and phosphate levels affect the growth of algae species found in Perry Pond. *Tillers* 4 21-24

Subehi, L., Uno, H., Nomosatryo, S., Yustiawati, Sulastri, Sulawesty, F., Toruan, R.L., Afandi, A.Y., Rusydi, A.F., Julzarika, A., Witasari, Y., Ajie, G.S and Sunthari, H (2024). Seasonal fluctuactions in water temperature and dissolved oxygen: A comparative study of oxbow lakes along the Kapuas Riverine System. *Earth and Environmental Science* 1436(2024) 012007

Sun, R (2010). Cereal straw as a Resource for Sustainable Biomaterials and Biofuels: Chemistry, Extractives, lignins, Hemicellulose and Cellulose; Elsevier: Amsterdam, The Netherlands, [Google Scholar]

Tahoon, M. A., Siddeeg, S. M., Salem Alsaiari, N., Mnif, W., and Ben Rebah, F. (2020). Effective heavy metals removal from water using nanomaterials: A review. *Processes*, *8*(6), 645

Tchounwou, P.B., Yedjou, C.G., Patlolla, A.K and Sutton, D.J. (2012). Heavy Metal Toxicity and the Environment. Exp. Suppl. 101, 133-164

Tejada-Tovar, C., Villabona-Ortíz, A., Ortega-Toro, R., López-Génes, J., and Negrete-Palacio, A. (2021). Elimination of Cadmium (II) in aqueaous solution using corn cob (Zea mays) in batch system: Adsorption kinetics and equilibrium. *Revista Mexicana de Ingeniería Química*, *20*(2), 1059–1077

Tochetto, G. A., Brandler, D., Pigatto, J., Pasquali, G. D. L., de Almeida Alves, A. A., Kempka, A. P., da Luz, C., and Dervanoski, A. (2023). Kinetic modeling of the adsorption and desorption of metallic ions present in effluents using the biosorbent obtained from Syagrus romanzoffiana. *Environmental Monitoring and Assessment*, *195*(7), 844

U.S. Environmental Protection Agency (EPA). (2021). E. coli: Indicator of faecal contamination. https://www.epa.gov/region8-waterops/addressing-total-coliform-positive-or-e-coli-positive-sample-results-epa-region-8

Ungureanu, E. L., Mocanu, A. L., Stroe, C. A., Panciu, C. M., Berca, L., Sionel, R. M., and Mustatea, G. (2023). Agricultural byproducts used as low-cost adsorbents for removal of potentially toxic elements from wastewater: A comprehensive review. *Sustainability*, *15*(7), 5999

USEPA (2005). Protecting Water Quality from Agricultural Runoff; United State Enviromental Protection Agency (USEPA): Washington, DC, US

Vafakhah, S., Bahrololoom, M., Bazarganlari, R., and Saeedikhani, M. (2014). Removal of copper ions from electroplating effluent solutions with native corn cob and corn stalk and chemically modified corn stalk. *Journal of Environmental Chemical Engineering*, *2*(1), 356–361

Van Vliet, M.T.H., Ludwig, F., Zwolsman, J.J.G, Weedon, G.P., Kabat, P. (2011). Global river temperature and the sensitivity to atmospheric warming and changes in river flow. *Water Resource* 9, 198

Vardhan, K.H., Kumar, P.S. and Panda, R.C. (2019). A review on heavy metal pollution, toxicity and remedial measures: Current trends and future perspectives. *J. Mol. Liq.* 290, 111-197

Vidyasagar, D. (2007). Global minute: Water and health - walking for water and water wars. *Journal of Perinatology*. 27, 56–58

Vierra, H.S.F. and Volesky, B. (2000) Biosorption a solution to pollution. *International Microbial,* 3, 17-21

Viviani, A., and Yanopa, S. (2023). The The Use of activated charcoal from corn cobs as adsorbent of heavy metals from groundwater. *Brazilian Journal of Biosystems Engineering*, 17

Wang, B., Lan, J., Bo, C., Gong, B., and Ou, J. (2023). Adsorption of heavy metal onto biomass-derived activated carbon. *RSC Advances*, *13*(7), 4275–4302

Wang, J., *et al*. (2018). Land use impacts on water quality in river systems. Science of the Total Environment, 633, 400–411. https://doi.org/10.1016/j.scitotenv.2018.03.221

Wang, X., Wang, X., and Cao, J. (2023). Environmental factors associated with Cryptosporidium and Giardia. Pathogens, 12(3), 420. https://doi.org/10.3390/pathogens12030420

Ward, A. J., Lewis, D. M., and Green, F. B. (2018). Anaerobic digestion of algae biomass: A review. Algal Research, 27, 129–144. https://doi.org/10.1016/j .algal.2017.09.018

Ward, M. H., Jones, R. R., *et al*. (2018). Drinking water nitrate and human health: An updated review. International Journal of Environmental Research and Public Health, 15(7), 1557. https://doi.org/10.3390/ijerph15071557

Welz, B. and Sperling, M. (2008). *Atomic absorption spectrometry*. John Wiley and Sons

Williams, A.P., Quilliam, R.S., Thorn, C.E., Cooper, D., Reynolds, B, Jones, D.L. (2012). Influence of land use and nutrient flux on metabolic activity of E. coli O157 in river water. *Water Air Soil Pollution*. 223, 3077–83

WHO. (2005). Guidelines for Laboratory and Field Testing of Mosquito Larvicides. WHO communicable disease control, prevention and eradication. WHO pesticide evaluation schemes

World Health Organization (2010). UN-water global annual assessment of sanitation and drinking-water GLAAS): Targeting resources for better results. Geneva: WHO Press Ramesh, Ram Prasanth. (2023). Re: Why peaks shift towards left in XRD Retrieved from: https://www.researchgate.net/post/Why_peaks_shift_towards_left_in_XRD/6550dc43d6929460c10ebeae/citation/download.

World Health Organization (2011). Water Sanitation and Health (WSH). Retrieved on May 20 2025 from http://www.who.inf/water_sanitation_health/en/

World Health Organization (WHO) (2001). Water quality: Guidelines, standards and health. Editted by Lorna Fewtrell and Jamie Bartram. Published by IWA publishing, London, UK

World Health Organization (WHO, 2006). Guidelines for Drinking Water Quality. First Addedum to 3rd edition vol.1, S.1; WHO press.

World Health Organization (WHO, 2009). Global health risks: Mortality and burden of disease attributable to selected major risks. Geneva

World Health Organization. (2017). Guidelines for drinking-water quality: Fourth edition incorporating the first addendum. World Health Organization. https://www.who.int/publications/i/item/9789241549950 retrieved on Friday 13/06/2025

World Health Organization. (2022). Drinking-water quality guidelines: Living guideline. WHO. https://www.who.int/publications/i/item/9789240045064 retrieved on Wednesday 30/07/2025

World Health Organization. (2022). Guidelines for drinking-water quality: Fourth edition incorporating the first and second addenda. WHO

World Health Organization. (2023). Drinking-water. https://www.who.int/news-room/fact-sheets/detail/drinking-water retrieved on Wednesday 13/08/2025

Zhang, X., Yan, L., Zhang, Z and Tan, C. (2019). Removal of different kinds of heavy metals by novel PPG-nZVI beads and their application in simulated stormwater in filtration facility. *Applied Science* 9(20) 4213

APPENDICES

Appendix I: Chuka University Ethics Review Committee Authorization

CHUKA UNIVERSITY

Knowledge is Wealth *(Sapientia divitia est)* Akili ni Mali

CHUKA UNIVERSITY INSTITUTIONAL ETHICS REVIEW COMMITTEE

Telephones: 020-2310512/18 **P. O. Box 109-60400, Chuka**
Direct Line: 0772894438 **Email: info@chuka.ac.ke,** **Website: www.chuka.ac.ke**

13th August, 2024

REF: CUIERC/ NACOSTI/632
TO: **Bertha Kinya Mwenda**

RE: **Determination of Water Quality and Effectiveness of Modified Corn Cob Powder in Remediation of Nguue Spring and River Mutonga in Tharaka Nithi County, Kenya**

This is to inform you that *Chuka University IERC* has reviewed and approved your above research proposal. Your application approval number is *NACOSTI/NBC/AC-0812.* The approval period is 13th August, 2024 – 13th August, 2025.

This approval is subject to compliance with the following requirements;

i. Only approved documents including (informed consents, study instruments, MTA) will be used
ii. All changes including (amendments, deviations, and violations) are submitted for review and approval by *Chuka University IERC.*
iii. Death and life threatening problems and serious adverse events or unexpected adverse events whether related or unrelated to the study must be reported to *Chuka University IERC* within 72 hours of notification
iv. Any changes, anticipated or otherwise that may increase the risks or affected safety or welfare of study participants and others or affect the integrity of the research must be reported to *Chuka University IERC* within 72 hours
v. Clearance for export of biological specimens must be obtained from relevant institutions.
vi. Submission of a request for renewal of approval at least 60 days prior to expiry of the approval period. Attach a comprehensive progress report to support the renewal.
vii. Submission of an executive summary report within 90 days upon completion of the study to *Chuka University IERC.*

Prior to commencing your study, you will be expected to obtain a research license from National Commission for Science, Technology and Innovation (NACOSTI) https://oris.nacosti.go.ke and also obtain other clearances needed.

Yours sincerely

Dr. Benjamin Kanga
SECRETARY

Appendix II: National Commission for Science, Technology and Innovation (NACOSTI) Research Permit

REPUBLIC OF KENYA

NATIONAL COMMISSION FOR SCIENCE,TECHNOLOGY & INNOVATION

Ref No: **577864**

Date of Issue: **10/September/2024**

RESEARCH LICENSE

This is to Certify that Miss.. Bertha Kinya Mwenda of Chuka University, has been licensed to conduct research as per the provision of the Science, Technology and Innovation Act, 2013 (Rev.2014) in Tharaka-Nithi on the topic: DETERMINATION OF WATER QUALITY AND EFFECTIVENESS OF MODIFIED CORN COB POWDER IN REMEDIATION OF NGUUE SPRING AND RIVER MUTONGA IN THARAKA NITHI COUNTY, KENYA for the period ending : 10/September/2025.

License No: **NACOSTI/P/24/39764**

577864

Applicant Identification Number

Director General
NATIONAL COMMISSION FOR SCIENCE,TECHNOLOGY & INNOVATION

Verification QR Code

NOTE: This is a computer generated License. To verify the authenticity of this document, Scan the QR Code using QR scanner application.

See overleaf for conditions

Appendix III: Physico-chemical Properties of Nguue Spring and River Mutonga in Dry Season

Physicochemical parameters for River Mutonga in dry season

Sample id	Temp (°C)	pH	EC (µs)	TDS (mg/l)	DO (mg/l)	TH (mg/l)	Nitrates (mg/l)	Phosphates (mg/l)
M1	25.9±0	7.4±0.5	202±1	0.886±0.001	4.47±0.01	268±2	17.95±0	2.07±0
M2	26.0±0	7.1±0.001	182.6±0.1	0.869±0.001	3.5±0.01	216±2	16.57±0	2.10±0
M3	26.1±0	7.3±0.001	176±0.1	0.852±0.001	3.48±0.01	258±2	18.72±0	2.11±0
M4	26.4±0	7.3±0.001	173.3±0.1	0.848±0.001	3.32±0.01	176±2	19.35±0	1.95±0
M5	26.5±0	7.2±0.001	172.5±0.1	0.844±0.002	3.25±0.02	230±2	19.01±0	2.03±0
M6	26.6±0	7.1±0.003	170.8±0.1	0.838±0.001	3.19±0.01	190±2	19.05±0	2.12±0
Mean	26.25	7.23	179.53	0.856	3.535	223	18.442	2.063
SD	0.27	0.19	11.1	0.017	0.4460	34.29	1.033	0.064
KEBS 2015	25	6.5-8.5	2500	1500	-	500	10	2.2
WHO2022	-	6.5-7.4	400	<1000	>4	10-500	-	0.5

Physicochemical parameters for Nguue spring in dry season

Sample	Temp (ºC)	pH	EC (µs)	TDS (Mg/l)	DO (Mg/l)	TH (Mg/l)	NO_3^- (mg/l)	PO_4^{3-} (mg/l)
N1	26.4	6.08	193.6	1.2	6.24	124	19.47	2.09
N2	26.5	6.43	157.0	0.651	2.61	160	19.09	2.03
N3	26.5	6.38	149	0.640	4.39	60	16.83	2.07
N4	26.2	6.58	147.6	0.552	3.61	58	16.83	2.12
N5	26.0	5.21	181.3	0.806	2.62	159.33	18.1	2.08
N6	25.9	6.20	185.6	0.838	4.62	157	18.6	2.04
WHO 2022	-	6.5-7.4	500	<1000	>4	10-500	45-100	0.5
KEBS 2015	25	6.5-8.5	2500	1500	-	500	10	2.2
Mean	26.25	6.690	174.28	0.7812	4.015	119.722	18.153	2.0717
SD	0.2588	0.4914	20.17	0.2318	1.381	48.94	1.124	0.033

EC=Electrical conductivity, TDS= Total dissolved solids, DO= Dissolved oxygen, TH= Total hardness, SD=Standard deviation, N= Nguue sampling point

Appendix IV: Physico-chemical Properties of River Mutonga and in Nguue Spring in Wet Season

Physico-chemical parameters for Mutonga River in wet season

Sample	Temp (ºC)	pH	EC (µs)	TDS (Mg/l)	DO (Mg/l)	TH (Mg/l)	NO_3^- (mg/l)	PO_4^{3-} (mg/l)
M1	21	5.973±0.001	57.2±0.1	36.1±0.1	8.72±0.01	108±1	9.15	2.01
M2	21	6.080±0.001	57.6±0.1	32.5±0.1	8.91±0.01	87.3±1	7.25	2.02
M3	21	6.033±0.001	58.1±0.1	31.3±0.1	8.87±0.01	120±1	7.98	2.24
M4	21	6.259±0.001	58.8±0.1	34.9±0.1	8.83±0.01	96±1	9.02	2.27
M5	21	6.280±0.001	59.2±0.1	33.5±0.1	8.873±0.01	122±1	11.67	2.26
M6	21	6.288±0.001	60.4±0.1	34.43±0.1	8.92±0.01	116±1	12.35	2.29
WHO 2022	-	6.5-7.4	500	<1000	>4	10-500	45-100	0.5
KEBS 2015	25	6.5-8.5	2500	1500	-	500	10	2.2
Mean	21	6.152	58.55	33.788	8.854	108.2	9.57	2.182
SD	0	0.14	1.17	1.73	0.073	13.97	2.03	0.13

EC=Electrical conductivity, TDS= Total dissolved solids, DO= Dissolved oxygen, TH= Total hardness, SD= Standard deviation, M=Mutonga sampling points

Physico-chemical parameters of Nguue spring in wet season

Sample	Temp (ºC)	Ph	EC (µs)	TDS (Mg/l)	DO (Mg/l)	TH (Mg/l)	NO_3^- (mg/l)	PO_4^{3-} (mg/l)
N1	21	5.231±0.001	55.6±0.2	32.5±0.1	8.86±0.01	84±2	7.8	2.04
N2	21	5.588±0.001	51.6±0.2	29.9±0.1	8.83±0.01	64±2	9.39	2.11
N3	21	5.561±0.001	51.2±0.2	27.7±0.1	8.78±0.01	64±2	9.21	1.95
N4	20.5	5.724±0.001	45.5±0.2	57.5±0.1	8.72±0.01	22.6±2	9.14	2.23
N5	20.5	4.344±0.001	38.7±0.2	59.5±0.1	8.61±0.01	32.0±2	14.65	2.03
N6	20.5	4.210±0.001	37.8±0.2	58.6±0.1	8.58±0.01	42±2	13.28	2.01
WHO 2022	-	6.5-7.4	500	<1000	>4	10-500	45-100	0.5
KEBS 2015	25	6.5-8.5	2500	1500	-	500	10	2.2
Mean	20.75	5.110	46.73	44.28	8.731	51.4	10.58	2.062
SD	0.274	0.666	7.333	15.67	0.115	23.13	2.718	0.097

EC=Electrical conductivity, TDS= Total dissolved solids, DO= Dissolved oxygen, TH= Total hardness, SD=Standard deviation, N=Nguue spring

Appendix V: Heavy Metals of Nguue Spring and River Mutonga in Dry and Wet Season

Heavy metal concentration in River Mutonga in dry and wet season

Sample id	Dry season		Wet season	
	Zinc(mg/l)	Iron(mg/l)	Zinc(mg/l)	Iron(mg/l)
M1	0.1333	1.0333	1.9458	2.5593
M2	0.1233	1.1	2.6298	2.7537
M3	0.1267	1.0933	1.6375	1.1025
M4	0.14	1.1767	2.4668	2.4025
M5	0.13	1.1133	2.5332	2.5215
M6	0.1267	1.1533	2.678	2.5575
KEBS 2015	5.0	0.3	5.0	0.3
WHO 2022	5.0	0.3	5.0	0.3
Mean	0.13	1.1117	2.3168	2.3162
SD	0.0060	0.0502	0.4236	0.6052

Heavy metal concentration in Nguue spring in dry and wet season

Sample id	Dry season		Wet season	
	Zinc(mg/l)	Iron(mg/l)	Zinc(mg/l)	Iron(mg/l)
N1	0.11	1.0	8.9155	6.4151
N2	0.1533	1.17	9.3430	4.2815
N3	0.18	1.1533	8.91	7.8080
N4	0.1833	1.1667	1.5915	2.3075

N5	0.14	1.14	2.3487	1.7828
N6	0.1867	1.19	2.3569	2.4589
KEBS 2015	5.0	0.3	5.0	0.3
WHO 2022	5.0	0.3	5.0	0.3
Mean	0.1587	1.1367	5.5776	4.1756
SD	0.0303	0.0690	3.8239	2.4651

Appendix VI: Analysis of Variance Table for Physico-chemical Parameters in Dry Season

Temp

Source	DF	Sum of Squares	Mean Square	F Value	Pr > F
Model	13	2.25000000	0.17307692	Infty	<.0001
Error	22	0.00000000	0.00000000		
Corrected Total	35	2.25000000			

Source	DF	Type III SS	Mean Square	F Value	Pr > F
Rep	2	0.00000000	0.00000000	.	.
Station	11	2.25000000	0.20454545	Infty	<.0001

pH

Source	DF	Sum of Squares	Mean Square	F Value	Pr > F
Model	13	14.49584358	1.11506489	61.09	<.0001
Error	22	0.40154117	0.01825187		
Corrected Total	35	14.89738475			

Source	DF	Type III SS	Mean Square	F Value	Pr > F
Rep	2	0.03809217	0.01904608	1.04	0.3690
RiverStation	11	14.45775142	1.31434104	72.01	<.0001

Electrical Conductivity

Source	DF	Sum of Squares	Mean Square	F Value	Pr > F
Model	13	9171.229167	705.479167	7766.74	<.0001
Error	22	1.998333	0.090833		
Corrected Total	35	9173.227500			

Source	DF	Type III SS	Mean Square	F Value	Pr > F
Rep	2	0.221667	0.110833	1.22	0.3144
RiverStation	11	9171.007500	833.727955	9178.66	<.0001

Dissolved Oxygen

Source	DF	Sum of Squares	Mean Square	F Value	Pr > F
Model	13	152107.3611	11700.5662	13.24	<.0001
Error	22	19442.9444	883.7702		
Corrected Total	35	171550.3056			

Source	DF	Type III SS	Mean Square	F Value	Pr > F
Rep	2	245.7222	122.8611	0.14	0.8710
RiverStation	11	151861.6389	13805.6035	15.62	<.0001

Total Dissolved Solids

Source	DF	Type III SS	Mean Square	F Value	Pr > F
Rep	2	0.00000203	0.00000102	0.96	0.3994
RiverStation	11	0.86107434	0.07827949	73681.8	<.0001

Source	DF	Type III SS	Mean Square	F Value	Pr > F
Rep	2	245.7222	122.8611	0.14	0.8710

Total Hardness

Source	DF	Sum of Squares	Mean Square	F Value	Pr > F
Model	13	152107.3611	11700.5662	13.24	<.0001
Error	22	19442.9444	883.7702		
Corrected Total	35	171550.3056			

Iron

Source	DF	Type III SS	Mean Square	F Value	Pr > F
Rep	2	0.00411667	0.00205833	0.63	0.5404
RiverStation	11	0.11480833	0.01043712	3.21	0.0096

Source	DF	Sum of Squares	Mean Square	F Value	Pr > F
Model	13	0.02269444	0.00174573	5.49	0.0002
Error	22	0.00699444	0.00031793		
Corrected Total	35	0.02968889			

Zinc

Source	DF	Type III SS	Mean Square	F Value	Pr > F
Rep	2	0.00087222	0.00043611	1.37	0.2745
RiverStation	11	0.02182222	0.00198384	6.24	0.0001

Appendix VII: Analysis of Variance Table for Physico-chemical Parameters in Wet Season

Temperature

Source	DF	Sum of Squares	Mean Square	F Value	Pr > F
Model	13	1.68750000	0.12980769	Infty	<.0001
Error	22	0.00000000	0.00000000		
Corrected Total	35	1.68750000			

Source	DF	Type III SS	Mean Square	F Value	Pr > F
Rep	2	0.00000000	0.00000000	.	.
RiverStation	11	1.68750000	0.15340909	Infty	<.0001

pH

Source	DF	Sum of Squares	Mean Square	F Value	Pr > F
Model	13	16.73523392	1.28732569	982237	<.0001
Error	22	0.00002883	0.00000131		
Corrected Total	35	16.73526275			

Source	DF	Type III SS	Mean Square	F Value	Pr > F
Rep	2	0.00000117	0.00000058	0.45	0.6464
RiverStation	11	16.73523275	1.52138480	1160825	<.0001

Electrical Conductivity

Source	DF	Type III SS	Mean Square	F Value	Pr > F
Rep	2	0.020000	0.010000	0.65	0.5333
RiverStation	11	2081.547500	189.231591	12244.4	<.0001

Total Dissolved Solid

Source	DF	Sum of Squares	Mean Square	F Value	Pr > F
Model	13	4731.811944	363.985534	29536.5	<.0001
Error	22	0.271111	0.012323		
Corrected Total	35	4732.083056			

Source	DF	Type III SS	Mean Square	F Value	Pr > F
Rep	2	0.035556	0.017778	1.44	0.2578
RiverStation	11	4731.776389	430.161490	34906.5	<.0001

Dissolved Oxygen

Source	DF	Sum of Squares	Mean Square	F Value	Pr > F
Model	13	0.41740278	0.03210791	299.17	<.0001
Error	22	0.00236111	0.00010732		
Corrected Total	35	0.41976389			

Source	DF	Type III SS	Mean Square	F Value	Pr > F
Rep	2	0.00010556	0.00005278	0.49	0.6181
RiverStation	11	0.41729722	0.03793611	353.48	<.0001

Total Hardness

Source	DF	Sum of Squares	Mean Square	F Value	Pr > F
Model	13	39977.90778	3075.22368	2026.54	<.0001
Error	22	33.38444	1.51747		
Corrected Total	35	40011.29222			

Source	DF	Type III SS	Mean Square	F Value	Pr > F
Rep	2	5.36222	2.68111	1.77	0.1943
RiverStation	11	39972.54556	3633.86778	2394.68	<.0001

Source	DF	Sum of Squares	Mean Square	F Value	Pr > F
Model	13	127.7636112	9.8279701	Infty	<.0001
Error	22	0.0000000	0.0000000		
Corrected Total	35	127.7636112			

Iron

Source	DF	Type III SS	Mean Square	F Value	Pr > F
Rep	2	0.0000000	0.0000000	.	.
RiverStation	11	127.7636112	11.6148737	Infty	<.0001

Zinc

Source	DF	Sum of Squares	Mean Square	F Value	Pr > F
Model	13	317.8179749	24.4475365	Infty	<.0001
Error	22	0.0000000	0.0000000		
Corrected Total	35	317.8179749			

Source	DF	Type III SS	Mean Square	F Value	Pr > F
Rep	2	0.0000000	0.0000000	.	.
RiverStation	11	317.8179749	28.8925432	Infty	<.0001

Appendix VIII: Experimental Data for Parameters

Time (mins)	% Adsorption of Zn		Time (mins)	% Adsorption of Fe	
	CCAC	CCC		CCAC	CCC
0	90.16	81.098	0	94.6	93.51
15	90.58	90.276	15	99.7	78.544
30	89.892	91.402	30	99.8	75.043
60	90.053	91.631	60	99.434	91.42
90	91.578	90.926	90	98.737	91.42
120	88.277	90.793	120	94.556	90.026
initial Conc. (ppm)	% Adsorption of Zn		Initial Conc. (ppm)	% Adsorption of Fe	
	CCAC	CCC		CCAC	CCC
5	90.522	90.522	5	79.29	86.46
10	92.31	94.687	10	86.90	89.13
15	90.884	97.682	15	88.74	88.68
20	87.5895	95.8245	20	87.44	88.09
25	85.7764		25	80.54	
Dosage (g)	% Adsorption of Zn		Dosage (g)	% Adsorption of Fe	
	CCAC	CCC		CCAC	CCC
0.025	57.91	46.35	0.025	53.97	55.83
0.05	80.34	74.12	0.05	75.31	70.56
0.1	94.086	93.157	0.1	88.451	89.435
0.2	88.512	88.157	0.2	78.469	82.405
0.3	87.763	84.441	0.3	73.267	79.945
0.4	86.34	81.07	0.4	70.78	76.8

Temperature (^{0}C)	% Adsorption of Zn		Temperature (^{0}C)	% Adsorption of Fe	
	CCAC	CCC		CCAC	CCC
25	94.58	94.179	25	86.06	93.793
35	94.81	94.933	35	88.8	93.231
45	95.51	95.179	45	88.59	91.755
55	92.802	94.632	55	81.42	89.857
pH	% Adsorption of Zn		pH	% Adsorption of Fe	
	CCAC	CCC		CCAC	CCC
2	93.703	94.742	2	83.652	93.955
4	94.487	95.097	4	84.326	94.668
5	95.678	95.987	5	85.639	94.947
6	96.182	96.605	6	86.201	95.582
8	94.995	94.933	8	82.476	92.985
10	93.066	93.761	10	80.716	92.512

Appendix IX: Experimental Data for Isotherms

zinc CCAC					
Conc.ppm	**Ce**	**qe**	**log ce**	**log qe**	**ce/qe**
5	**0.4739**	**1.131525**	**-0.32431**	**0.053664**	**0.418815**
10	**0.769**	**2.30775**	**-0.11407**	**0.363189**	**0.333225**
15	**1.3674**	**3.40815**	**0.135896**	**0.532519**	**0.401215**
20	**2.4821**	**4.379475**	**0.394819**	**0.641422**	**0.566757**
25	**3.5559**	**5.361025**	**0.55095**	**0.729248**	**0.663287**
zinc CCC					
Conc.ppm	**Ce**	**qe**	**log ce**	**log qe**	**ce/qe**
5	**0.4739**	**1.131525**	**-0.32431**	**0.053664**	**0.418815**
10	**0.5313**	**2.367175**	**-0.27466**	**0.37423**	**0.224445**
15	**0.5477**	**3.613075**	**-0.26146**	**0.557877**	**0.151588**
20	**0.6051**	**4.848725**	**-0.21817**	**0.685628**	**0.124796**
iron CCAC					
Conc.ppm	**Ce**	**qe**	**log ce**	**log qe**	**ce/qe**
5	**1.0354**	**0.99115**	**0.015108**	**-0.00386**	**1.044645**
10	**1.3096**	**2.1726**	**0.117139**	**0.33698**	**0.60278**
15	**1.6892**	**3.3277**	**0.227681**	**0.522144**	**0.507618**
20	**2.5112**	**4.3722**	**0.399881**	**0.6407**	**0.574356**
25	**2.364**	**5.659**	**0.373647**	**0.75274**	**0.417742**
iron CCC					
Conc.ppm	**Ce**	**qe**	**log ce**	**log qe**	**ce/qe**
5	**0.6769**	**1.080775**	**-0.16948**	**0.033735**	**0.62631**
10	**1.0875**	**2.228125**	**0.036429**	**0.34794**	**0.488079**
15	**1.698**	**3.3255**	**0.229938**	**0.521857**	**0.5106**
20	**2.3824**	**4.4044**	**0.377015**	**0.643887**	**0.540914**

Appendix X: Experimental Data for Pseudo 1st and 2nd Order

Fe CCC							
Time	Initial conc. Fe (ppm)	Ce (mg/l)	qe	Qt	**qe−qt**	**log(qe−qt)**	**t/qt**
0	10	0.649	2.25065	2.33775	-0.0871	#NUM!	0
15	10	3.1456	2.25065	1.7136	0.53705	-0.269985279	8.753501
30	10	2.4957	2.25065	1.876075	0.374575	-0.426461212	15.99083
60	10	0.858	2.25065	2.2855	-0.03485	#NUM!	26.25246
90	10	0.858	2.25065	2.2855	-0.03485	#NUM!	39.37869
120	10	0.9974	2.25065	2.25065	0	#NUM!	53.31793
	Fe CCAC						
Time	Initial conc. of Fe (ppm)	Ce	qe	Qt	qe-qt	log(qe-qt)	t/qt
0	10	0	2.495	2.5	-0.005	#NUM!	0
15	10	0.03	2.495	2.4925	0.0025	-2.602059991	6.018054
30	10	0.02	2.495	2.495	0	#NUM!	12.02405
60	10	0.0566	2.495	2.48585	0.00915	-2.038578906	24.13661
90	10	0.1263	2.495	2.468425	0.026575	-1.575526727	36.4605
120	10	0.5444	2.495	2.3639	0.1311	-0.882397308	50.76357
	Zn CCAC						
Time	Initial conc. of Fe (ppm)	Ce	qe	qt	qe-qt	log(qe-qt)	t/qt
0	10	0.984	2.2895	2.254	0.0355	-1.449771647	0
15	10	0.942	2.2895	2.2645	0.025	-1.602059991	6.623979
30	10	1.0108	2.2895	2.2473	0.0422	-1.374687549	13.34935
60	10	0.9947	2.2895	2.251325	0.038175	-1.418220954	26.65097
90	10	0.8422	2.2895	2.28945	0	#NUM!	39.31075
120	10	1.1723	2.2895	2.206925	0.082575	-1.083151418	54.3743
	Zn CCC						
Time	Initial conc. of Fe (ppm)	Ce	qe	qt	qe-qt	log(qe-qt)	t/qt
0	10	1.8902	2.2908	2.0275	0.26335	-0.579466677	0
15	10	0.9724	2.2908	2.2569	0.0339	-1.469800302	6.646285
30	10	0.8598	2.2908	2.2851	0.00575	-2.240332155	13.12882
60	10	0.8369	2.2908	2.2908	0	#NUM!	26.19201
90	10	0.9074	2.2908	2.2732	0.01765	-1.75325529	39.59264
120	10	0.9207	2.2908	2.2698	0.020975	-1.67829803	52.86751

Appendix XI: Graphs for Pseudo 1st and 2nd Order

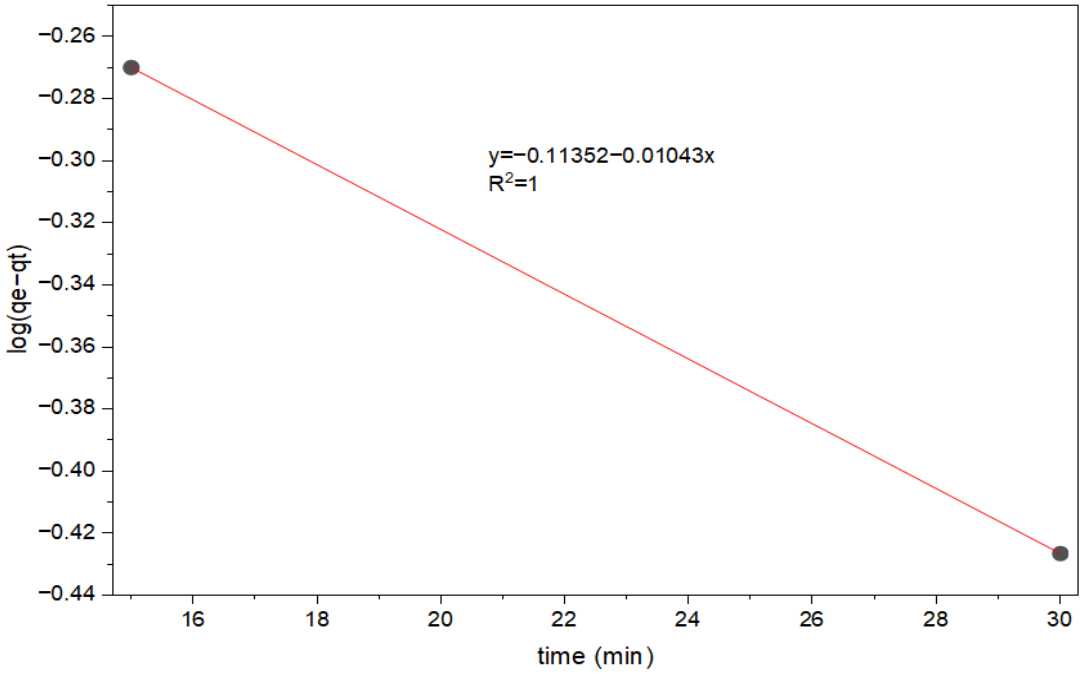

Figure 15: Pseudo first order of Fe using corn cob charcoal

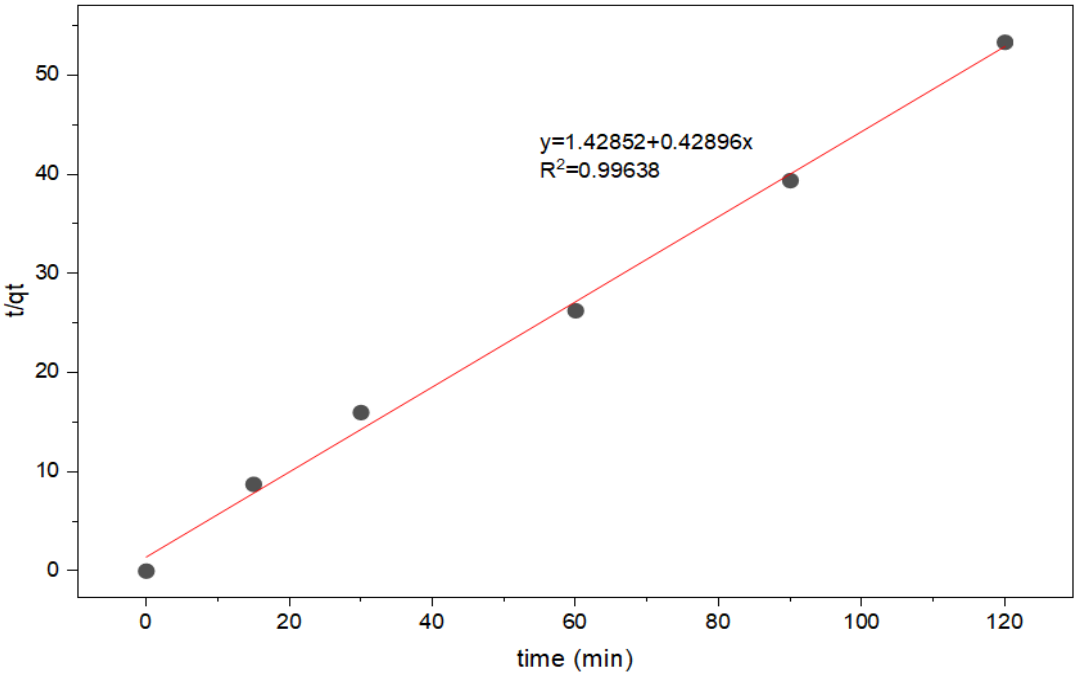

Figure 16: Pseudo second order of Fe using corn cob charcoal

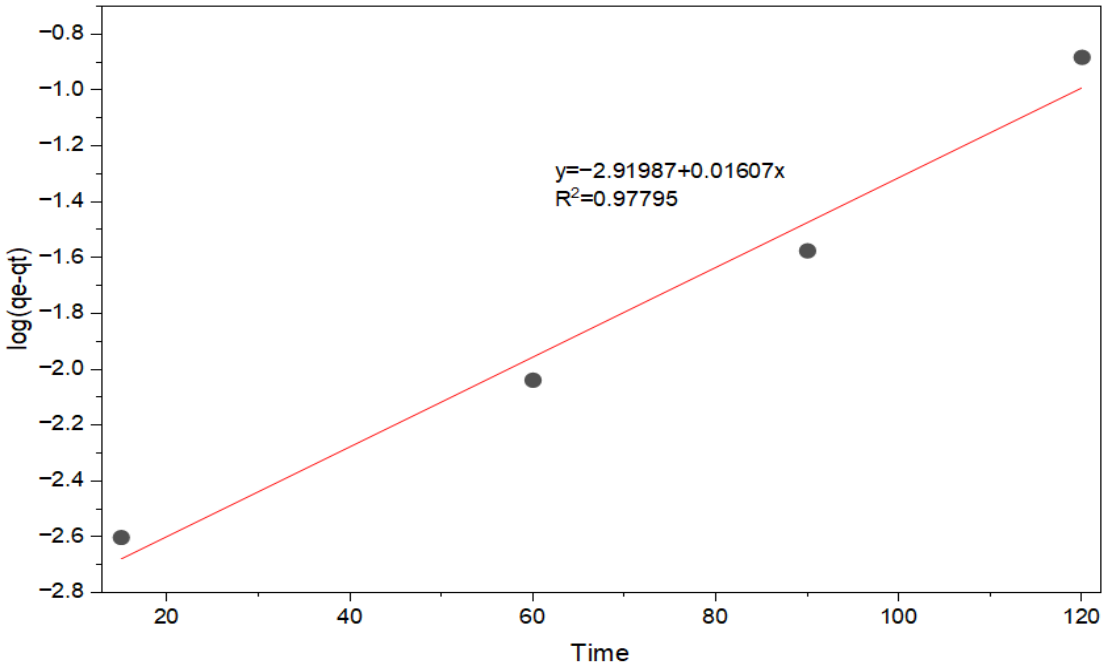

Figure 17: Pseudo first order of Fe using corn cob activated carbon

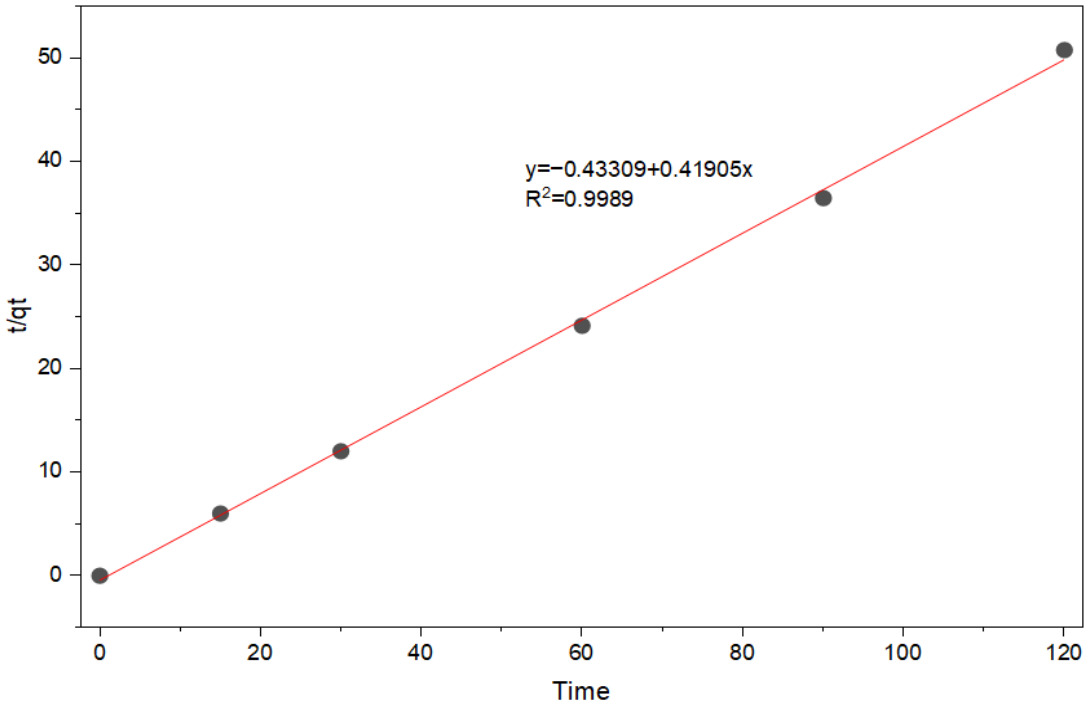

Figure 18: Pseudo second order of Fe using corn cob activated carbon

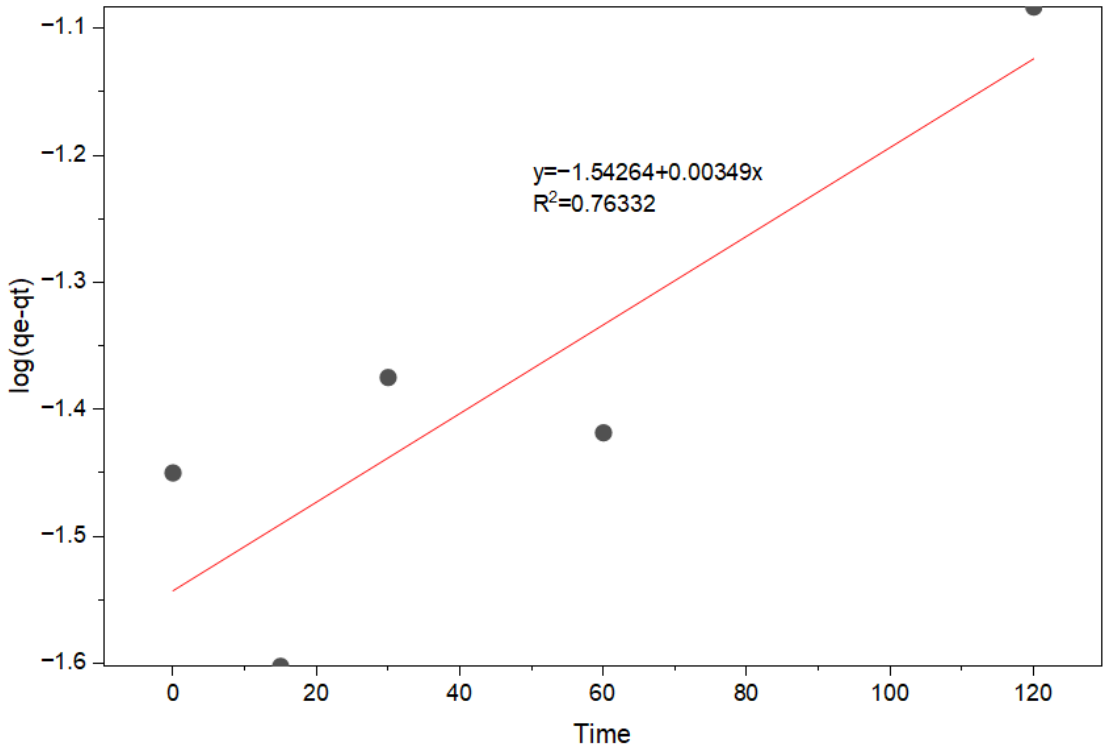

Figure 19: Pseudo first order of Zn using corn cob activated carbon

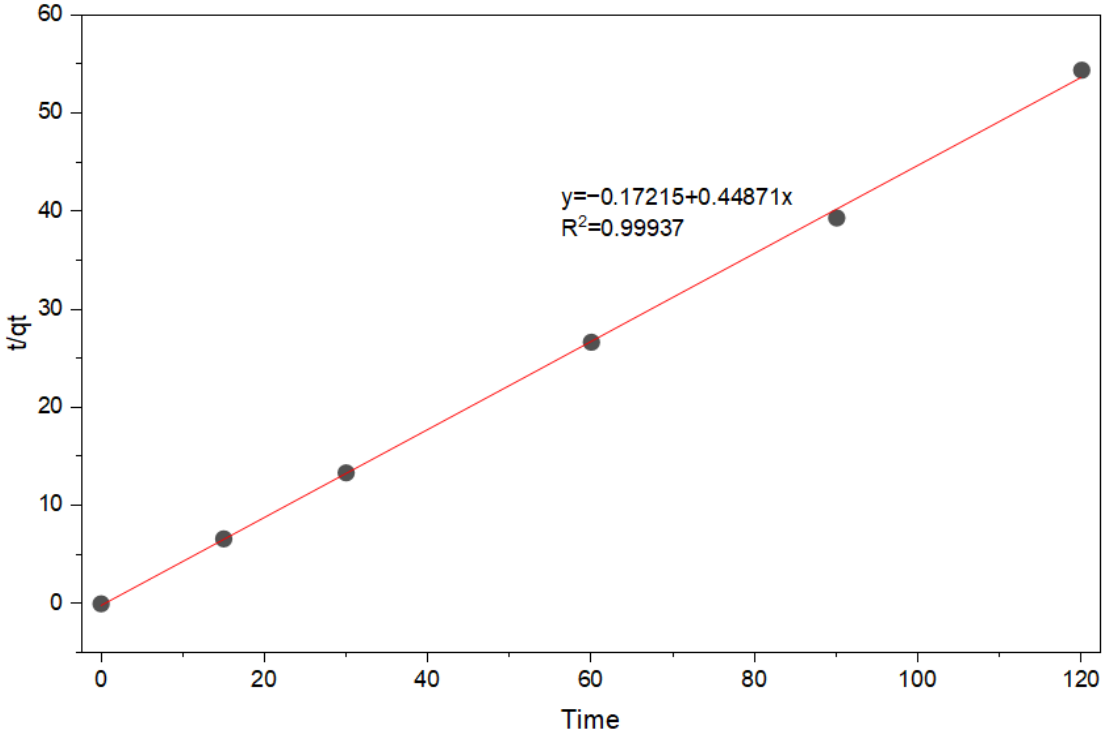

Figure 20: Pseudo second order of Zn using corn cob activated carbon

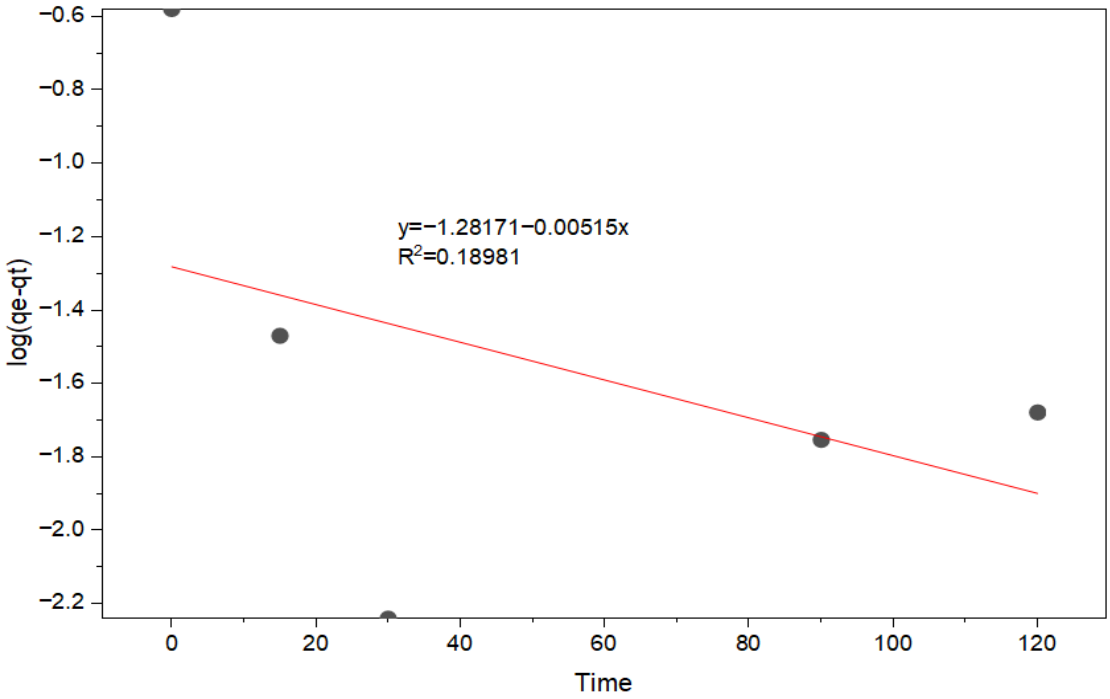

Figure 21: Pseudo first order of Zn using corn cob charcoal

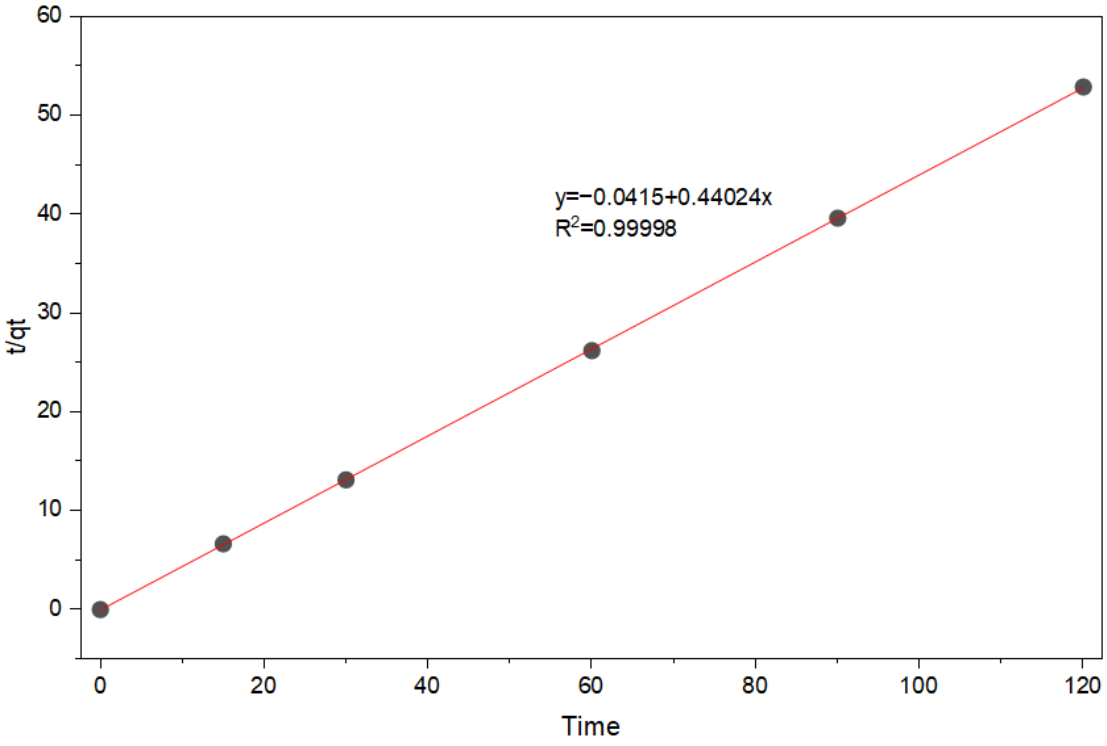

Figure 22: Pseudo second order of Zn using corn cob charcoal

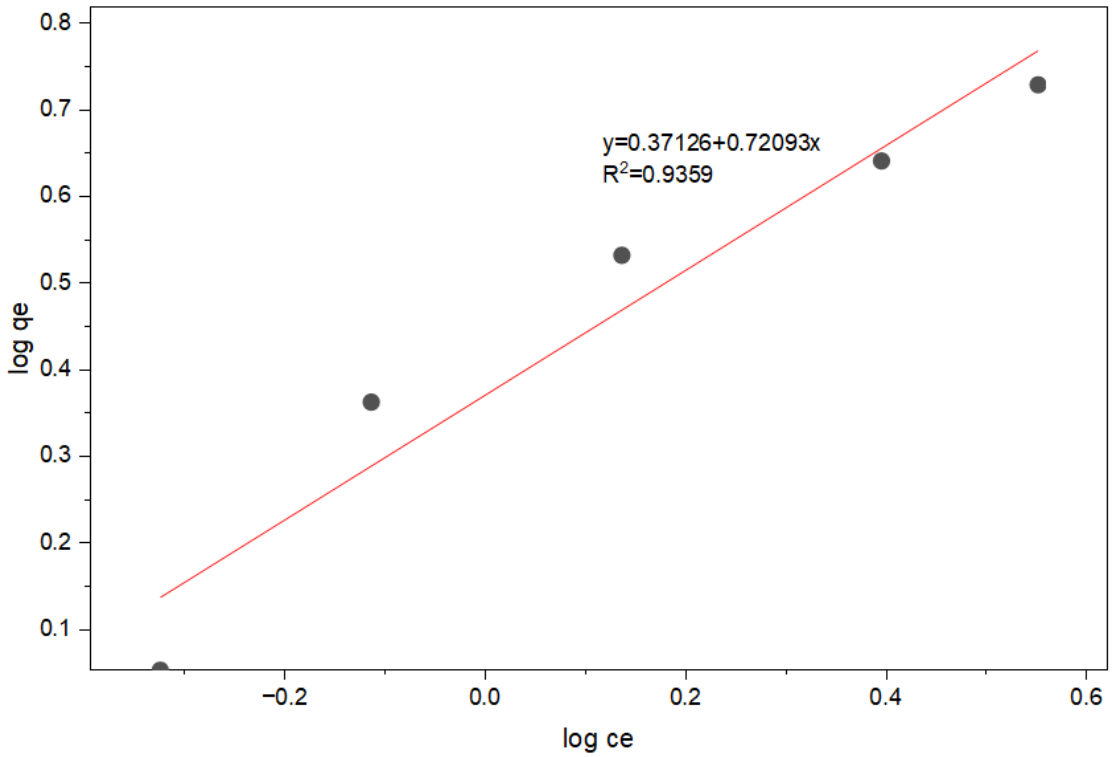

Figure 23: Freundlich isotherm for Zn using corn-cob activated charcoal

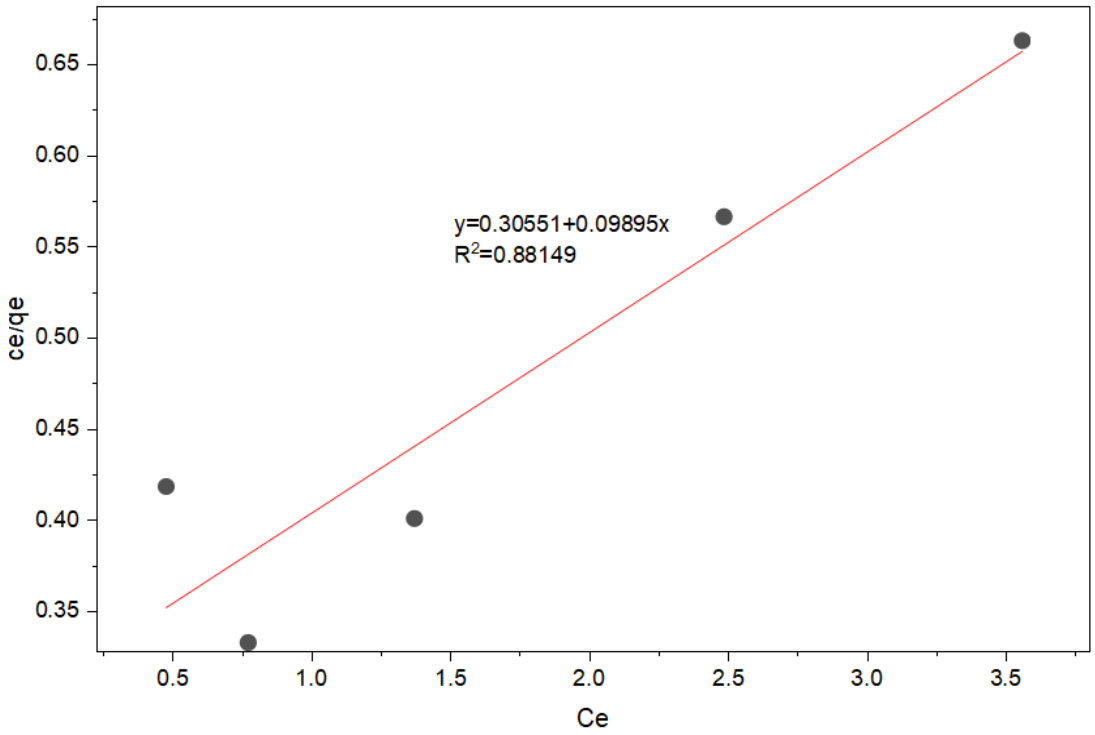

Figure 24: Langmuir isotherm of Zn using corn-cob activated charcoal

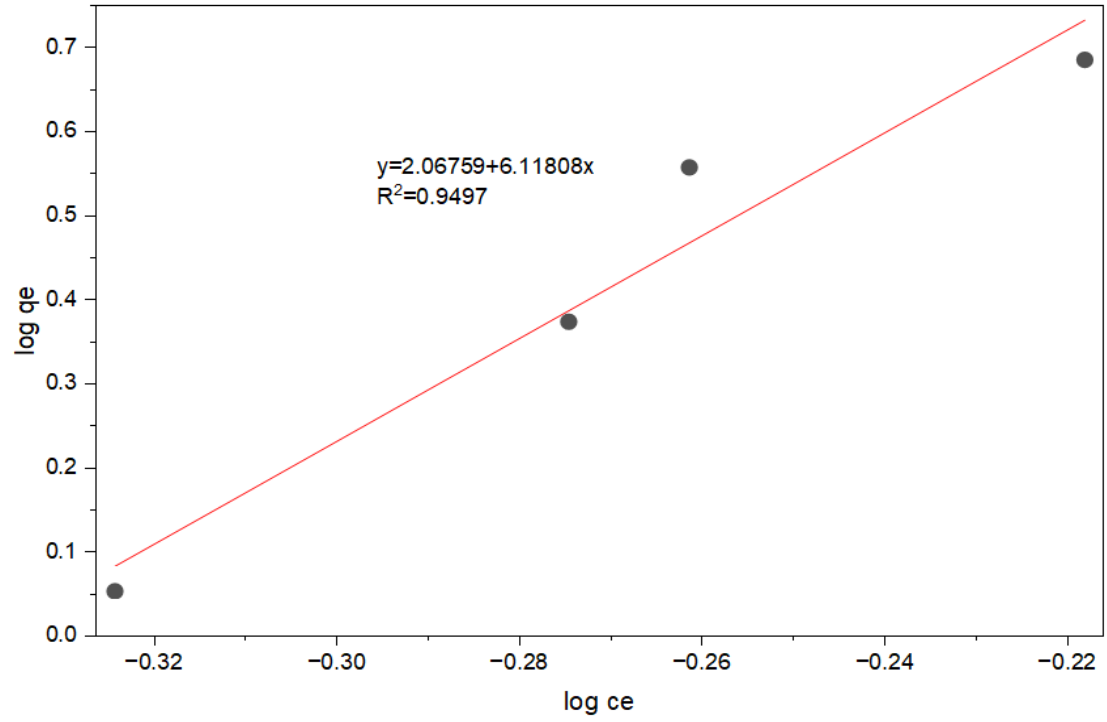

Figure 25: Freundlich isotherm for Zn using corn-cob charcoal

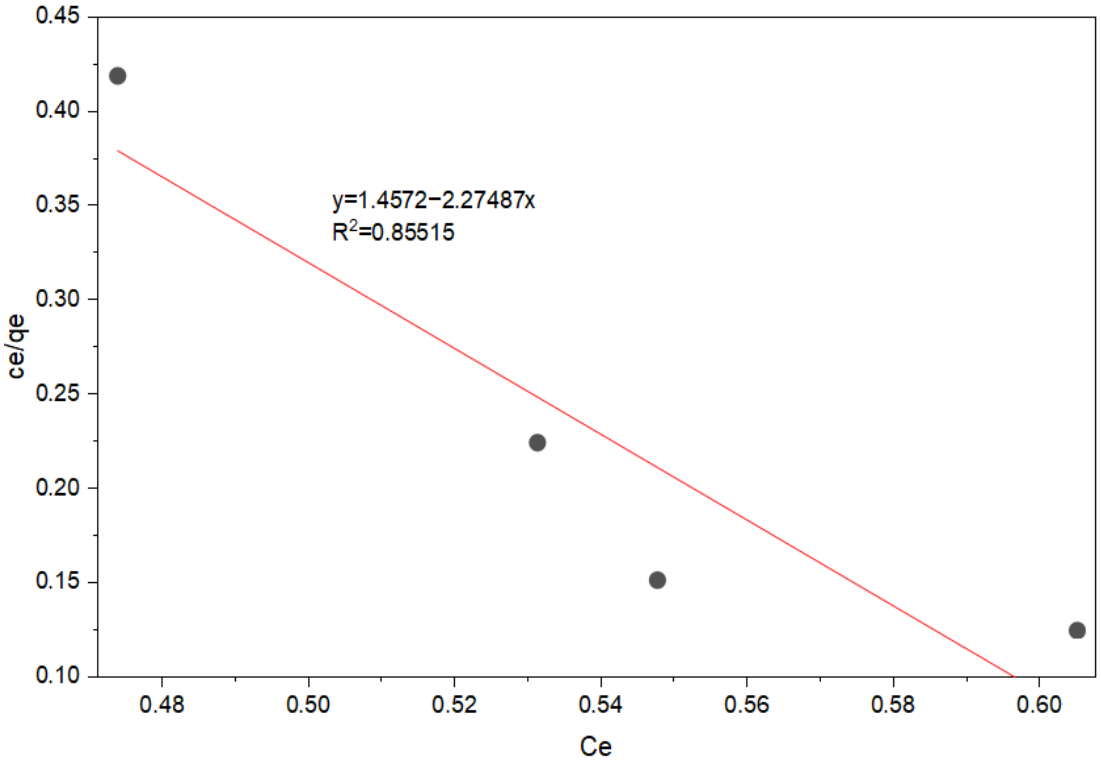

Figure 26: Langmuir isotherm of Zn using corn-cob charcoal

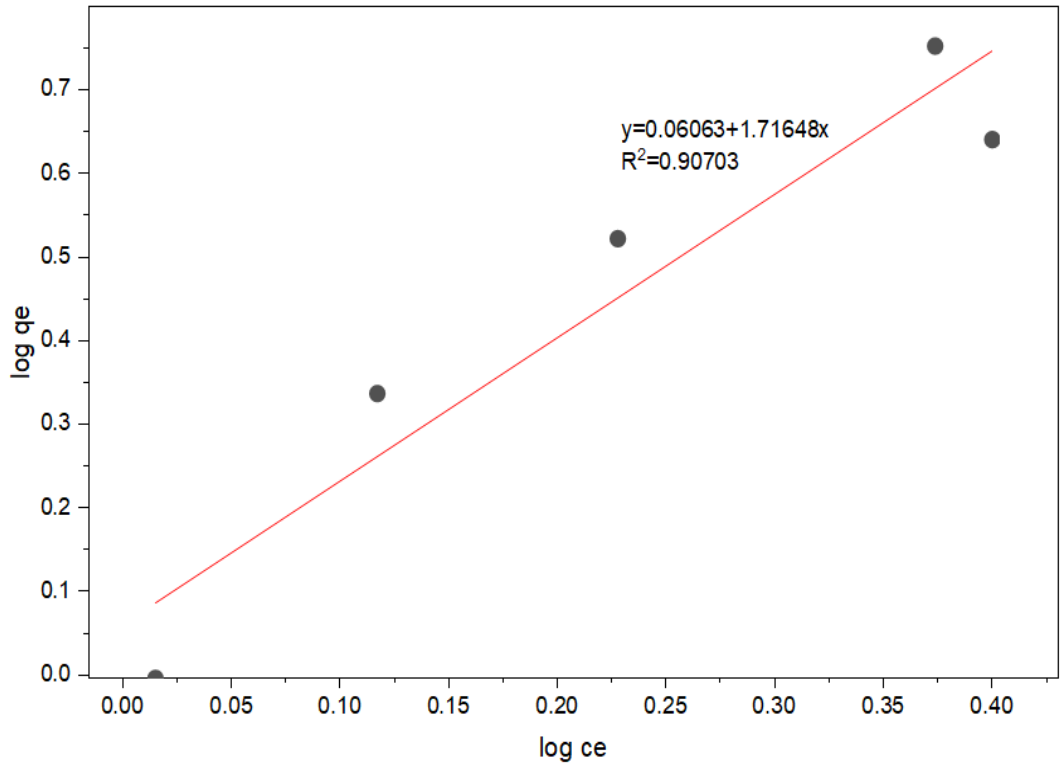

Figure 27: Freundlich isotherm for Fe using corn cob activated carbon

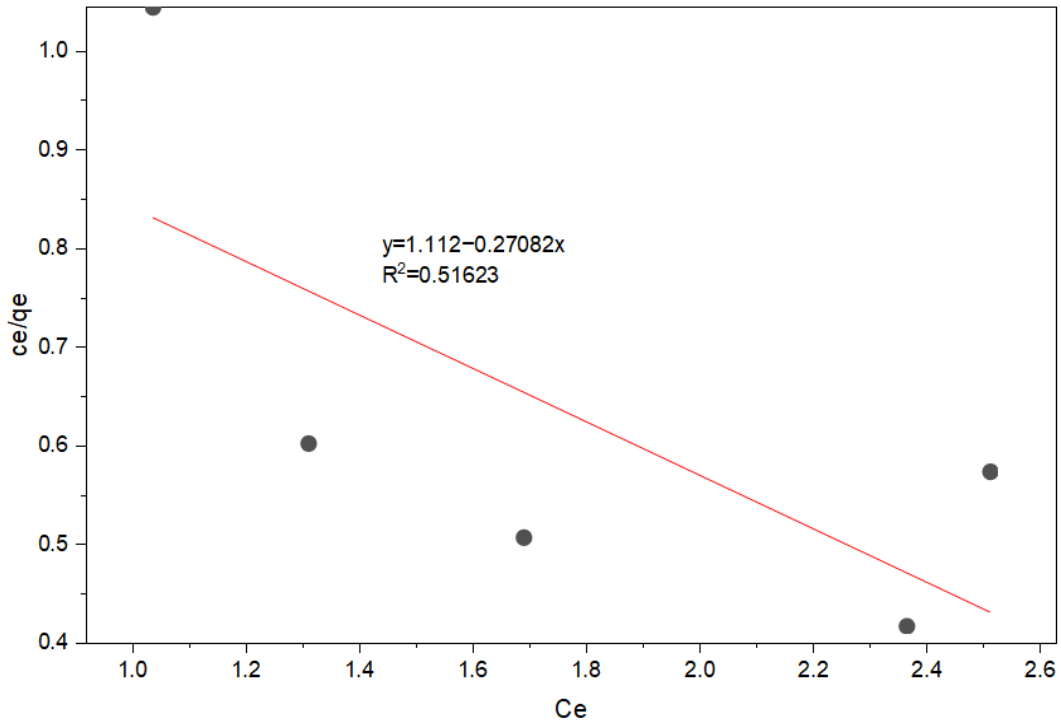

Figure 28: Langmuir isotherm of Fe using corn cob activated carbon

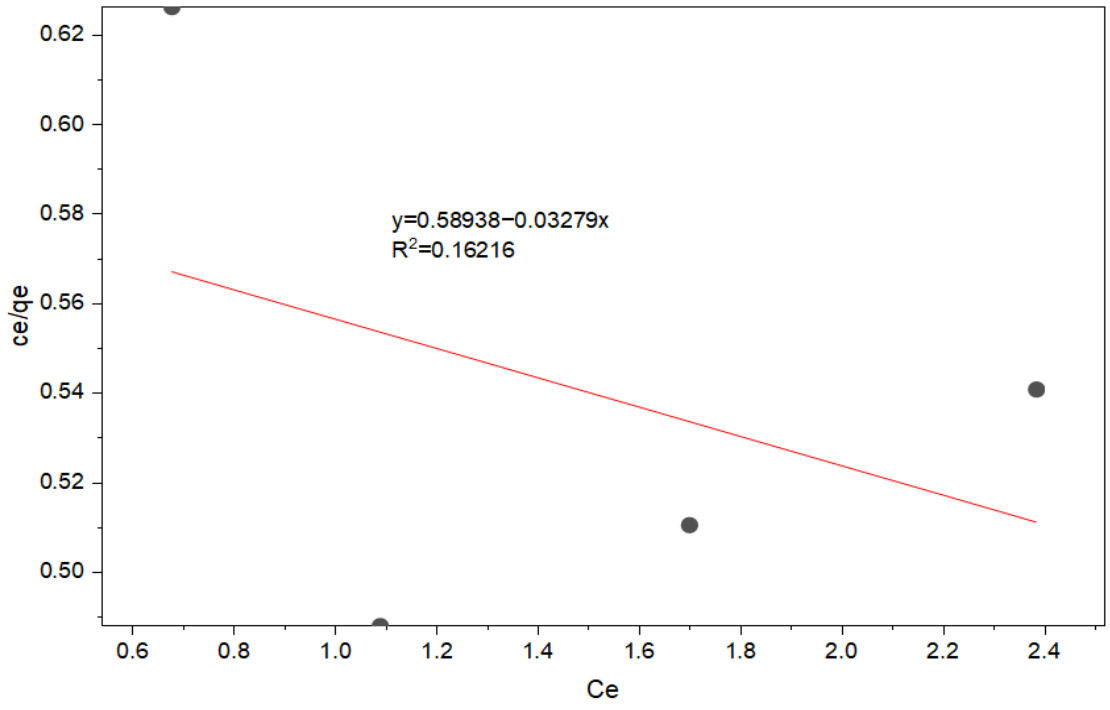

Figure 29: Langmuir isotherm of Fe using corn-cob charcoal

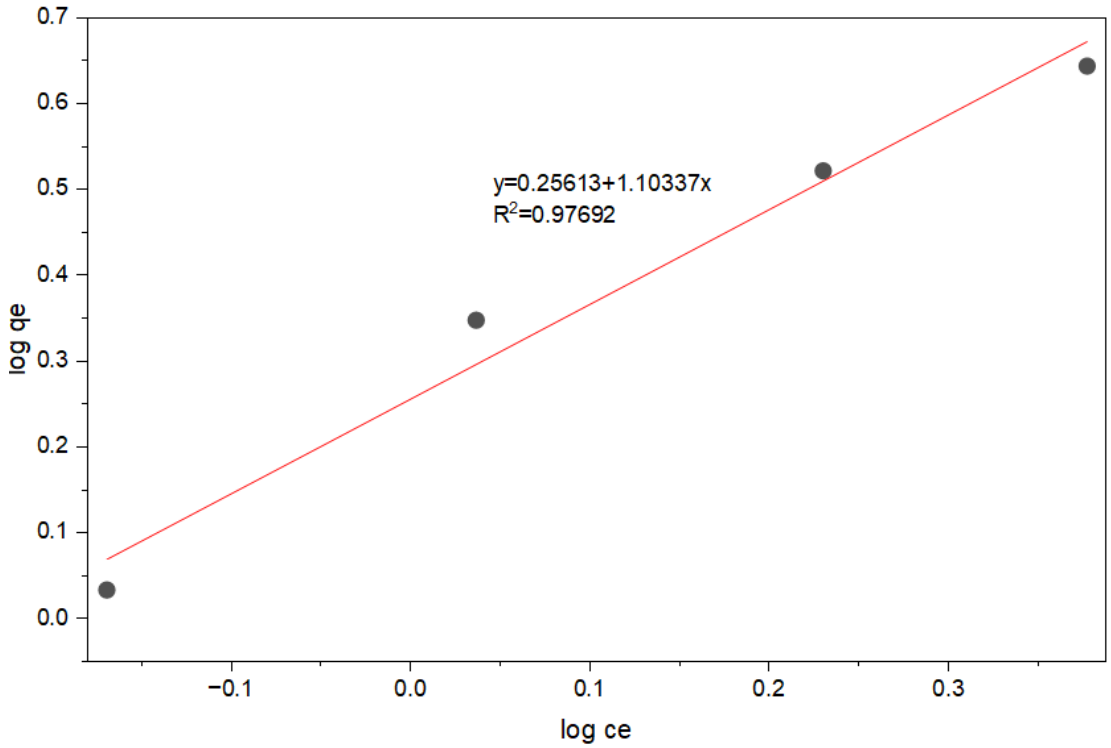

Figure 30: Freundlich isotherm for Fe using corn-cob charcoal